EVALUATION OF EARLY-AGE CRACKING SENSITIVITY IN BRIDGE DECK CONCRETE

Except where reference is made to the work of others, the work described in this thesis is my own or was done in collaboration with my advisory committee. This thesis does not include proprietary or classified information.

Akash Rao

Certificate of Approval:

Robert W. Barnes Associate Professor Civil Engineering	Anton K. Schindler, Chair Gottlieb Associate Professor Civil Engineering
Mary L. Hughes Assistant Professor Civil Engineering	George T. Flowers Interim Dean Graduate School

EVALUATION OF EARLY-AGE CRACKING SENSITIVITY IN BRIDGE DECK CONCRETE

Akash Rao

A Thesis

Submitted to

the Graduate Faculty of

Auburn University

in Partial Fulfillment of the

Requirements for the

Degree of

Master of Science

Auburn, Alabama
December 19, 2008

EVALUATION OF EARLY-AGE CRACKING SENSITIVITY IN BRIDGE DECK CONCRETE

Akash Rao

_____
Signature of Author

_____
Date of Graduation

THESIS ABSTRACT

EVALUATION OF EARLY-AGE CRACKING SENSITIVITY IN BRIDGE DECK CONCRETE

Akash Rao

Master of Science, December 19, 2008

134 Typed Pages

Directed by Anton K. Schindler

Early-age cracking is a problem in bridge deck concrete as it can have several detrimental effects on long-term behavior and durability. The primary objective of this project was to evaluate the early-age cracking tendency of bridge deck concrete.

The research presented in this thesis involved testing of a rigid cracking frame and a free shrinkage frame, under match-cured and isothermal conditions, to explore early-age cracking mechanisms of bridge deck concrete. The rigid cracking frame was used to evaluate the development of restrained stresses due to thermal and autogenous deformations. The free shrinkage frame was used to evaluate the thermal and autogenous deformations under zero-stress conditions. The laboratory testing program was designed to evaluate the effects of placement temperature, ambient temperature, aggregate type

and supplementary cementing materials on the cracking sensitivity of bridge deck concrete mixtures.

The laboratory testing program revealed that the heat generated during hydration greatly affects the restrained stress development of concrete. The temperature, at which the cracking occurred, decreased and time of cracking was delayed, when the control mixtures were placed in cold weather conditions. Use of supplementary cementing materials (SCMs) was found to be very effective in reducing the heat generation in bridge deck concrete and in reducing the restraint stresses, which significantly delayed the time of cracking.

The behavior of concrete under isothermal conditions was also investigated. The rigid cracking frame was held at a constant temperature for the duration of the test. Use of SCMs was found to reduce the magnitude of shrinkage stress and development associated with autogenous shrinkage. The use of SCMs during hot weather conditions significantly reduced the cracking tendency of bridge deck concrete.

ACKNOWLEDGMENTS

I sincerely thank my advisor Dr. Anton Schindler. His technical guidance, time, patience and friendship have been greatly appreciated. Billy Wilson, graduate students, and undergraduate assistants deserve thanks, for without them this project would never have been completed.

I thank the Alabama Department of Transportation (ALDOT) for their support and financial funding, which has made this project possible.

I also thank my family and friends. Their support and encouragement have been greatly appreciated.

Style manual or journal used Chicago Manual of Style

Computer software used Microsoft® Word, Microsoft® Excel

TABLE OF CONTENTS

LIST OF TABLES

LIST OF FIGURES

CHAPTER 1

INTRODUCTION

1.1 BACKGROUND

Concrete bridge deck cracking has been a prevalent problem in the United States. Transverse cracking occurs in most geographical locations and climates, and in many types of bridge superstructures (Krauss and Rogalla 1996). Engineers and researchers began documenting early-age cracking concerns relating to the generation of heat during hydration. It has been noted, that deck cracking can be caused by thermal stresses, shrinkage stresses and plastic shrinkage (Krauss and Rogalla 1996).

The work of National Cooperative Highway Research Program (NCHRP) 380 (Krauss and Rogalla 1996) included a survey sent to all U.S. Departments of Transportation (DOTs) and several transportation agencies overseas to learn the extent of deck cracking. Sixty-two percent of the agencies that responded considered transverse cracking at early age to be a problem. A survey conducted by the Federal Highway Administration (FHWA) found that more than 100,000 bridges suffered from early-age cracking (FHWA 2005). These types of cracks are often mistakenly called drying shrinkage cracks. However, in addition to the drying shrinkage effects, cracks are also caused by restrained volume change, due to temperature changes in concrete (due to

ambient temperature fluctuations) and heat of hydration of the concrete mixture (Krauss and Rogalla 1996).

These shrinkage and temperature stresses develop in all bridge decks, because the girders restrain the natural thermal and shrinkage movements of the deck. Further, when the deck and girders consist of different materials (e.g., steel and concrete, or different concretes) with different thermal expansion rates, even a constant temperature change across the entire bridge will cause stresses, because different materials expand differently and cannot freely expand, where they are attached (Mehta and Monteiro 2006). In addition to thermal and shrinkage stresses, heat is generated due to hydration of the cement and water. As the hydration continues, concrete matures, and it develops stiffness, which leads to the development of stresses when coupled with restrained thermal and shrinkage deformations. Cracking initiates once stresses exceed the tensile stress capacity of the concrete.

Understanding why cracking is a problem is important. Cracking in bridge decks may lead to durability-related issues, in addition to affecting the performance of the bridge. Increased permeability from cracks could not only result in steel corrosion, but could also decrease the service life of the concrete. Corrosion of reinforcing steel due to permeability is a major problem in cold and marine environments. The transportation agencies that responded to the FHWA survey found that weather conditions during placement greatly influenced cracking (Krauss and Rogalla 1996). Cracking was found to be worse in low humidity conditions and when concrete was cast at low or hot temperatures (Krauss and Rogalla 1996).

In addition to placement conditions discussed above, drying, autogenous, and chemical shrinkage have been found to cause early-age volume changes in concrete. Autogenous shrinkage was documented for the first time in the 1930s by Lynam (1934). At that time, autogenous shrinkage was thought to only occur at very low water-to-cement ratios (w/c) that were beyond the practical range of concrete. But with the advancement of chemical admixtures, low water-to-cement ratios are very common in modern construction.

Hence, in order to evaluate the cracking sensitivity of concrete mixtures, it is important to understand all of the mechanisms driving early-age volume change and restraint stresses which lead to early-age cracking.

1.2 EARLY-AGE VOLUME CHANGE AND STRESS DEVELOPMENT

A brief overview of the early-age volume change mechanisms and stress development is given in this section. However, it is discussed in detail in Section 2.4.

Concrete shrinkage is due to migration or loss of water from the hydrated cement paste phase. The shrinkage due to evaporation of water is called drying shrinkage. This type of shrinkage in unsealed concrete surfaces is highly dependent on environmental conditions such as wind, humidity and temperature. In addition to drying shrinkage, autogenous shrinkage occurs over time, which is the macroscopic volume change of the concrete with no accompanying moisture transfer with the exterior environment. Further, chemical shrinkage also occurs due to reaction of the cement with water. Thermal shrinkage is another phenomenon due to exposure of concrete to environmental conditions and the heat of hydration. All these shrinkage mechanisms induce strain in the

concrete, which, when restrained, causes stress, as the stiffness of the concrete develops. These stresses build up over time, and may exceed the tensile strength of concrete, leading to cracking.

1.3 RESEARCH OBJECTIVE

The objective of this project was to evaluate the effects of placement temperature, ambient temperature, cementitious materials and aggregate type on the cracking tendency of concrete mixtures.

1.4 RESEARCH APPROACH

Two sets of cracking frame and free shrinkage frame tests were implemented for this project. The first set included one match-cured rigid cracking frame and a match-cured free shrinkage frame. The second set included one isothermal rigid cracking frame, and an isothermal free shrinkage frame.

The rigid cracking frame, with overall dimensions of 6 x 6 x 65 in., illustrated in Figure 1-1, is comprised of two mild steel crossheads and two Invar side bars. In order for the concrete to be restrained, the crossheads are constructed using dovetails on each end. These connections are tapered to reduce the stresses in the crosshead. The dovetail is lined with teeth that grip the concrete. To further prevent slippage of the concrete, cross head braces are bolted to the top and bottom of the crosshead; these restrain expansion as the concrete goes into tension. Invar side bars are used to minimize the effect of temperature change on the length and stress of the concrete member. The Invar bars have a coefficient of thermal expansion (α), of 1 x 10^{-6}/°C, which is significantly less than that

of ordinary mild steel, 12 x 10^{-6}/°C (Whigham 2005). The forces developed within the bars causes an elastic deformation, which is recorded by means of strain gauges.

Insulated formwork is used to prevent moisture loss and to allow proper heating and cooling in the concrete specimen. The formwork is designed to insulate the test specimen, producing a heat of hydration approximately equal to a 50-cm-thick specimen (Breitenbucher 1989).

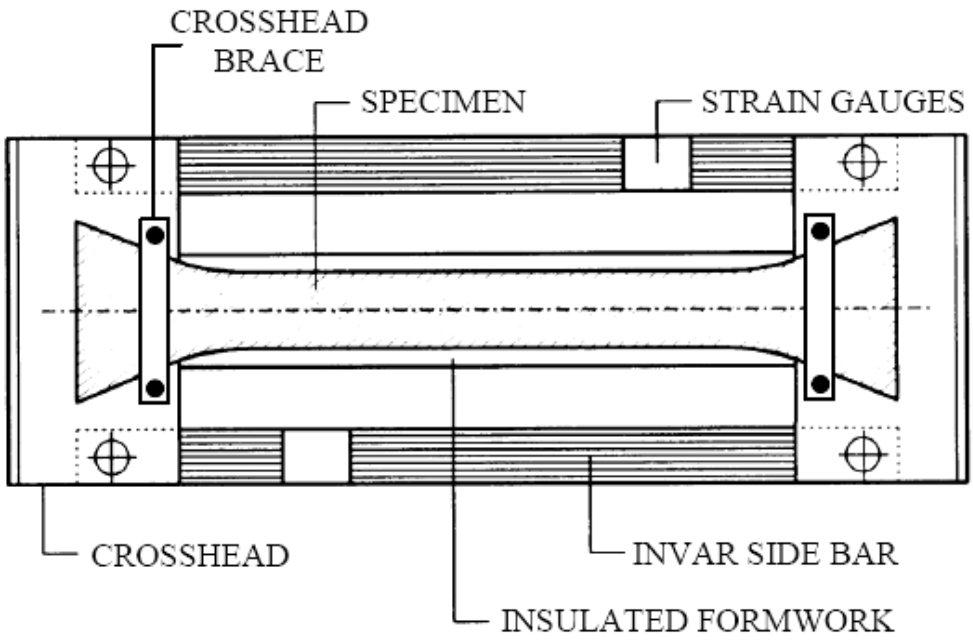

Figure 1-1: Diagram of the Rigid Cracking Frame (Springenschmid et al. 1994)

The formwork also provides support for the fresh concrete, which allows measurements to be taken as soon as the concrete has been placed. The formwork can be connected to an external heating and cooling water circulator. Copper tubing is built within the formwork, which allows temperature control without contamination of the test

specimen; therefore, measurement of thermal stresses can be determined for an arbitrary temperature profile (Mangold 1998).

In addition to the rigid cracking frame, a free shrinkage frame was also used to measure the shrinkage of the concrete specimen under no restraint conditions. The free shrinkage frame essentially consists of a box of dimensions, 6 x 6 x 24 in., supported by an Invar steel frame, as shown in Figure 1-2. The box formwork is lined with two layers of plastic separated by a layer of lubricant. Concrete is poured into the inner layer, which is not taped to the formwork and covers the concrete when the frame is ready for testing. Hence, the concrete inside is free to move because of the lubricant and lack of restraint. Linear Variable Differential Transformers (LVDTs) and temperature probes measure the shrinkage and the temperature of the specimen. A detailed discussion of the shrinkage frame design and testing procedure is given in Section 3.1.4

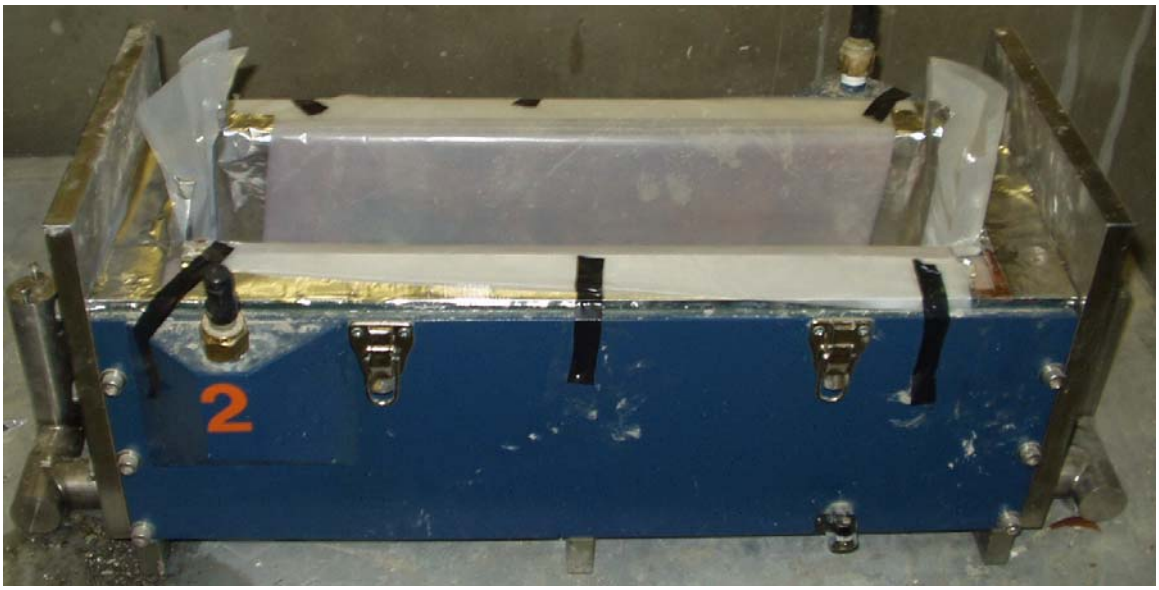

Figure 1-2: Free shrinkage frame (Meadows 2007)

The rigid cracking frame was used to evaluate the development of restrained stresses due to thermal and autogenous deformations. The free shrinkage frame was used to evaluate the thermal and autogenous deformation under zero-stress conditions. This study consists of an evaluation of the manner in which certain variables affect early-age cracking. The evaluation provides both researchers and practicing engineers with knowledge of how these variables affect the cracking tendency of concrete.

1.5 SCOPE OF REPORT

Chapter 2 of this report provides a thorough discussion of the early-age cracking phenomena. The discussion includes description of the development of heat of hydration, development of mechanical properties, early-age volume change, and early-age creep behavior.

The experimental laboratory testing program is documented and discussed in Chapter 3. It includes the description of the laboratory testing setup and materials.

All the results obtained from the execution of the laboratory testing program are presented in Chapter 4. Results regarding the development of mechanical properties, results from the rigid cracking frame, and results from the free shrinkage frame are included.

A thorough discussion of the laboratory testing results presented in Chapter 4 is provided in Chapter 5. Stress development due to thermal and autogenous deformations is thoroughly discussed.

Conclusions and recommendations resulting from the work documented in this thesis are offered in Chapter 6

Appendix A contains fresh concrete properties for each concrete batch. It includes slump, unit weight, air content, temperature and setting times.

All the hydration parameters used in generating the temperature history for a particular concrete mixture are summarized in Appendix B.

CHAPTER 2

LITERATURE REVIEW

Early-age cracking in bridge deck concrete is a severe problem that can reduce its functional life. Cracking originates from stresses induced by volume change as a result of thermal, drying, autogenous, and chemical shrinkage, coupled with restraint conditions that prevent movement of the concrete. These stresses develop due to strains that are induced by early-age volume change as the concrete stiffness increases. Over time, these stresses may exceed the tensile strength of the concrete, which will result in cracking. The mechanisms driving early-age cracking are influenced by many complex variables, and the mechanisms which drive the volume change are not clearly understood. In order to better understand the mechanisms driving early-age cracking, the variables that influence the cracking sensitivity of the concrete have to be studied. The current state of the art related to these mechanisms and variables are reviewed in this chapter.

2.1 HYDRATION OF CEMENTITIOUS MATERIALS

The hydration of portland cement is a chemical reaction during which heat is liberated. Many variables affect the heat generated during this hydration process. Factors such as cement composition, cement fineness, mixture proportions, replacement of cement by supplementary cementing materials (SCMs), and curing temperature can increase or

decrease the rate of heat generated during hydration (Mehta and Monteiro 2006). Excessive heat generated, coupled with non-uniform cooling, results in thermal gradients in the concrete elements. This uneven distribution of heat can lead to thermal deformations which, when restrained, can introduce cracking long before the structure is exposed to externally applied loads.

2.1.1 CEMENT COMPOSITION

The composition of cement is a major contributor to heat of hydration. Variables such as chemical composition and fineness affect the temperature rise of concrete. Some of these factors can be varied as a technique for controlling temperature, while others must be accepted as given conditions.

2.1.1.1 Chemical Composition

The chemical composition of the clinker compounds consists primarily of tricalcium silicate (C_3S), dicalcium silicate (C_2S), tricalcium aluminate (C_3A), and tetracalcium aluminoferrite (C_4AF), which are commonly referred to as Bogue compounds. The relative proportions of these chemical compounds and their fineness determine the different types of cement, as well as the amount of heat they generate during hydration (Bjøntegaard 1999, Mehta and Monteiro 2006).

The hydration of cement is a mixture of simultaneous and consecutive reactions (Bjøntegaard 1999). When the cement is dispersed in water, C_3A, the high-temperature compound of calcium, begins to go into solution and the liquid phase gets rapidly saturated with various ionic species. Needle-shaped crystals of Ettringite (calcium

trisulfoaluminate hydrate), is the first hydration product to be formed by the reaction of C_3A with water. The reaction of C_3A is followed by the hydration of C_3S. Finally, C_3A and C_4AF react simultaneously after C_3S.

Figure 2-1 demonstrates the heat evolution of cement as it hydrates. The initial reaction (Phase I) is caused by the reaction of C_3A forming ettringite. This process is very fast and a dormant period follows. After the dormant period, the second heat peak (II) is exhibited by the hydration of C_3S. The last heat peak (III) is produced by the transformation of ettringite to monosulfate (Bjøntegaard 1999).

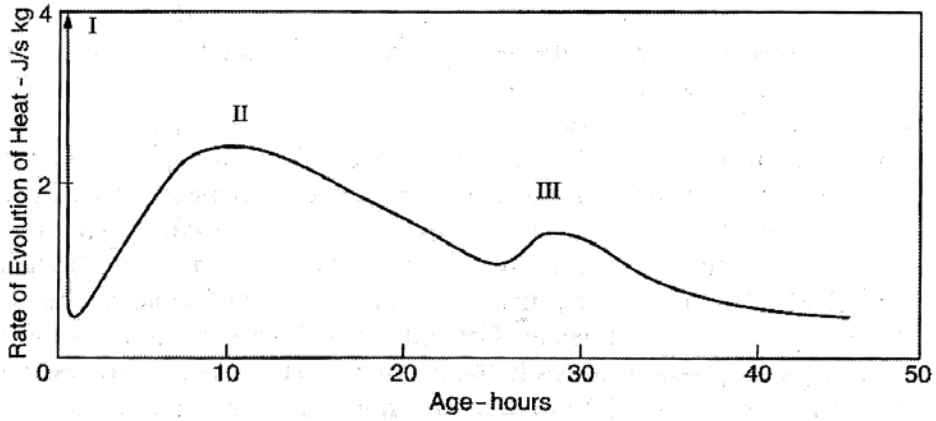

Figure 2-1: Heat evolution of hydrating cement (Bjøntegaard 1999)

Table 2-1 gives the typical values for heat evolution and rate of reactions for four primary chemical compounds in a Type I cement. Type I cement is the standard cement and is most commonly used in general construction applications in the United States (ACI 116R 1997). Type II and IV cements are low-heat generating cements during early ages, due to relatively low C_3A and high C_4AF content (Townsend 1965). Type III cement is high early-age strength cement, due to high C_3A content and fineness, which generates much more heat during hydration than Type I, II, or IV cements.

Table 2-1: Heat evolution of Bogue compounds (Bogue 1929)

Compound	Heat evolution after complete hydration (J/g)	Rate of reaction with water
C_3S	500	"medium"
C_2S	260	"slow"
C_3A	866	"fast"
C_4AF	125	"medium"

2.1.1.2 Fineness

Cement fineness affects the rate of heat generation rather than the magnitude of heat generation (ACI 207.2R 1997). The higher the fineness, the more surface area the cement is exposed to react with the water, and higher is the rate of hydration.

2.1.2 Mixture Proportions

The rate and magnitude of heat generation are affected by the quantity of cement used (ACI 207.2R 1997). This is due to the quantity of reactive products that are available to hydrate and liberate heat. The higher the cement content, the greater the temperature rise potential.

2.1.3 Replacement of Cement with Supplementary Cementing Materials

To reduce the amount of heat liberated during the hydration of cement, some SCMs can be used as a replacement for portland cement. SCMs such as fly ash and ground granulated blast furnace slag (GGBF Slag) have been found to be effective means of reducing the quantity of cement, therefore reducing the heat due to hydration (ACI

207.2R 1997). Springenschmid and Breitenbucher (1998) stated that it is current practice to reduce the cement content as much as possible in order to reduce heat development.

2.1.3.1 Fly Ash

Fly ash comes from many different sources. The calcium oxide (CaO) content of the fly ash can be used as an indicator of its cementitious nature (Schindler and Folliard 2005).

Class C fly ash is classified as fly ash containing more than 20% of CaO. Class F fly ash contains less than 15% CaO (ACI 232.2R 1997). Class F fly ash is generally more pozzolanic in nature as compared to Class C fly ash, which is more cementitious. Therefore Class F fly ash reduces the total heat of hydration more than Class C (Mehta and Monteiro 2006). Figures 2-2 and 2-3 demonstrate the reduction in heat liberation due to hydration of cementitious systems containing fly ash and cement-only systems.

2.1.3.2 GGBF Slag

Hardly any literature is available on the use of slag in bridge deck concrete. The reduction of early-age heat generation is directly proportional to the slag quantity used (ACI 233R 1997). The peak rate of temperature rise is delayed due to the inclusion of slag (Sioulas and Sanjayan 2000, Schindler and Folliard 2005), as seen in Figure 2-4.

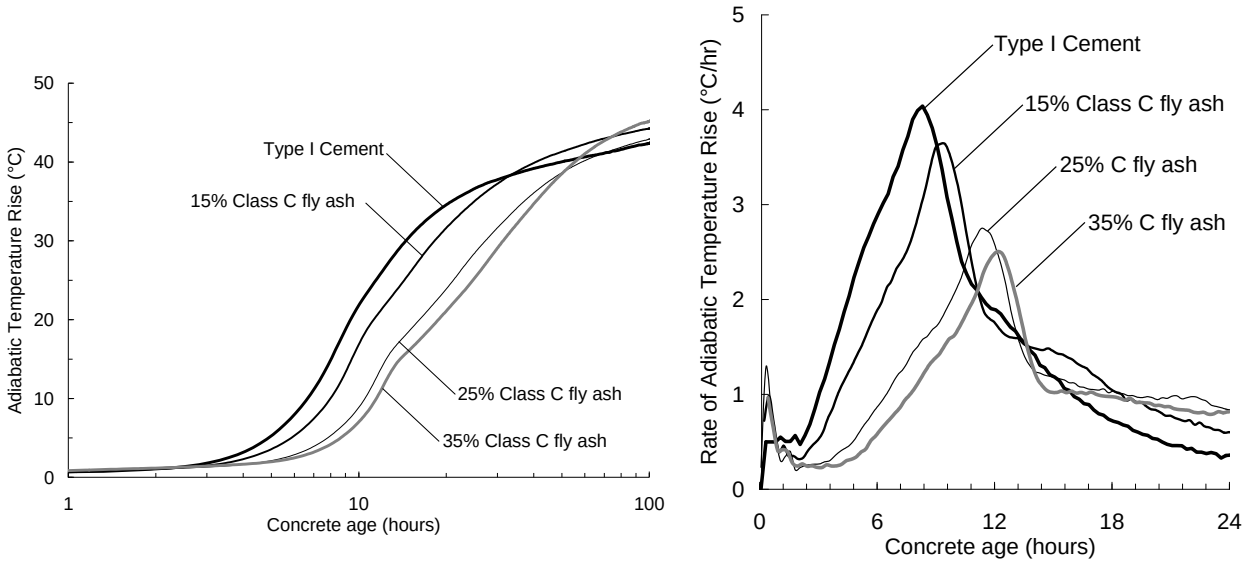

Figure 2-2: Total temperature rise and rate of temperature rise using Class C fly ash as a replacement (Schindler and Folliard 2005)

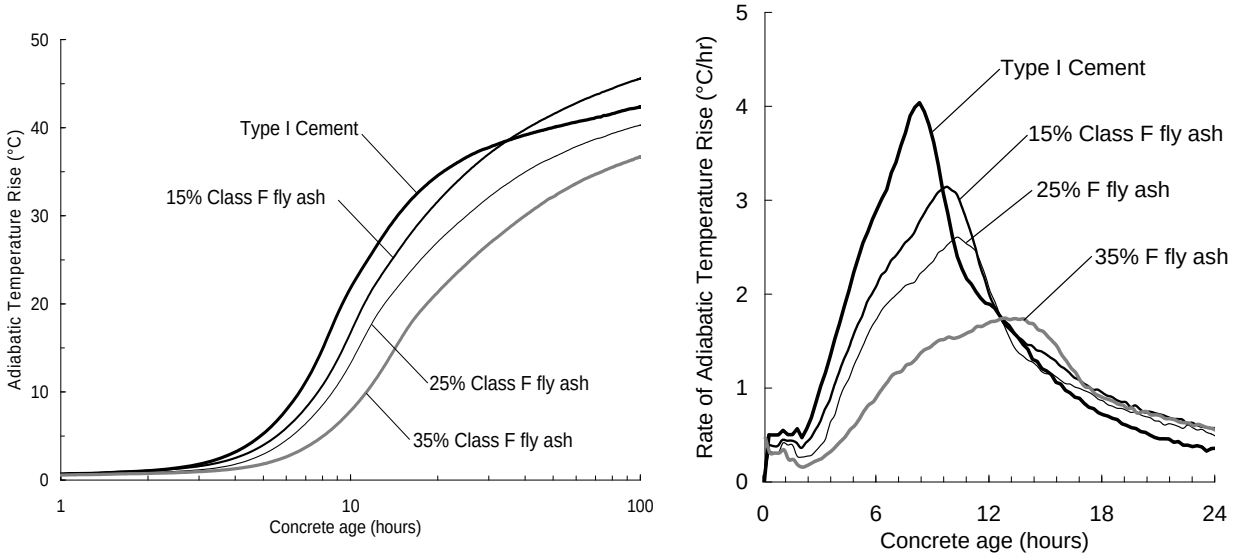

Figure 2-3: Total temperature rise and rate of temperature rise using Class F fly ash as a replacement (Schindler and Folliard 2005)

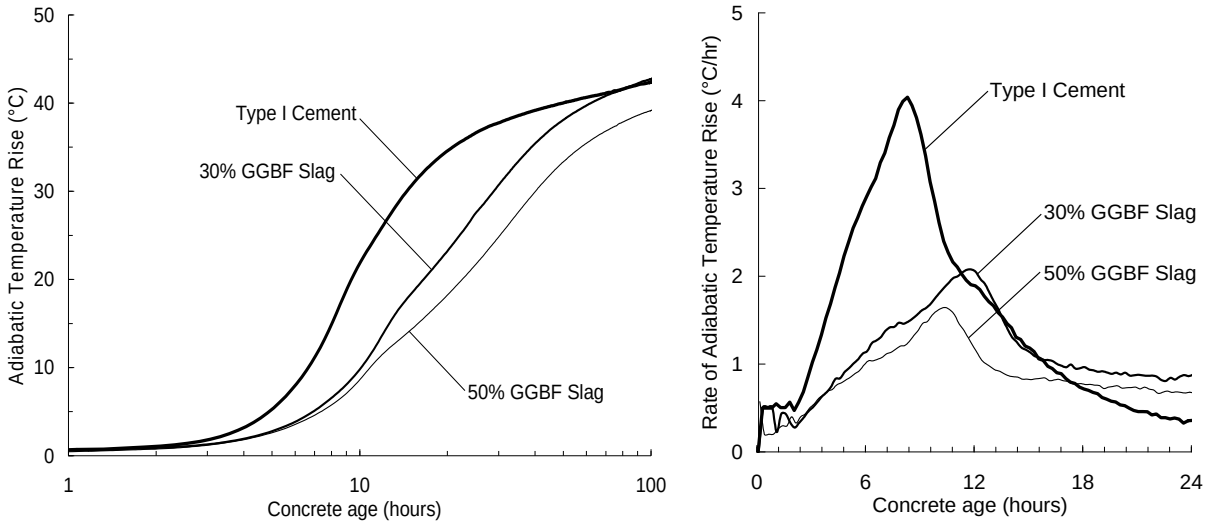

Figure 2-4: Total temperature rise and rate of temperature rise using GGBF slag as a replacement (Schindler and Folliard 2005)

2.1.4 CURING TEMPERATURE

The curing temperature has a direct influence on the rate of hydration. If the curing temperature is increased, then the rate of hydration is increased. As placement temperatures increase, adiabatic temperature rises faster due to the acceleration of hydration.

2.2 SETTING OF CONCRETE

Setting is the change in the concrete from a fluid to a rigid state. It is caused by the sufficient formation of hydration products, which is accompanied by a sudden change in temperature rise in the concrete (Mehta and Monteiro 2006). According to ASTM C 403, initial set is achieved when the concrete paste has reached a bearing pressure of 500 psi.

Final set is achieved when the concrete paste has reached a bearing pressure of 4,000 psi. A plot of penetration resistance over time, like the one shown in Figure 2-5, is used to determine initial and final set.

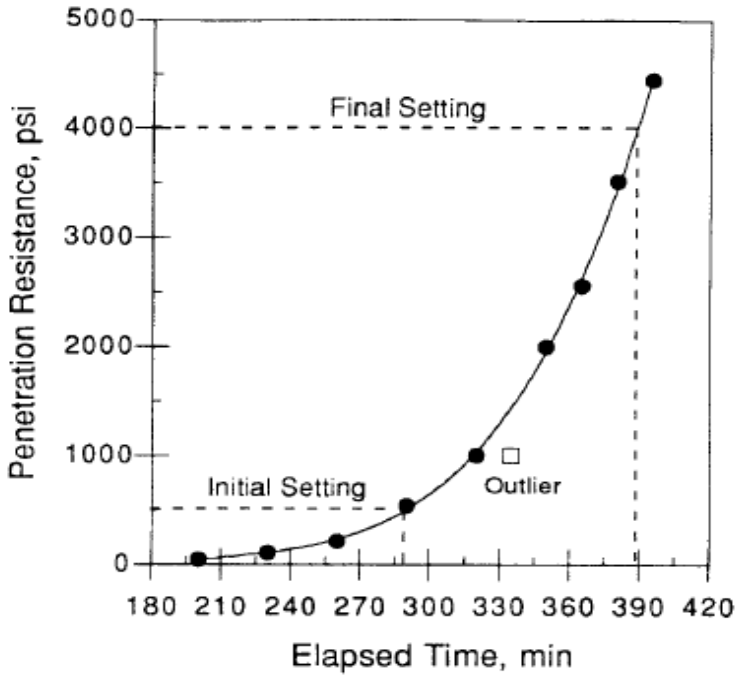

Figure 2-5: Typical plot of penetration resistance versus time (ASTM C 403 1999)

2.3 DEVELOPMENT OF MECHANICAL PROPERTIES

Cracking in early-age concrete is not just a function of stress development. Cracking is also a function of mechanical properties such as tensile strength and elastic modulus. These properties are time- and temperature-dependent. The modulus of elasticity relates strains and stresses and will be discussed in Section 2.3.3. The tensile strength of the concrete resists the stresses from restrained contraction of the concrete and will be discussed in Section 2.3.2.

2.3.1 COMPRESSIVE STRENGTH

The development of compressive strength in concrete has been widely studied for many years. Factors such as amount and type of cement and admixtures, temperature, curing conditions, and water-to-cementitious materials ratio affect the development of concrete strength (Mehta and Monteiro 2006).

As discussed in Section 2.1, cement type and amount may affect the amount of heat developed in the concrete member. Temperature affects the rate at which the cement hydrates. Therefore, early-age and long-term strength can be affected due to changes in these mixture proportions. Variables such as water-to-cementitious ratio (w/cm), air entrainment, and cement type can be varied to increase or decrease strength. Figure 2-6 demonstrates the effect of w/cm on concrete compressive strength. As the w/cm is increased, the compressive strength is decreased. Figure 2-7 illustrates the decrease in the compressive strength as air entrainment is introduced to the mixture proportions at the same w/cm. Figure 2-8 demonstrates the effect of cement type on concrete strength. As discussed in Section 2.1.1.1, Types II and IV have low early-age strength due to lower C_3A content. However, Type III cement has high early-age strength due to higher C_3A content.

The curing temperature also affects the rate at which the cement hydrates as discussed in Section 2.1.4. As the curing temperature is increased, the cement hydrates more rapidly. As a result, the concrete develops mechanical properties at a faster pace; however, the long-term strengths are reduced as shown in Figure 2-9.

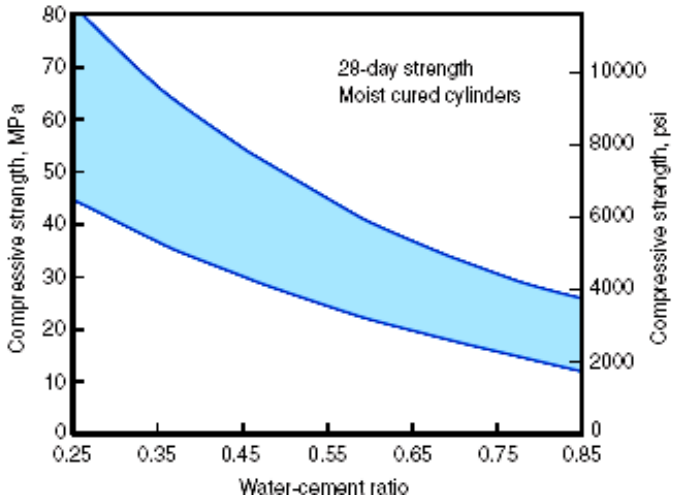

Figure 2-6: Effect of w/c ratio on concrete strength (Kosmatka et al. 2002)

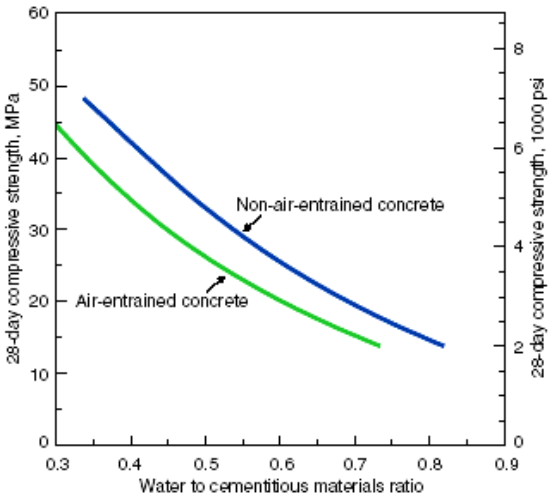

Figure 2-7: Effect of air entrainment on concrete strength (Kosmatka et al. 2002)

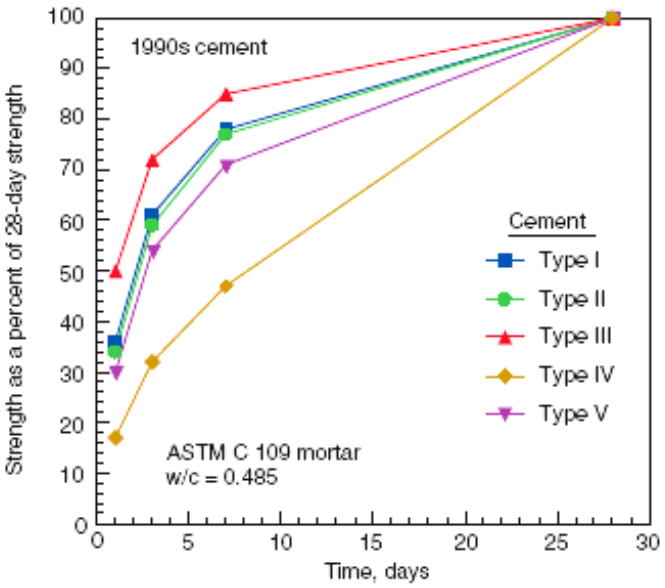

Figure 2-8: Effect of cement type on concrete strength (Kosmatka et al. 2002)

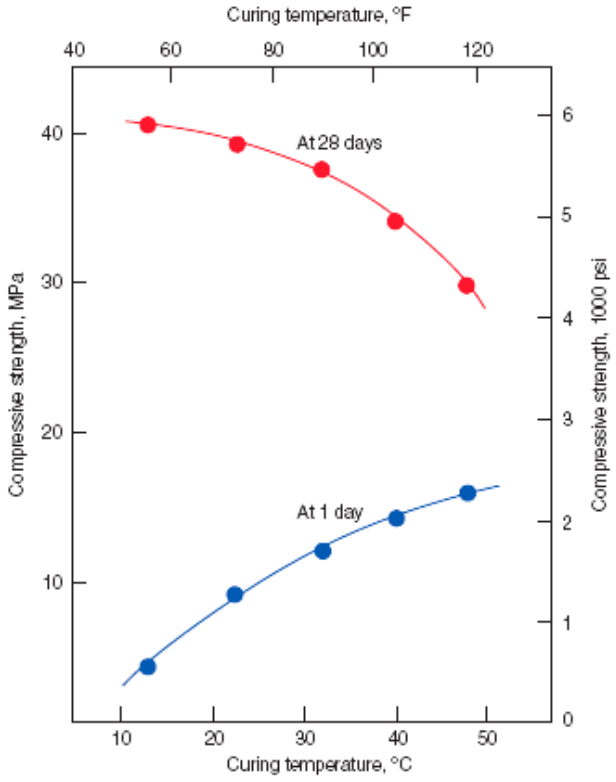

Figure 2-9: Effect of curing temperature on concrete strength (Kosmatka et al. 2002)

2.3.2 TENSILE STRENGTH

Tensile strength of concrete develops due to the same factors as compressive strength; however, concrete's tensile strength is much lower than its compressive strength, due to ease of crack propagation under tensile loads (Mindess and Young 2002). The development of tensile strength is an important property in the mitigation of early-age cracking.

Microcracking originates in the interfacial transition zone (ITZ), and cracking develops as load is applied. The ITZ develops from a water film, that forms around large aggregate particles as bleeding occurs. As hydration progresses, calcium silicate hydrate (C-S-H) forms to fill the empty voids left behind from the water film. This helps to improve the strength and density of the ITZ (Mehta and Monteiro 2006).

The ITZ is the strength-limiting phase in concrete (Mehta and Monteiro 2006). This is primarily due to the microcracking that can be present in the ITZ before the structure is loaded. It is also the reason why, concrete displays inelastic behavior, while its constituents exhibit elastic behavior until fracture.

Aggregate characteristics influence the tensile strength of concrete (Mehta and Monteiro 2006). Aggregate texture has a substantial impact on the tensile strength of concrete. Rough textured or crushed aggregates have shown higher tensile strengths, especially at early ages, than smoother aggregates (Mehta and Monteiro 2006).

2.3.3 ELASTIC MODULUS

The development of the elastic modulus of concrete varies in proportion to the square root of the compressive strength gain in concrete (ACI 318 2005). The same factors that

alter the development of strength affect the development of the elastic modulus, with some exceptions. The modulus of elasticity is affected primarily by the aggregate type and quantity used in the concrete mixture (Mindess and Young 2002). As the stiffness and amount of the aggregate fraction in concrete increases, the stiffness of the concrete increases, as shown in Figure 2-10.

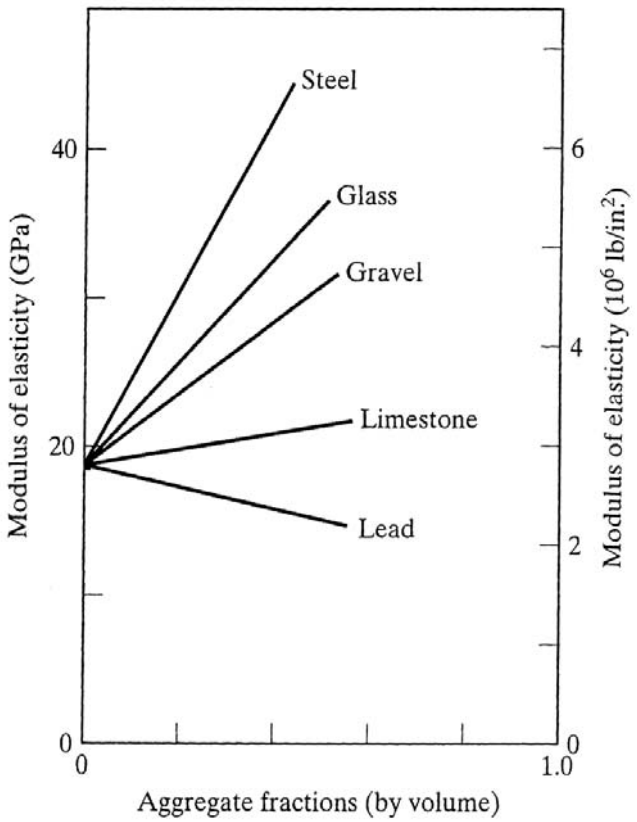

Figure 2-10: Effect of aggregates on modulus of elasticity (Mindess and Young 2002)

The modulus of elasticity is also a function of the porosity of the paste fraction of the concrete. As the water-to-cementitious materials ratio is increased, the porosity of the paste fraction is increased. If the porosity is increased, the elastic modulus will decrease (Mindess and Young 2002).

2.4 FACTORS THAT PRODUCE EARLY-AGE VOLUME CHANGE

Early-age volume change in concrete is a well-known phenomenon that has been studied for many years. Factors such as thermal changes, drying shrinkage, and autogenous shrinkage are known to produce early-age volume change. If the concrete is restrained from movement, the volume changes will induce compressive or tensile stresses. If these stresses are greater than the corresponding strength of the concrete, then cracking may occur. In this section, the various factors that contribute to early-age volume changes are discussed.

2.4.1 THERMAL EFFECTS

Thermal stresses have been a major cause of early-age cracking of bridge deck concrete (Lange and Altoubat 2002). Many factors such as heat of hydration (as discussed previously), environmental conditions (weather and time of placement) and thermal conductivity affect the rate of temperature rise. Concrete, like many other materials, expands when it is heated and contracts when it is cooled. If the concrete is restrained from movement, the change in temperature will induce stresses.

Figure 2-11A demonstrates the temperature development of a concrete element, due to heat generated during hydration, that is fully restrained from movement. The mechanical properties begin to develop as shown in Figure 2-11C, after the concrete has reached final set (at approximately 6 hours). As the temperature and stiffness of the specimen increases, the concrete experiences compressive stresses as shown in Figure 2-11B (negative value in the figure indicates compression). As the temperature of the concrete subsides, the compressive stresses diminish and the concrete has zero-stress at

approximately 24 hours at a temperature of T_{02}. Since the concrete has gained stiffness, since the time from final set to zero-stress condition, the temperature at zero-stress condition is higher than the setting temperature. As the temperature subsides further, the concrete experiences tensile stresses. Once the tensile stresses reach the tensile strength of the concrete, cracking occurs at approximately 48 hours. The concrete cracked at a temperature change of 8°K (14°F), relative to the zero-stress temperature, T_{02}. According to Thielen and Hintzen (1994), if the restraint factor is reduced to 50%, then the temperature change to induce cracking would double. Therefore, the reduction of the degree of restraint will reduce the cracking tendency.

However, it is to be noted that there is a noted difference between calculated stress due to the given temperature change, and the actual measured stress. This is due to the visco-elastic nature of the concrete at early ages, which allows much of the compressive stresses to be relaxed. However, due to the relaxation, concrete experiences tensile stresses much earlier than the calculated, and hence a higher risk of cracking at an earlier age than predicted.

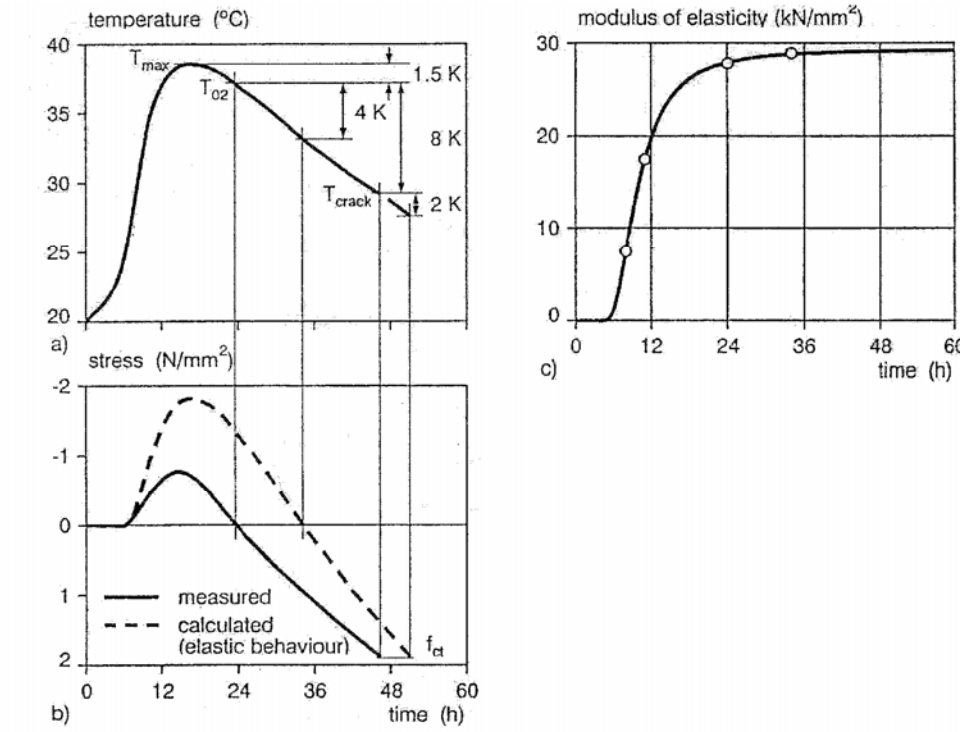

Figure 2-11: (A) Temperature development of restrained concrete specimen (B) Stress development of restrained specimen (C) Development of elastic modulus of concrete (Thielen and Hintzen 1994)

The magnitude of thermal stresses further depends on the creep-adjusted elastic modulus, the coefficient of thermal expansion, and amount of restraint as defined in Equation 2-1 (Bamforth and Price 1995).

$$\Delta\sigma_{Thermal} = \Delta T \cdot \alpha_t(t) \cdot E_{cr}(t) \cdot K_r \qquad \textit{Equation 2-1}$$

where,

$\Delta\sigma_{Thermal}$ = change in concrete stress due to temperature change (psi),

ΔT = change in concrete temperature (°F),

$\alpha_t(t)$ = coefficient of thermal expansion of the concrete at time t (in/in/°F),

$E_{cr}(t)$ = creep-adjusted modulus of elasticity at time t (psi), and

K_r = restraint factor.

2.4.1.1 Coefficient of Thermal Expansion

The coefficient of thermal expansion, $\alpha_t(t)$, is the key parameter that relates temperature change in the concrete to strain. As indicated in Equation 2-2, the magnitude of strain developed in an unrestrained specimen, is directly proportional to the temperature change and the coefficient of thermal expansion (CTE).

$$\Delta\varepsilon_{Thermal} = \Delta T \cdot \alpha_t(t) \qquad \textit{Equation 2-2}$$

where,

$\Delta\varepsilon_{Thermal}$ = change in concrete strain due to temperature change (in/in),

ΔT = change in temperature (°F), and

$\alpha_t(t)$ = coefficient of thermal expansion of the concrete at time t (in/in/°F).

The $\alpha_t(t)$ varies as a function of the individual constituents of the concrete (Emanuel and Hulsey 1977). Variables such as aggregate type, water-to-cementitious materials ratio, and age affect α_t of concrete. The variations of α_t of concrete due to the use of different aggregates can be seen in Figure 2-12. The α_t of concrete is directly related to the α_t of the aggregate used in the mixture proportions (Mehta and Monteiro 2006). As the α_t of the aggregate is increased, the α_t of the concrete is increased. The influence of aggregate type on α_t of hardened concrete is easy to evaluate because it is directly related to the α_t of the aggregate used in the mixture proportions.

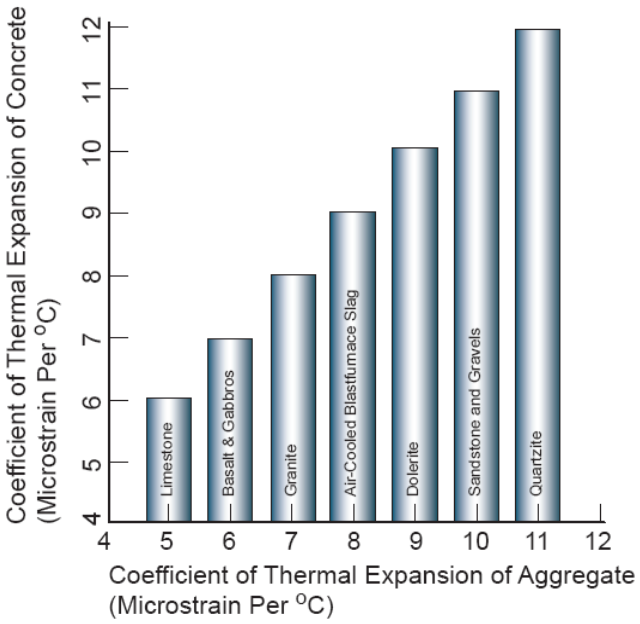

Figure 2-12: Influence of aggregate α(t) on α(t) of hardened concrete (Mehta and Monteiro 2006)

2.4.1.2 Environmental conditions

Bridges are continuously subjected to changing temperatures, therefore, a significant factor in the behavior and performance is thermal loading due to environmental factors. Thermal stresses induced from seasonal temperatures changes, are linearly proportional (not accounting for relaxation effects) to the differences between material thermal expansion coefficients and differences between concrete stiffness of various elements in the bridge. Through the study conducted by NCHRP Report 380 (Krauss and Rogalla 1996), it is now known that the diurnal temperature changes affect the bridge deck more than the supporting girders and the resulting thermal stresses are proportional to the coefficient of thermal expansion. However, usually, temperature changes are not taken

into consideration during design because temperature steel is considered sufficient to control widths after cracking.

When a deck is cast monolithically with the girders, thermal stresses caused by hydration are generally reduced because both the deck and girders generate heat and then cool at the same time. However thermal stresses are worse in steel-girder bridges (Krauss and Rogalla 1996). Bridge decks in moderate or extreme climates often experience high stresses due to temperature changes. The upper surface of the deck typically heats and cools more quickly, because it is exposed to direct solar radiation, wind, and humidity. Hence, these factors have to be taken into account when determining the thermal effects on early-age cracking.

2.4.2 EARLY-AGE SHRINKAGE

Concrete shrinkage is a result of the migration or loss of water from the hydrated cement paste phase. Holt (2001) states that "as water is lost to evaporation (drying shrinkage) or internal reactions (autogenous shrinkage), tensile stresses are generated." As a result of a slow elastic modulus development, large strains may only create small stresses at early ages. However, these stresses at early-ages are more critical because the concrete has not developed much strength. Even if the resulting stresses are small, microscopic cracks may still form. If early cracks are internal and microscopic, long-term shrinkage may cause the cracks to widen and spread. A discussion of drying shrinkage, autogenous shrinkage, and chemical shrinkage can be found in Sections 2.4.2.1, 2.4.2.2, and 2.4.2.3, respectively.

2.4.2.1 Drying Shrinkage

Drying shrinkage is the decrease in volume of the concrete with time due to moisture loss (Mindess and Young 1981). The rate of water loss from unsealed concrete surfaces is highly dependent upon environmental conditions. Conditions such as wind, relative humidity, and temperature affect the rate of evaporation. Unlike heat dissipation of mass concrete elements, moisture loss from the core of mass concrete occurs extremely slowly. The slow migration of moisture from within concrete elements is highly dependent upon the length it has to travel; therefore, thinner members tend to dry faster than larger members.

2.4.2.2 Autogenous Shrinkage

Autogenous shrinkage of cement paste and concrete is defined as the macroscopic volume change occurring with no moisture transferred to the exterior surrounding environment. It is a result of chemical shrinkage affiliated with the hydration of cement particles (Holt 2001).

Autogenous shrinkage was documented for the first time in the 1930s by Lynam (1934). At that time, autogenous shrinkage was thought to only occur at very low water-to-cement ratios that were beyond the practical range of concrete. But with the advancement of concrete, low water-to-cement ratios are a very common occurrence in today's structural design. Even though many strength and durability aspects are now improved, the risk of autogenous shrinkage is greater and needs to be accounted for.

A graphic depiction of a sealed concrete's composition change due to the cement hydration reactions is given in Figure 2.13 where C is the cement volume, W is the

volume of water, H_y is the volume of the hydration products and V is the volume of voids. This bar graph relates how the autogenous shrinkage is a portion of the chemical shrinkage. While the chemical shrinkage is an internal volume reduction, the autogenous shrinkage is an external volume change.

The factors influencing the magnitude of autogenous shrinkage are often disputed. It is agreed that autogenous shrinkage cannot be prevented by casting, placing or curing methods, but must be addressed when proportioning the concrete mixture. It appears that the internal components or ingredients have the most significant influence (Holt 2001).

Autogenous shrinkage occurs over three different stages, as described in following sections (Holt 2001). Immediately after mixing water and cement, a chemical shrinkage change will occur due to the reduction in volume of the reaction products.

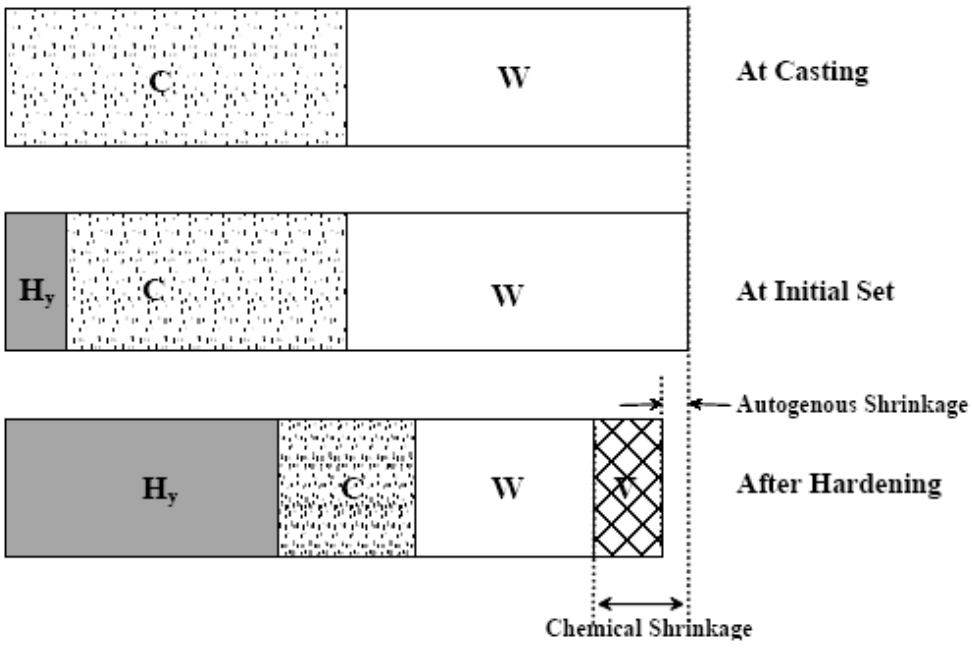

Figure 2-13: Volume reduction due to autogenous shrinkage (Holt 2001).

In this early phase, while the concrete is still liquid, the autogenous shrinkage is equivalent to chemical shrinkage.

The point when autogenous shrinkage changes from being a function of chemical shrinkage to self-desiccation is a function of the degree of cement hydration. Self-desiccation is defined as the localized drying of the concrete's internal pores and will be further described in the next stage. During this stage, capillary pressure will start to develop and may cause shrinkage. This pressure mechanism works as the water, or meniscus, is moving between the pores. As the water is lost from subsequently smaller pores, the water meniscus will continue to be pulled into the capillary pores and will generate more stress on the capillary pore walls.

As described in the previous paragraphs, when the concrete is still liquid, immediately after mixing, the autogenous shrinkage is proportional to the degree of hydration. This means the autogenous shrinkage is due only to chemical changes. Once a skeleton has formed, the chemical shrinkage becomes more and more restrained. Beyond a certain stage, the material is rigid and autogenous shrinkage is comprised of less and less chemical shrinkage. The further volume reductions are only due to self-desiccation (Holt 2001).

Once concrete has hardened with age (> 1 day), the autogenous shrinkage may no longer be a result of only chemical shrinkage. During the later ages, the autogenous shrinkage can also result from self-desiccation since a rigid skeleton is formed to resist chemical shrinkage. Self-desiccation is the localized drying resulting from a decreasing relative humidity. This drying is caused due to the accumulation of the water in the

narrow pores, gradually drying out the wider pores (Van Breugel 2001). The lower humidity is due to the cement requiring extra water for hydration.

In a high-strength concrete with a low w/c, finer porosity causes the water meniscus to have a greater radius of curvature. These menisci cause a large compressive stress on the pore walls, thus causing greater autogenous shrinkage as the paste is pulled inwards. Self-desiccation occurs over a longer time period than chemical shrinkage and does not begin immediately after casting. It is only a risk when there is not enough localized water in the paste for the cement to hydrate; thus, the water is drawn out of the capillary pore spaces between solid particles. This would typically begin after many hours or days in high-strength (low w/c) concretes. At later ages, a strong correlation exists between internal relative humidity and free autogenous shrinkage, as shown in work by Baroghel-Bouny (1996).

The use of mineral admixtures, such as silica fume, may also refine the pore structure towards a finer microstructure. If there is a finer pore structure, the water consumption will be increased and thus the autogenous shrinkage due to self-desiccation will be increased.

Although autogenous shrinkage has been investigated for many years, only recently have studies resulted in models, to estimate the autogenous shrinkage. In 1999, Hedlund and Westman published an empirical formula for the estimation of autogenous shrinkage, as shown in Equation 2-3 and Equation 2-4.

$$\varepsilon_{co}(t) = \varepsilon_{co\infty} \cdot \beta_{so}(t) \qquad \textit{Equation 2-3}$$

where,

$\varepsilon_{co}(t)$ = autogenous shrinkage at time t (microstrains)

t = age of concrete (days),

$\varepsilon_{co\infty}$ = final value of autogenous shrinkage, and

$$\beta_{so}(t) = -1.14.\left[\frac{t_{so}}{t - t_{start}}\right]^{0.3} \qquad \textit{Equation 2-4}$$

where,

$\beta_{so}(t)$ = time distribution function for autogenous shrinkage,

t_{so} = time parameter (days), and

t_{start} = starting time (days).

The starting time for shrinkage measurements varies between 9 and 24 hours (Hedlund and Westman 1999). This is when the concrete is stiff enough to take a measurement, which is established by judgment. The time parameter, t_{so}, is a constant for all high-performance concrete (HPC) and is typically taken as 5 days. The final value of autogenous shrinkage, $\varepsilon_{co\infty,}$ can be calculated from the following equation (Hedlund and Westman 1999):

$$\varepsilon_{so\infty} = (-0.6 + 1.2 \cdot \frac{w}{b}) \cdot 10^{-3} \qquad \textit{Equation 2-5}$$

where,

w = weight of the water (lbs) and

b = weight of the binder (lbs).

The European Standard was the first to include a method for the prediction of long-term autogenous shrinkage strains (Holt 2001). The model in European standard, given in Equation 2-6 and Equation 2-7 is very similar to the model of Hedlund and Westman.

$$\varepsilon_{cs} = \beta_{cc}(t) \cdot \varepsilon_{cs,\infty} \qquad \textit{Equation 2-6}$$

where,

ε_{cs} = autogenous shrinkage strain (microstrain),

$\varepsilon_{cs,\infty} = 2.5\left(f_c^{'} - 10\right)\times 10^{-3}$, and

$f_c^{'}$ = characteristic compressive strength of concrete at 28 days (MPa).

$$\beta_{cc}(t) = \exp\left\{ s\left[1 - \left(\frac{28}{t/t_1} \right)^{1/2} \right] \right\} \qquad \textit{Equation 2-7}$$

where,

$\beta_{cc}(t)$ = time distribution of autogenous shrinkage,

s = coefficient depending on the type of cement,

t = age of concrete (days), and

t_1 = 1 day.

The values of s in Equation 2-7 are 0.20 for rapid-hardening high-strength cement, 0.25 for normal and rapid-hardening cements, and 0.38 for slowly hardening cements.

According to Holt (2001), variations in autogenous shrinkage over the cross section or depth of the concrete member do not occur. This is due to the low porosity of high-strength concrete where the internal water will be distributed once the material has hardened and thermal equilibrium has been reached. Unlike autogenous shrinkage, drying shrinkage is dependent upon the moisture gradient across the concrete element, which is caused by uneven evaporation due to large volume-to-surface ratios.

2.4.2.3 Chemical Shrinkage

As discussed in the previous section, autogenous shrinkage is a result of chemical shrinkage during the first few hours after hydration has started. Chemical shrinkage, commonly referred to as Le Chatlier shrinkage, is the internal volume reduction associated with the reaction of cement and water (Holt 2001). It is caused by the volume changes that occur as a result of Bogue compounds reacting with water as seen in Figure 2-14.

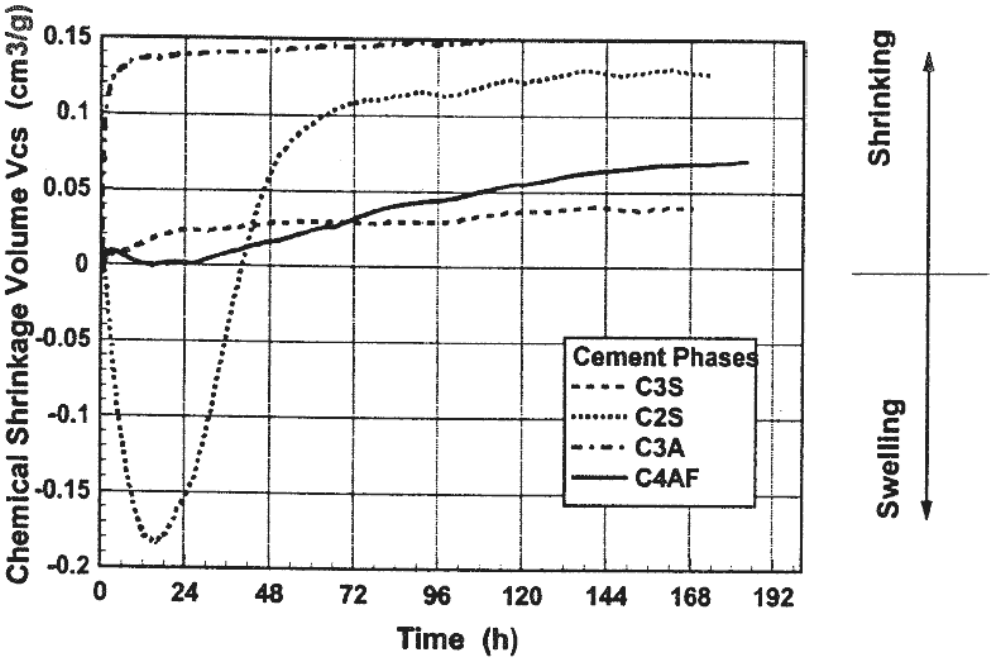

Figure 2-14: Influence of cement composition on chemical shrinkage (Paulini 1996)

Many other variables affect the rate of chemical shrinkage; however, they do not affect the overall magnitude (Holt 2004). The rate of chemical shrinkage is dependent upon concrete mixture proportions and cement composition such as fineness. The fineness of the cement and the water-to-cement ratio affect the rate of the reaction rather

than the overall magnitude of shrinkage. Other variables such as cement type, admixture type and dosage, and addition of pozzolans have been found to affect the rate of chemical shrinkage (Sellevold et al. 1994). Higher reaction rates of cement will lead to larger chemical shrinkage magnitudes, which will lead to greater autogenous shrinkage (Holt 2004). Conditions that lead to large autogenous shrinkage magnitudes may produce greater total shrinkage, which increases the cracking risk of concrete structures.

2.5 DEVELOPMENT OF EARLY-AGE STRESSES

Early-age stresses originate from volume change as a result of thermal, drying, and autogenous shrinkage, coupled with restraint conditions that prevent or alter the movement of concrete. The stresses are time-dependent and are proportional to the restraint against movement. Over time, stresses may exceed the tensile strength of the concrete which will result in cracking.

2.5.1 RESTRAINT CONDITIONS

Restraint conditions of the concrete element are of utmost importance when determining stresses induced by early-age volume change. Restraint stresses can be divided into two major categories, internal and external. Internal restraint is caused by temperature or gradients that form as a result of uneven cooling and/or moisture loss within the concrete member. During cooling, the surface of the concrete cools more rapidly than the interior of the element, which creates thermal gradients.

External restraint is caused by the conditions surrounding or supporting the concrete element that prevents free movement. External restraints associated with bridge decks

could include, but are not limited to deck form type, deck-girder systems, girder type, girder end constraints, relative stiffness of the girder and the deck. The reduction of the overall restraint of the concrete member can significantly decrease the cracking tendency. Figure 2-15 demonstrates the temperature, stress, and strength development of a concrete element that is fully restrained (100%) from movement. As shown, reducing the restraint factor diminishes the risk of cracking due to the reduction in stresses.

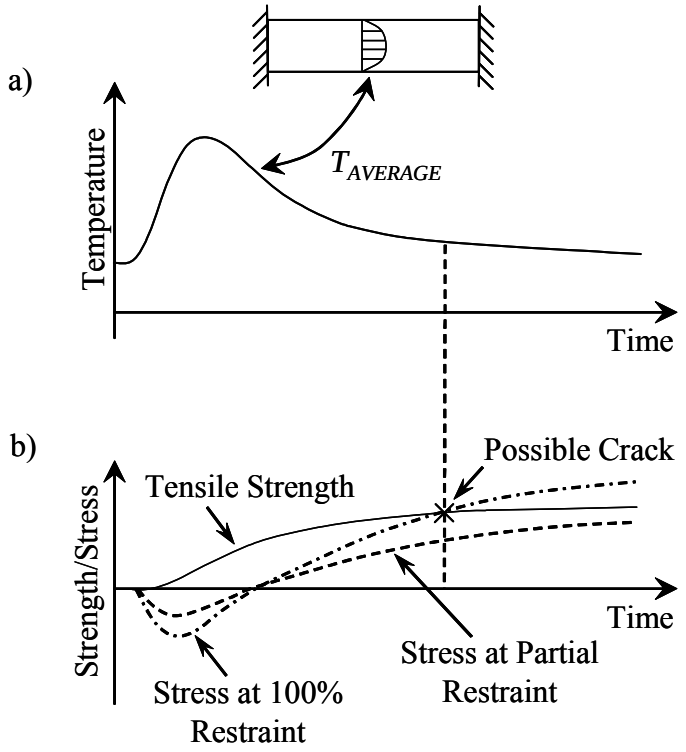

Figure 2-15: Evolution of temperature and thermal stresses for different restraint conditions (Nilsson 2003)

2.5.2 EARLY-AGE CREEP BEHAVIOR

Early-age concrete undergoes deformations due to volume change as discussed previously. Restraint of these deformations creates stresses in the concrete. Creep and

associated relaxation occur due to the viscoelastic response of early-age concrete; therefore, these properties must be considered when assessing the cracking risk of concrete during the first few days after placement.

Creep is the increase in strain with respect to time under a constant load. If a linear-elastic material is subjected to a constant load, then it will respond instantaneously with a deformation that remains constant. However, if the load is removed, then the material will return to its original shape. Concrete, on the other hand, is not a linear-elastic material especially at early-ages; therefore, understanding early-age nonlinear creep behavior is very important when calculating restraint stresses in early-age concrete (Westman 1999).

Concrete creep can be divided into two major categories; recoverable and irrecoverable deformation (Mehta and Monteiro 2006). Recoverable deformation is recovered fully after unloading due to the elastic nature of the concrete. Irrecoverable deformation causes the concrete paste to behave plastically; therefore not recovering all deformation after the load is removed. Figure 2-16 illustrates the general behavior of hardening concrete with loading and unloading taking place. Elastic deformation can be recovered instantaneously after the load is removed. The delayed elastic recovery, commonly referred to as creep recovery, is the portion of creep-induced deformation that will be recovered over time. The net effect after loading and unloading has taken place, is the irrecoverable deformation (Emborg 1989).

Factors that influence creep can be divided into two major categories: internal and external. The internal factors are cement type, mixture proportions, water-to-cement ratio, etc. (Emborg 1989). External factors include the type and intensity of loading,

duration of loading, age at loading, moisture content, and the change in relative humidity and temperature of the ambient conditions.

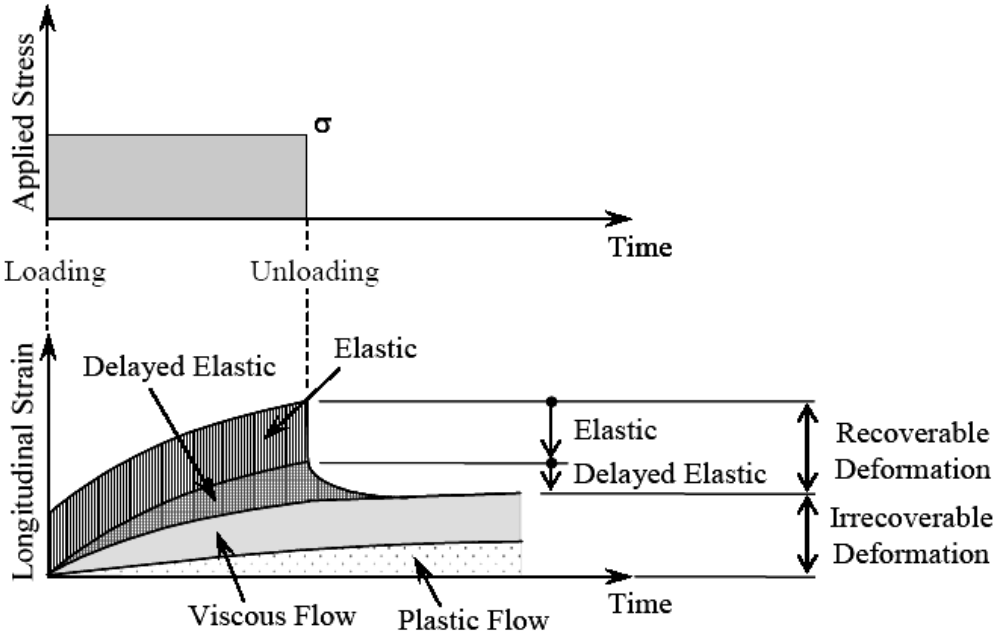

Figure 2-16: Generalized creep behavior of hardening concrete (Emborg 1989)

Creep in early-age concrete members is very complex. Due to the low strength of young concrete, the nonlinear portion of the stress-strain relation is reached at much lower stress levels than in concrete at later ages. As a result, many complex models have been proposed to describe the time varying nature of creep (Westman 1999, Bazant and Chern 1985, Emborg 1989). These models were developed using prior models for long-term creep estimates (Larson 2003).

2.6 METHODS FOR DETERMINING EARLY-AGE STRESSES

The mechanisms that cause internal volume changes in early-age concrete are very complex. The stresses that are generated cannot be determined by measuring deformations alone (Breitenbucher 1990). As a result, accurate measurement of restraint-induced stresses is very difficult. Many laboratory tests have been developed to measure the restraint stresses and quantify the cracking tendency of concrete. Tests such as the concrete ring test, restrained prism test, and temperature-stress testing machine (TST) are methods of determining the cracking tendency of various concrete mixtures (Whigam 2005, Mangold 1998); however, this thesis only involves the use of the rigid cracking frame as a testing method, as used by Meadows (2007), which was described earlier in Section 1.4. Additionally, environmental conditions were simulated by using the ConcreteWorks Version 2.0 software (Poole et al. 2006).

2.7 CONCLUDING REMARKS

Cracking in concrete due to early-age volume change is a complex phenomenon and is caused by many variables. Effects such as thermal, drying, and autogenous shrinkage, coupled with restraint conditions, create stresses that can exceed the tensile strength of the concrete. In order to fully understand the mechanisms driving early-age cracking, each variable must be studied. Quantification of these variables can be an extremely hard task, particularly at early ages, therefore making prediction of cracking tendencies very difficult. A practical way to assess the effect of these variables is to perform restrained cracking tests such as those performed with the rigid cracking frame used in this study.

CHAPTER 3

LABORATORY TESTING PROGRAM AND MATERIALS

In order to accomplish the objective set forth in Section 1.3, an experimental laboratory testing program was undertaken. The laboratory testing program was designed to evaluate the effects of placement temperature, ambient temperature, supplementary cementing materials and aggregate type on the cracking tendency of concrete typically used in bridge deck applications. The laboratory test setup developed by Whigham (2005) was implemented with some modifications that will be described in this chapter.

3.1 EXPERIMENTAL TESTING PROGRAM

The experimental testing program was designed to primarily investigate the restraint stresses due to early-age volume change. In order to study the mechanisms controlling early-age restraint stresses, the following equipment was used: a rigid cracking frame, a free shrinkage frame, a match-curing box, and a semi-adiabatic calorimeter. Each concrete mixture was tested for two weeks.

Figure 3-1 shows a schematic of the experimental testing program. In the first week, the fresh concrete was placed in the rigid cracking frame, free shrinkage frame and match-curing box, and was subjected to a match-curing temperature profile that is representative of temperatures experienced in bridge deck applications.

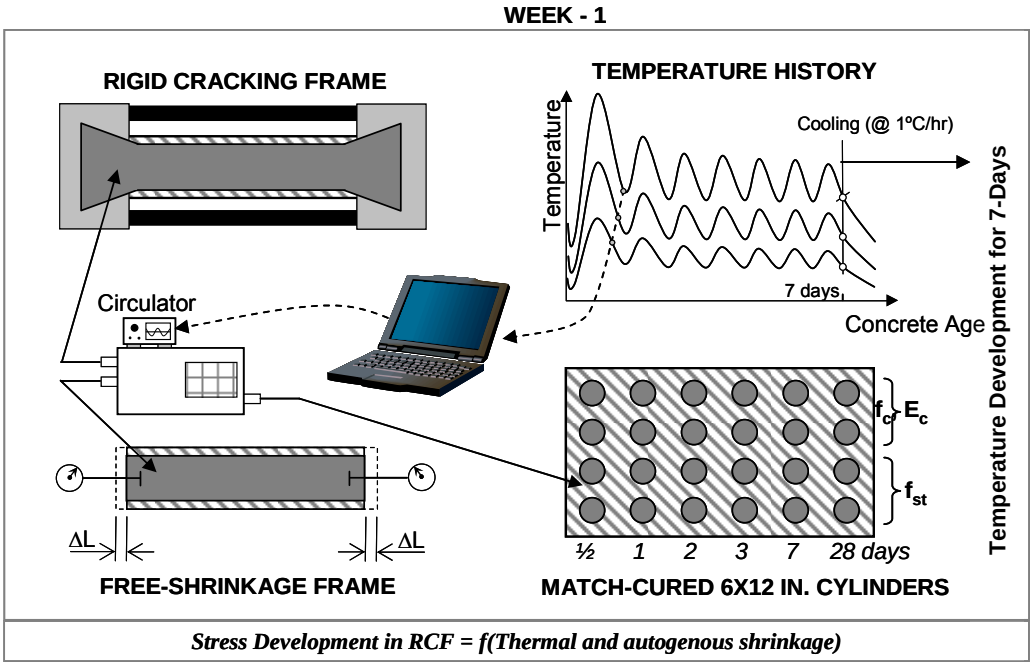

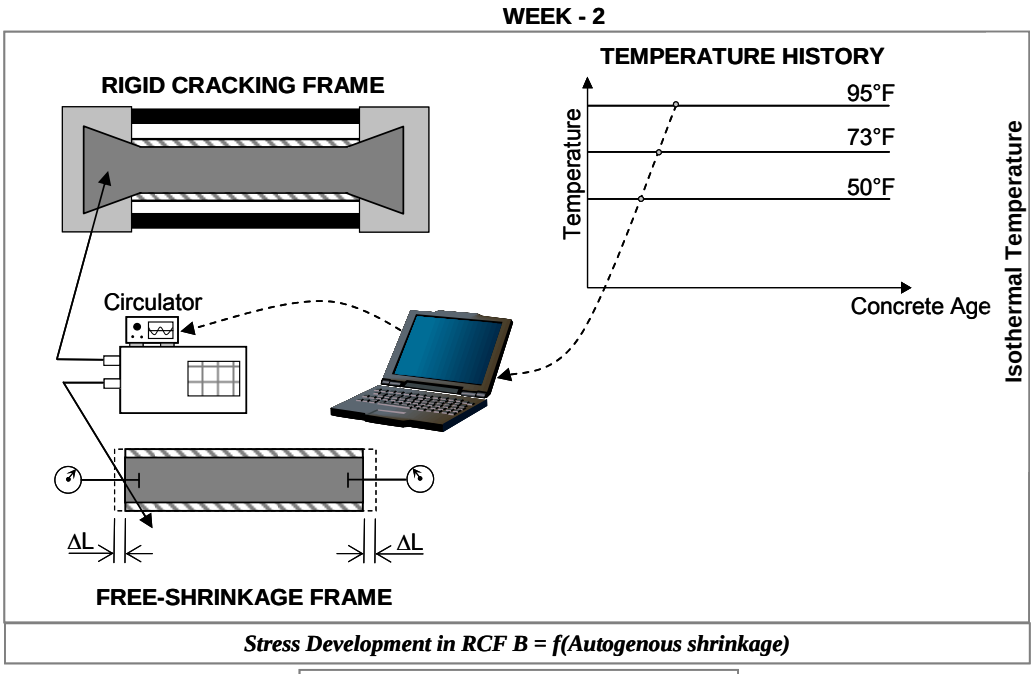

ADDITIONAL TESTS

- Semi-adiabatic calorimetry
- Conventional drying shrinkage
  - Start drying at 7-days
- f_c at 7, and 28-day (moist cured)
- Fresh concrete properties
  - Slump, Air
- Setting

Figure 3-1: Schematic of experimental testing program

The rigid cracking frame, free shrinkage frame, and match-curing box are connected to a computer and circulator, which drive the concrete to a specific bridge deck temperature history. This variation was imposed to study the combined effects of autogenous and thermal shrinkage on the development of restraint stresses. In addition, the match-curing box was used to condition the temperature history of the molded concrete cylinder specimens, so that the development of mechanical properties could be determined.

In the second week, fresh batch of concrete was mixed and placed in the cracking frame and shrinkage frame under isothermal conditions. This change in testing protocol was made in order to separate thermal and autogenous shrinkage effects.

During the two weeks of testing, the cracking frame provided valuable information about thermal and autogenous stresses under restrained conditions, whereas the free shrinkage frame allowed the measurement of volume change of the concrete under restraint-free conditions.

A list of the additional tests performed on the fresh and hardened concrete is provided later in the chapter. The semi-adiabatic calorimeter was used to obtain hydration parameters to calculate the temperature history for match-curing the concrete specimens.

3.1.1 SEMI-ADIABATIC CALORIMETER

The semi-adiabatic calorimeter (Quadrel iQdrum 300) was used to record the heat signature of each concrete mixture. The semi-adiabatic calorimeter is shown in Figure 3-2. The data recovered from the hydration drum were then used to calculate the parameters that define the progress of hydration for a specific mixture (Schindler and Folliard 2005).

These hydration parameters, given in Appendix B, were then used to model the temperature evolution in a typical bridge deck, as described in the next section.

Figure 3-2: Semi-adiabatic calorimeter

3.1.2 ESTIMATION OF BRIDGE DECK TEMPERATURES

The next step for each mixture was to generate a temperature history that could be expected if that mixture were to be placed in a typical bridge deck. A cracking frame temperature development software package, developed as part of Texas Department of Transportation (TxDOT) Research Project 0-4653 was used to generate a temperature profile by modeling an 8-inch thick deck with stay-in-place metal forms, as shown in Figure 3-3.

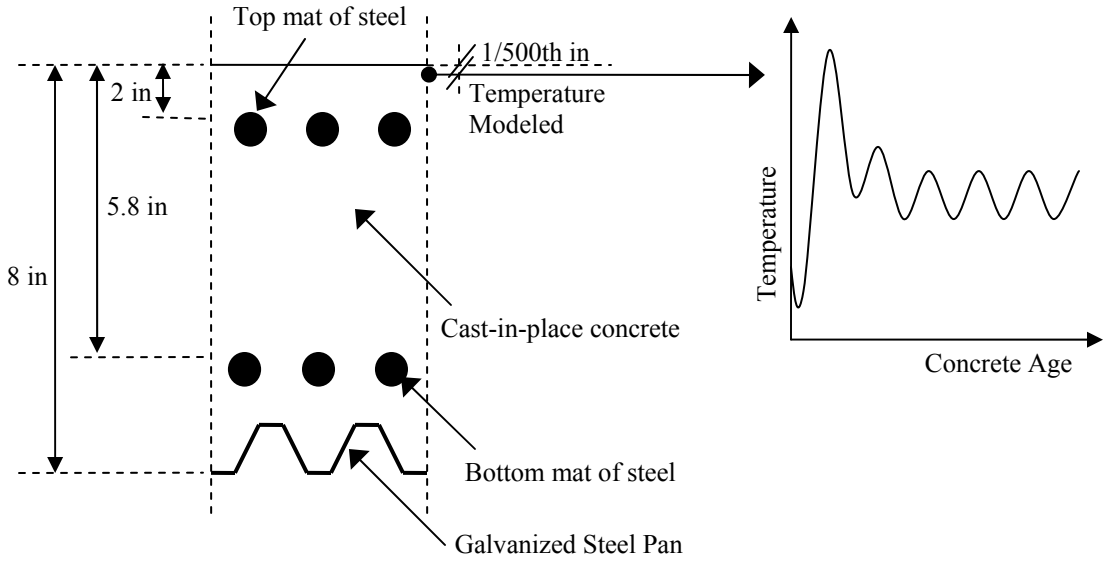

Figure 3-3: Schematic of deck geometry used to model the concrete (Concrete Works Version 2.01, User's Manual)

The inputs for generating the temperature profile were the following:

- General parameters
  - Placement time = 8 a.m.
  - Placement date: Summer = August 15th
    Spring/Fall = October 15th
    Winter = January 15th
  - Place: Montgomery, AL
- Mixture proportion parameters
- Cement content, water content, coarse aggregate content, fine aggregate content, coarse aggregate type, fine aggregate type, supplementary cementitious material

type, chemical admixture type, air content, hydration properties, and fresh concrete temperature.

- Hydration parameters
- Environmental parameters
    - Wind speed (constant at 5 mph), Relative humidity (constant at 50%), Cloud cover (constant at 25%)

Using these inputs, the software estimated the temperature profile for specified fresh concrete placement temperatures of 50 °F, 73 °F, and 95 °F. The resulting temperature profile was exported and converted into a text document. The computer program used to control the match-curing test used the text document as input when driving the concrete to the desired temperature profile. Typical temperature profiles from the cracking frame temperature development program can be seen in Figure 3-4.

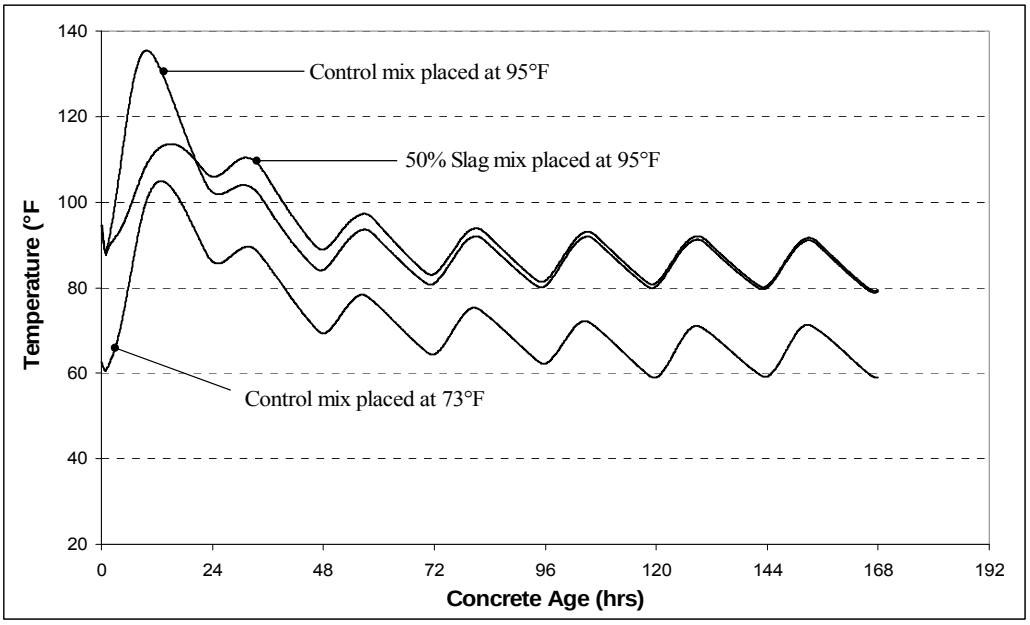

Figure 3-4: Temperature profiles estimated by cracking frame temperature development program

3.1.3 RIGID CRACKING FRAME

In Section 1.4, an introduction to the rigid cracking frame test setup was provided. The testing program, as discussed in Meadows (2007) is used with some exceptions. The changes to the testing program of Meadows (2007) are:

- Each concrete mixture is tested separately under a match-curing temperature profile and under isothermal temperature conditions on consecutive weeks.
- One rigid cracking frame and one free shrinkage frame is used each week to retrieve information about temperature stresses, shrinkage stresses and deformations. This testing is conducted for specimens under match-cured temperature profile and isothermal temperature profile on successive weeks.
- 6 x 12 in. cylinders were used to study development of mechanical properties

Reasons for these changes are as follows:

- To produce temperatures representative of those experienced by bridge decks
- To isolate and evaluate the effects of autogenous stresses and autogenous deformations.
- From the earlier study (Meadows 2007) it was found that 4 x 8 in cylinders gave inconsistent results when tested for split-tensile strength and elastic modulus. Hence 6 x 12 in cylinders was used in this study.

Depending on whether one particular concrete mix was mixed at 50 °F, 73 °F, or 95 °F on the first week, the isothermal temperature for the next week's testing would be set correspondingly. These temperatures were selected to match the fresh concrete placement temperatures for the cracking frame subjected to varying temperature profiles.

Figure 3-5: Rigid cracking frame under test conditions

The rigid cracking frame under test conditions is shown in Figure 3-5. The inside of the formwork was lined with a layer of plastic sheeting that is taped to the formwork. This layer was used to protect and prevent the concrete from adhering to the formwork. Silicone was used to smooth the area between the crossheads and formwork to prevent stress concentrations.

After the concrete was mixed, the fresh concrete was placed into the rigid cracking frame formwork with two lifts. Each lift was vibrated to ensure proper

consolidation. The concrete was smoothed using a wooden trowel. A layer of plastic was secured to the formwork over the concrete to prevent moisture loss. All edges of the plastic was sealed with adhesive aluminum foil tape. The thermally insulated lid was then secured to the formwork. Two temperature probes were embedded into the concrete via holes through the lid. The strain gauge wires were securely fastened to the Invar rods. Quick disconnect hoses were fastened to the formwork and circulator so that concrete in the rigid cracking frame could be temperature controlled.

The concrete in the cracking frame of week one was allowed to hydrate naturally until the concrete specimen cracked. If the specimen did not crack after 7 days (168 hours), the concrete in the cracking frame was cooled at 1°C/hr until cracking occurred.

The isothermal frame was also allowed to run for 144 hours at a constant temperature. This time was selected so that the test could be conducted every week.

3.1.4 FREE SHRINKAGE FRAME

The specimen in this frame was match-cured using the same temperature profile as the concrete in the match-curing cracking frame. An addition to the testing program of Meadows (2007), a free shrinkage frame subjected to isothermal conditions was also employed. This test was added to isolate autogenous deformations of concrete.

3.1.4.1 Free Shrinkage Frame Design

The free shrinkage frame consists of a thermally insulated box, four steel plates, and a supporting invar steel frame as shown in Figures 3-6 and 3-7. The box serves as the formwork for the freshly placed concrete as well as the system to match cure the concrete

to the temperature profile used for the cracking frame. The dimensions of the concrete specimen are 150 mm x 150 mm x 600 mm; however, the effective gauge length of the test specimen is 500 mm as indicated in Figure 3-6. There are two stainless steel plates at each end of the formwork. The outer plate is connected via bolts to the formwork. The inner plate is connected to the outer plate with bolts that allow for retraction once the concrete has reached initial set. Initial set was determined with the procedure outlined in ASTM C 404 (1999).

As shown in Figure 3-6, a 1/8-in diameter Invar rod is placed through the inner and outer plates on each side which hold it into position. The rod is connected to an anchorage disk within the concrete and to the Linear Variable Differential Transformer (LVDT). The LVDT is securely fastened to the supporting frame using standard mounting holes and small bolts. A small plastic sleeve is placed around each Invar bar to allow easy recovery after testing is complete.

In Figure 3-7, the supporting steel frame is shown. The frame consists of Invar steel bars to reduce the effect that ambient temperature changes may have on the recorded length change. The reduction in movement allows for accurate measurements to be taken without significant effects due to ambient temperature changes. For further details of free shrinkage frame, the reader is encouraged to refer Appendix A of Meadows (2007).

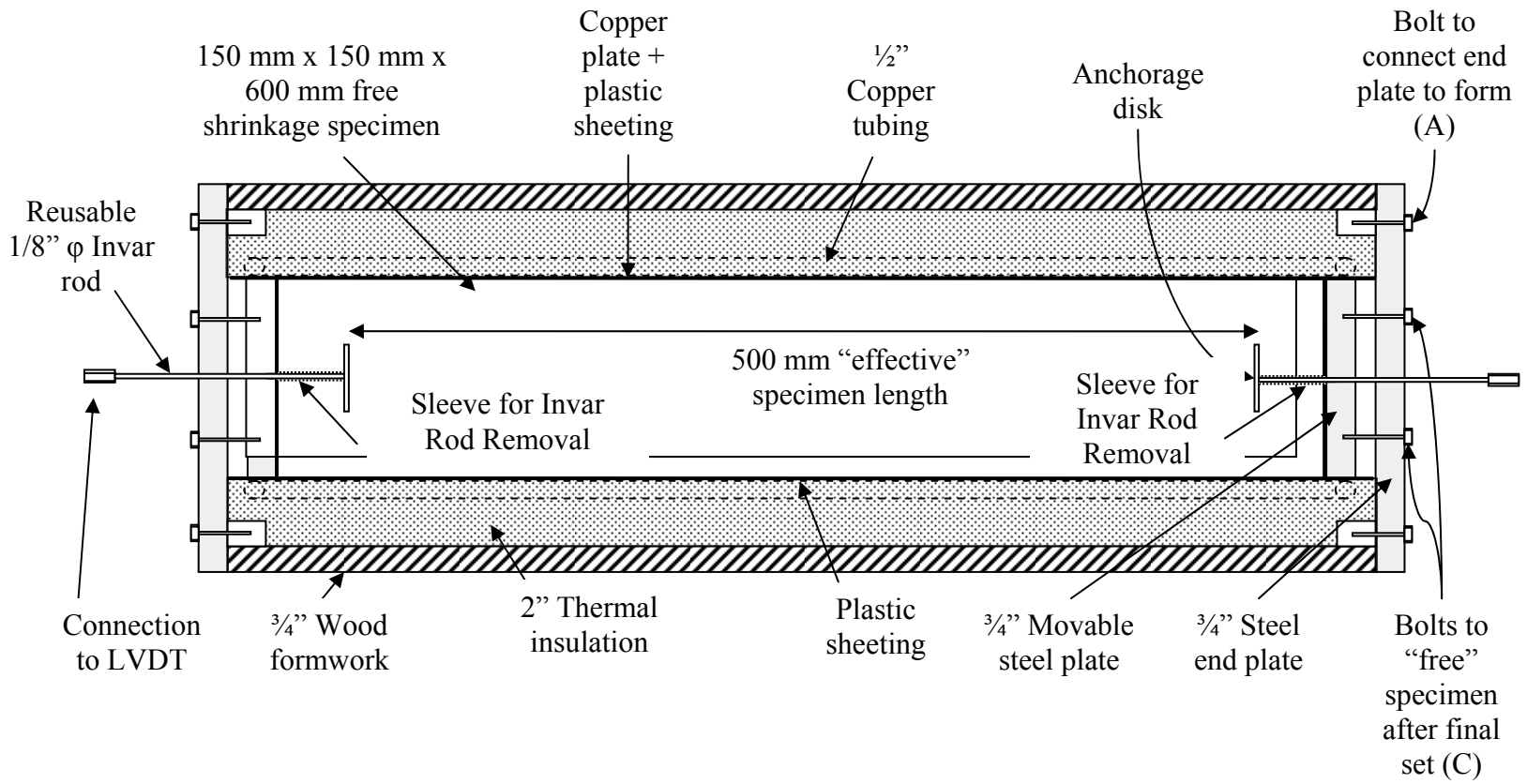

Figure 3-6: Free shrinkage frame detail in plan view (Meadows 2007)

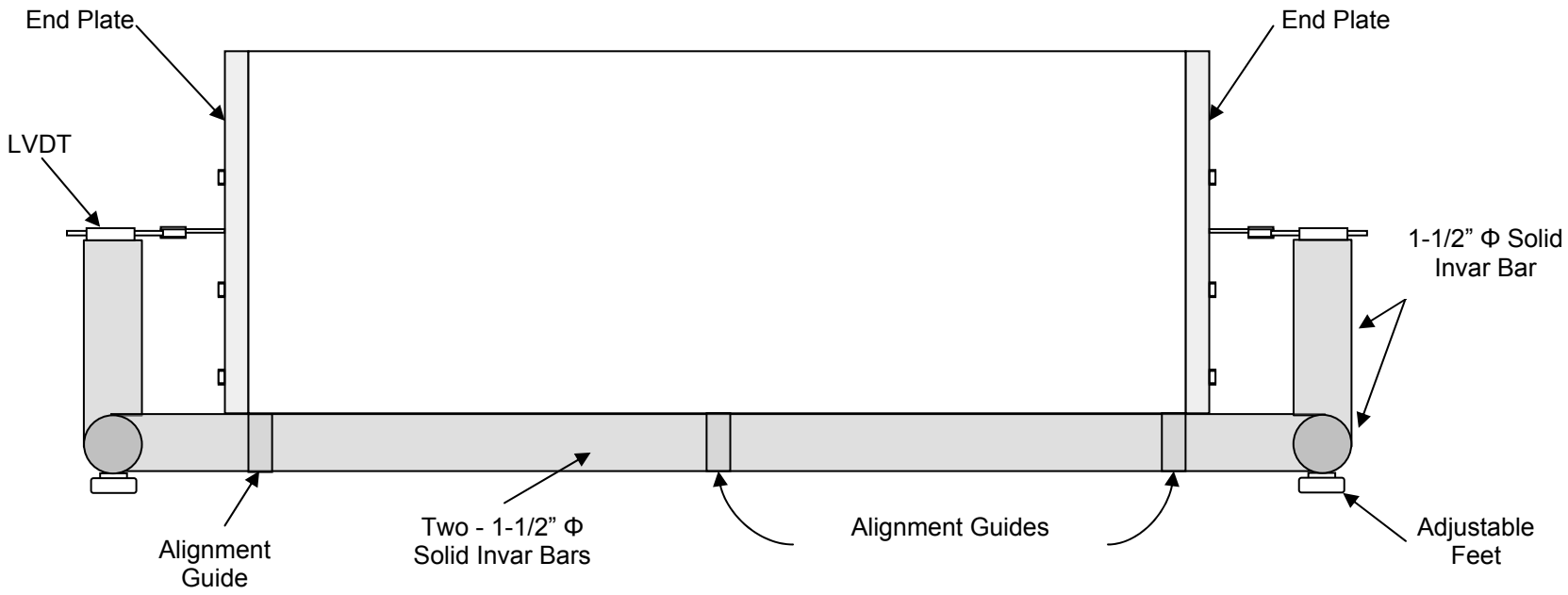

Figure 3-7: Elevation view of free shrinkage frame (Meadows 2007)

3.1.4.2 Free Shrinkage Frame Preparation

The inside of the formwork is lined with an outer layer of plastic sheeting that is taped to the formwork. This layer is used to protect and prevent the concrete from adhering to the formwork. A lubricant (WD40®) is sprayed onto the outer layer of plastic sheeting. Care has to be taken to see that this lubricant is sprayed just prior to the concrete placement in the free shrinkage frame to avoid crumpling of the plastic sheeting caused by drying of the lubricant. An inner layer of plastic sheeting is placed inside the outer layer. Thus, the lubricant is between the two layers of plastic sheeting. The inner layer of plastic is not taped to the formwork, because this could restrain the movement of the concrete specimen; the inner layer is folded over the concrete after placement. Therefore, the concrete prism is completely sealed by the inner layer of plastic, yet able to move freely inside the formwork.

3.1.4.3 Free Shrinkage Frame Test Method

The fresh concrete is placed into the free shrinkage frame formwork in two lifts. Each lift is vibrated to ensure proper consolidation. Care has to be taken to see that the LVDT rods are not disturbed/damaged while using the vibrator. The concrete surface is finished using a wooden trowel. The inner layer of plastic sheeting is folded over the top of the fresh concrete and a layer of plastic is secured to the formwork over the concrete to prevent moisture loss. All edges of the plastic are sealed with adhesive aluminum foil tape. The thermally insulated lid is then secured to the formwork. Two temperature probes are embedded into the concrete via holes through the lid. The LVDTs are securely fastened to the Invar rods and the supporting steel frame. Quick disconnect hoses are

fastened to the formwork and circulator so that concrete in the free shrinkage frame can be temperature controlled. The free shrinkage frame ready for testing is shown in Figure 3-8. After the concrete has reached initial set, the inner plate is backed away to allow measurement of expansion and contraction of the prism.

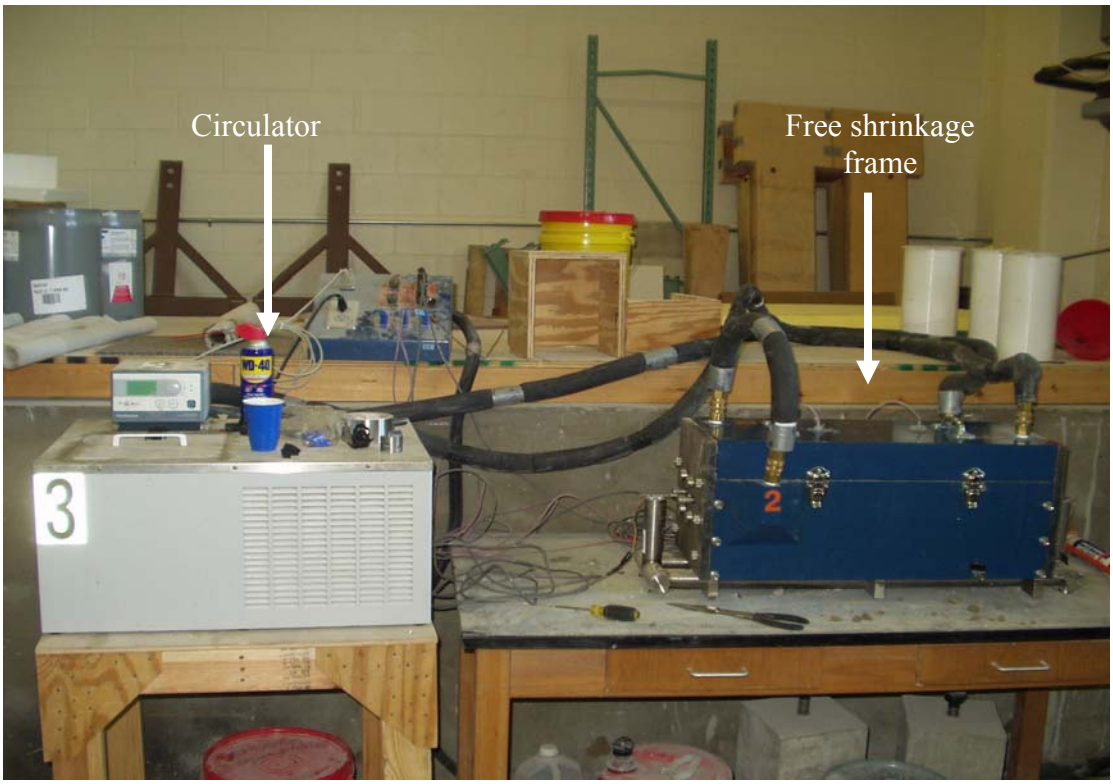

Figure 3-8: Free shrinkage frame ready for testing

3.1.5 CYLINDER MATCH-CURING SYSTEM

A match-curing system was required to condition the temperature of all molded cylinders and the setting test specimen. The cylinders in the match-curing system were subjected to the same temperature profile as the match-cured cracking frame and the free shrinkage frame. The match-curing box is as shown in Figure 3-9.

Figure 3-9: Match-curing system

3.1.6 SETTING TEST

A setting test box, as shown in Figure 3-10, was prepared to hold a 7 ½ x 6 in. cylindrical can. This box was set next to the free shrinkage frame, and the circulator hoses from the free shrinkage frame were connected to this box, such that the free shrinkage frame with its circulator and the setting test box acted as one unit and went through the same temperature profile (either match-cured or isothermal). The setting test can was periodically removed from the box, so as to determine the initial set of the concrete, at which time the inner plates of the free shrinkage frame were backed away to allow measurement of expansion and contraction of the concrete prism. After this, the setting test was continued until the final set was reached.

Figure 3-10: Setting test box construction

3.1.7 DATA ACQUISITION

The data acquisition system is similar to the system used by Meadows (2007), except that instead of testing two cracking frames simultaneously, only one of the frames was activated using the system. No changes had to be made to the datalogger program to incorporate the new testing program.

3.2 CONCRETE MIXTURES EVALUATED

The laboratory testing program was designed to evaluate the effects of placement temperature, ambient temperature, cementitious materials, and aggregate type on the

cracking tendency of concrete mixtures. Table 3-1 outlines the laboratory testing program used to test these variables. Table 3-2 outlines the mixture proportions of each concrete mixture. All the concrete mixtures had a water-to-cementitious materials ratio (w/cm) of 0.44.

In order to systematically evaluate the effects of concrete constituents and temperature on the cracking sensitivity of a mixture, a control mixture was established for comparison purposes. The control mixture, identified by I-CTRL, consists of standard Type I Portland cement, water-to-cement ratio of 0.44, with No. 67 siliceous river gravel. The placement temperature and ambient temperature conditions were varied to study the effects of seasonal changes.

Table 3-1: Laboratory Testing Program

Mix ID	Mixture	Placement Temperature	Ambient Temperature	Aggregate Type
I-CTRL	Type I Portland Cement	50 °F 73 °F 95 °F	50 °F 73 °F 95 °F	No.67 Silicious River Gravel
I-30C	70% Type I + 30% Class C Fly ash	95 °F	95 °F	
I-20F	80% Type I + 20% Class F Fly ash	95 °F	95 °F	
I-50S	50% Type I + 50% GGBF Slag	95 °F	95 °F	
I-LS	Type I Portland Cement	73 °F 95 °F	73 °F 95 °F	No.67 Dolomitic Limestone

Table 3-2: Concrete Mixture Proportions

Mix ID	Water (pcy)	Type I cement (pcy)	Class F Fly Ash (pcy)	Class C Fly Ash (pcy)	GGBF Slag (pcy)	Coarse Aggregate (pcy)	Fine Aggregate (pcy)	Pozzolith 200N (oz./cwt)	Target slump (inches)	Total Air Content (%)	w/cm
I-CTRL	273	620	--	--	--	1950	1149	6	4	2	0.44
I-30C	273	434	--	186	--	1854	1213	6	4	2	0.44
I-20F	273	496	124	--	--	1854	1208	6	4	2	0.44
I-50S	273	310	--	--	310	1854	1223	6	4	2	0.44
I-LS	273	620	--	--	--	1950	1217	6	4	2	0.44

These changes are denoted by the Batch ID. For example, the following notation will be used to present and discuss the control mix.

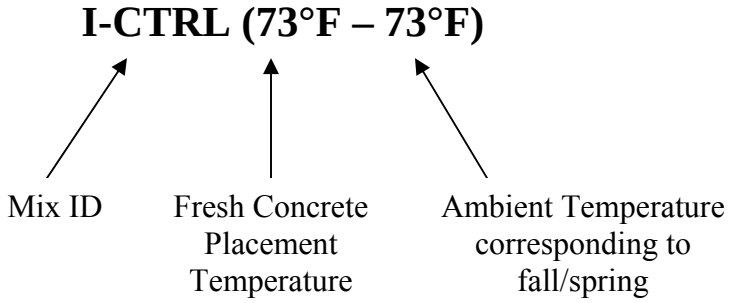

In the above mixes, supplementary cementing materials were also used as a replacement in the control mixture. The replacement percentages were 30% for Class C fly ash, 20% for Class F fly ash and 50% GGBF Slag, because they reflect the upper limit of dosages permitted by the Alabama Department of Transportation.

3.3 EXPERIMENTAL PROCEDURES

The experimental procedure outlined in Meadows (2007) was closely followed. All concrete mixing for this project was performed in an air-conditioned room. The raw materials used in the production of the concrete batches were also stored in the air-conditioned laboratory. Portland cement was stored in standard 94-lb sacks while the supplementary cementing materials were stored in sealed 5-gallon buckets or sealed 55-gallon drums. The coarse and fine aggregates were stored in sealed 55-gallon drums and placed in the air-conditioned laboratory. These aggregates were replenished time-to-time from large stockpiles stored outdoors at the Sherman Concrete Co. plant in Auburn, Alabama.

3.3.1 BATCHING

Moisture corrections were conducted using a small digital scale and a hot plate. After the moisture content of the aggregates was determined, the materials were placed in 5-gallon buckets with lids to prevent any moisture loss.

To produce concrete with a cold or hot placement temperature, the raw materials were placed in an environmental chamber for at least 48 hours prior to mixing. To produce concrete with placement temperatures of 50 °F or 95 °F, the environmental chamber was set to corresponding temperatures. To produce concrete at room temperature (approximately 73 °F), the raw materials were placed in the air-conditioned concrete laboratory for at least 24 hours prior to mixing.

3.3.2 MIXING PROCEDURE

Just prior to mixing each batch, the concrete mixer was "buttered" using cement, sand, and water to produce a mortar to coat the inside of the mixer. Once this mortar was removed, the raw materials were added. Approximately one third of the aggregates were then placed in the mixer, alternating rock and sand to ensure proper mixing. Then, one third of the cement and water was added. The materials were allowed to mix thoroughly before the next one third of the materials was added. This process was continued until all materials were added to the concrete mixer. Once all materials were placed in the mixer, the concrete was allowed to mix for five minutes to ensure thorough mixing of all constituents.

3.3.3 FRESH CONCRETE TESTING

After completion of mixing, the following fresh concrete properties were tested:

- Slump according to ASTM C 143 (2003),
- Unit weight according to ASTM C 138 (2001),
- Air content according to ASTM C 231 (2004),
- Fresh concrete temperature according to ASTM C 1064 (2004), and
- Setting times according to ASTM C 403 (1999).

3.3.4 HARDENED CONCRETE TESTING

Hardened concrete properties were evaluated using the following test methods:

- Compressive strength according to ASTM C 39 (2003),

- Static modulus of elasticity according to ASTM C 469 (2002),
- Splitting-tensile strength according to ASTM C 496 (2004), and
- Drying shrinkage according to ASTM C 157 (2004).
- Test ages for compressive strength, modulus of elasticity and split-tensile strength were 12 hours, 1 day, 2 day, 3 day, 7 day and 28 days.
- The drying shrinkage specimens were 6 x 6 x 12 in. prisms and were demolded 24 hours after they were cast. The specimens were then placed in a lime-saturated bath for seven days, including the period in the molds, in accordance with ASTM C 157. After curing, the specimens were placed in a temperature-and humidity-controlled room and readings were taken for up to 64 weeks.

3.4 MATERIALS

To determine the effect of aggregate type and supplementary cementing materials on the cracking sensitivity of concrete mixtures, several different raw materials were used to produce concrete. The following sections provide a detailed discussion of the cement type, supplementary cementing materials, aggregates, and chemical admixtures used to produce the concrete mixtures outlined in Table 3-2.

3.4.1 CEMENT TYPE

Type I portland cement, manufactured by Lafarge North America in Calera, Alabama was used in all the concrete mixtures. The result of the chemical analysis and fineness for the cement is shown in Table 3-3.

3.4.2 SUPPLEMENTARY CEMENTING MATERIALS

In order to evaluate the effects of SCMs on the cracking sensitivity of a concrete mixture, three different types of SCMs were used:

- Class C fly ash – distributed by Holcim Ltd. in Quinton, Alabama,
- Class F fly ash – distributed by Boral Materials in Cartersville, Alabama, and
- Grade 120 GGBF Slag – distributed by Buzzi Unicem in New Orleans, Louisiana

The chemical compositions of the SCMs as provided by the companies are shown in Table 3-4.

Table 3-3: Properties of the portland cement

Parameter	Value
Silicon dioxide, SiO_2 (%)	21.06
Aluminum oxide, Al_2O_3 (%)	4.82
Iron oxide, Fe_2O_3 (%)	3.07
Calcium oxide, CaO (%)	63.06
Magnesium oxide, MgO (%)	3.39
Alkalies ($Na_2O + 0.658K_2O$) (%)	0.56
Sulfur trioxide, SO_3 (%)	2.91
Loss on ignition, LOI (%)	0.85
Tricalcium silicate, C_3S (%)	51.63
Dicalcium silicate, C_2S (%)	21.42
Tricalcium aluminate, C_3A (%)	7.58
Tetracalcium aluminoferrite, C_4AF (%)	9.34
Blaine fineness (m^2/kg)	350

3.4.3 COARSE AGGREGATE

Two types of coarse aggregates were used in this project viz. Silicious river gravel and Dolomitic limestone. The No. 67 River Gravel was obtained from Martin Marietta Materials, Shorter, Alabama. The No. 67 Dolomitic limestone was obtained from Vulcan

Table 3-4: Chemical properties of supplementary cementing materials

Parameter	Class C fly ash	Class F fly ash	GGBF Slag
Silicon dioxide, SiO_2 (%)	36.09	51.86	38.63
Aluminum oxide, Al_2O_3 (%)	18.05	24.62	9.16
Iron oxide, Fe_2O_3 (%)	6.42	4.04	0.54
Calcium oxide, CaO (%)	25.20	13.38	35.84
Magnesium oxide, MgO (%)	5.73	2.10	13.01
Alkalies ($Na_2O + 0.658K_2O$) (%)	2.19	0.92	0.57
Sulfur trioxide, SO_3 (%)	2.30	0.44	0.19
Loss on ignition, LOI (%)	0.40	0.43	0.48
Bulk specific gravity	2.63	2.34	2.91

Materials, Calera, Alabama. These aggregates were trucked to the Twin City Concrete mix plant in Auburn and were subsequently used. The aggregates were sampled and tested to determine the gradation, bulk specific gravity, and absorption capacity. The No. 67 river gravel and the No. 67 limestone were found to be in accordance with gradation requirements of ASTM C 33 (2003). The gradation of these aggregates can be found in Figures 3-11 and 3-12. The bulk specific gravity and absorption capacity for each aggregate type can be found in Table 3-5.

Table 3-5: Aggregate specific gravity and absorption capacity

Material	Bulk Specific Gravity (SSD)	Absorption Capacity (%)
Siliceous River Gravel	2.634	0.52
Dolomitic Limestone	2.730	0.99
Siliceous River Sand	2.608	0.41

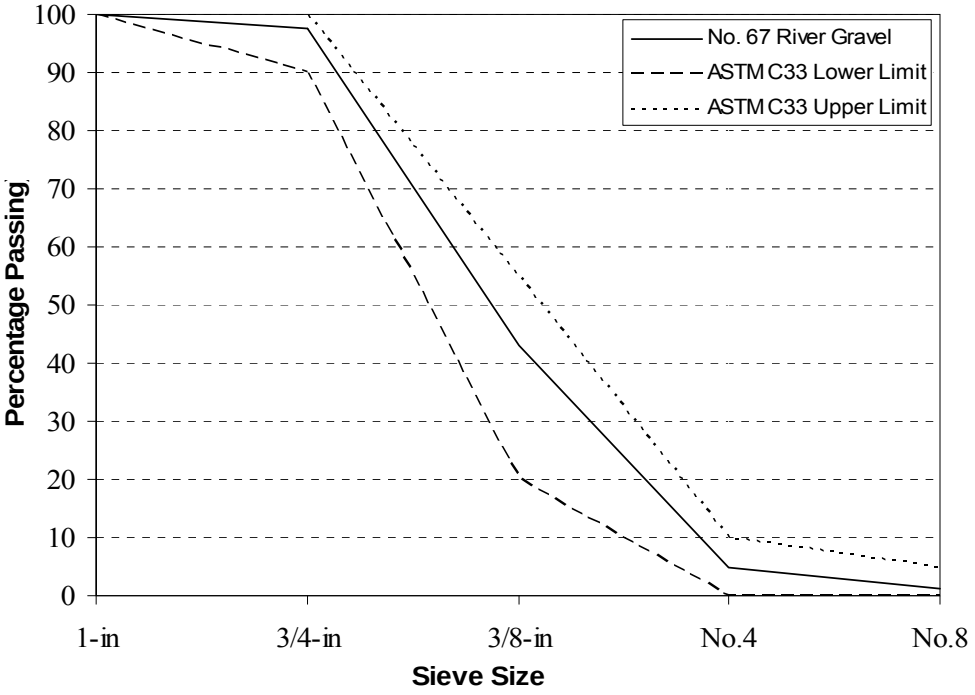

Figure 3-11: No. 67 siliceous river gravel gradation

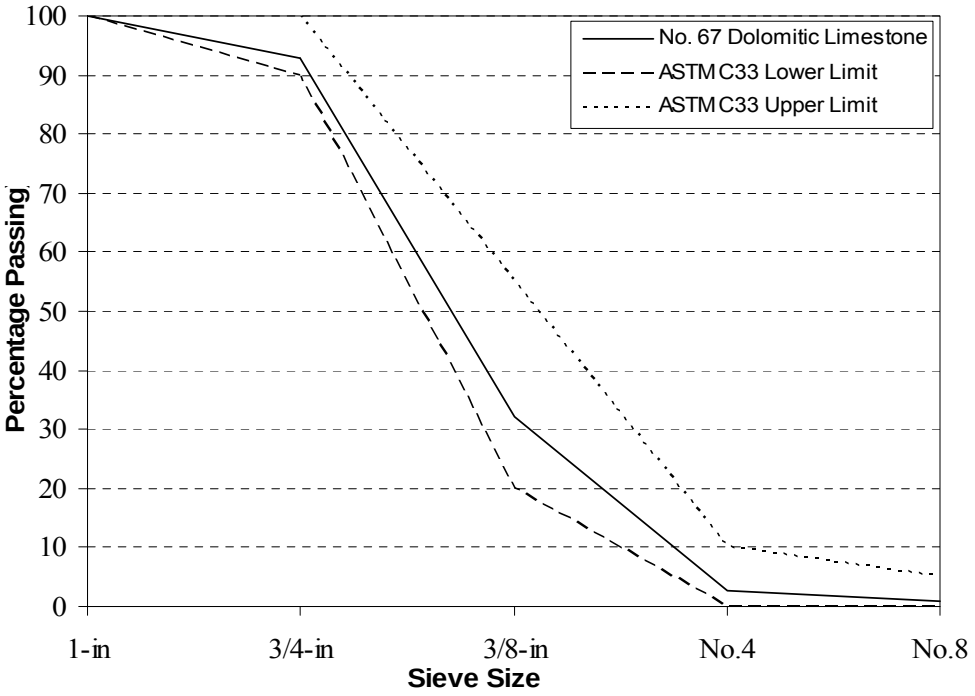

Figure 3-12: No. 67 Dolomitic limestone gradation

3.4.4 FINE AGGREGATE

The fine aggregate used throughout this project was siliceous river sand provided by Martin Marietta Materials, Shorter, Alabama. The fine aggregate was sampled, and the gradation, bulk specific gravity, and absorption capacity were determined. The fine aggregate was found to satisfy the gradation requirements of ASTM C33 (2003). The gradation of the sand is given in Figure 3-13. The bulk specific gravity and absorption capacity are shown in Table 3-5.

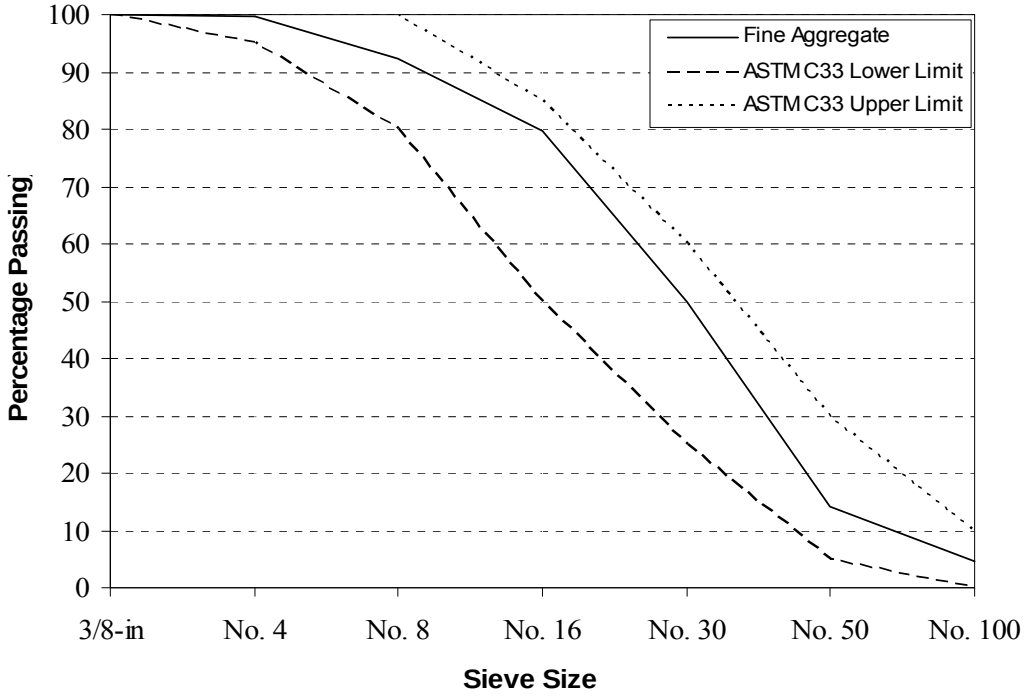

Figure 3-13: Fine aggregate gradation

3.4.5 CHEMICAL ADMIXTURE

The chemical admixture used throughout this project was obtained from BASF Admixtures Inc, Ohio. The admixture mixture proportions can be found in Table 3-2.

Pozzolith 200 N, a mid-range water reducer, was used in all the concrete mixtures. This admixture meets ASTM C 494/C 494M requirements for Type A, water-reducing, Type B, retarding, and Type D, water-reducing and retarding admixtures.

CHAPTER 4

PRESENTATION OF RESULTS

The results obtained from the laboratory testing program outlined in Chapter 3 are presented in this chapter. The fresh and hardened concrete properties of each mixture are presented first. The remainder of the chapter focuses on the results obtained from the two rigid cracking frames and the free shrinkage frame. Discussion of these results can be found in Chapter 5. The notation used throughout this chapter is consistent with the notation described in Section 3.2 of Chapter 3.

4.1 FRESH CONCRETE PROPERTIES

As discussed in Chapter 3, several tests were performed on the fresh concrete before placement and cylinder preparation. These tests included slump, unit weight, air content, temperature, and setting. All tests were conducted according to their respective ASTM standard.

In order to produce the desired amount of concrete for testing, three different batches were used. The batch sizes were 5 ft^3 and 6.50 ft^3 for week 1 of testing. The batch size for week 2 was 4.5 ft^3. The fresh concrete properties did not differ very much between the batches of concrete prepared for the two weeks of testing. These properties were found to be within acceptable limits. See Appendix A for actual test values of each batch.

Additionally, the fresh concrete placement temperature of each batch varied from the targeted fresh concrete temperature. However, since ethylene glycol was circulated within the formwork and crosshead, the placement temperature was quickly altered to reach its target temperature. An evaluation of the concrete temperature test data revealed that each mixture reached ±1°C of its target temperature within 2 hours.

4.2 HARDENED CONCRETE PROPERTIES

As previously discussed in Chapter 3, the hardened concrete properties were tested at multiple intervals. A summary of the 7-day and 28-day splitting tensile strength, compressive strength, and modulus of elasticity results for all the mixtures under match-cured conditions are given in Table 4-1. The early-age development graph for each property is presented in Section 4.2.1 for each mixture.

Table 4-1: 7-day and 28-day mechanical properties

Mixture	Splitting Tensile Strength (psi)		Compressive Strength (psi)		Modulus of Elasticity (ksi)	
	7-day	28-day	7-day	28-day	7-day	28-day
I-CTRL (50 °F - 50 °F)	670	700	4900	6300	6220	6780
I-CTRL (73 °F - 73 °F)	570	610	5420	5800	5800	6120
I-CTRL (95 °F - 95 °F)	530	550	5070	5400	5740	6080
I-30C (95 °F - 95 °F)	500	550	5440	5780	5740	6120
I-20F (95 °F - 95 °F)	480	560	5620	6130	5680	6120
I-50S (95 °F - 95 °F)	520	560	5430	5770	5930	6200
I-LS (73 °F - 73 °F)	530	580	5070	5200	5740	6100
I-LS (95 °F - 95 °F)	470	510	4540	5130	5740	5920

4.2.1 EARLY-AGE MECHANICAL PROPERTIES

Early-age mechanical properties are important when studying the cracking tendency of concrete mixtures. The compressive strength of the concrete at early ages has little direct influence; however, the tensile strength and modulus of elasticity are vital components to understanding the cracking tendency of various mixtures.

As discussed in Chapter 2, as the stiffness of the concrete grows, small temperature changes create large tensile stresses if restrained. Once stresses exceed the tensile capacity of the concrete, cracking may occur. This section presents the early-age mechanical behavior of the concrete mixtures outlined in Chapter 3.

4.2.1.1 Control Mixture

As previously discussed in Chapter 2, the curing temperature of the concrete has an effect on the rate of development of early-age mechanical properties. The mechanical properties test results of the control mixture are shown in Figure 4-1, which illustrates the effect of temperature. Compressive strength development for the 50 °F-50 °F mixture is slow, compared to other two control mixtures. However at later ages, the 50 °F-50 °F mixture has a higher compressive strength. Similar trend is observed in splitting tensile strength and stiffness development. In addition, after 2 days, the 50 °F-50 °F mixture has better splitting tensile strength and stiffness, than the other two control mixtures. The 7-day compressive and tensile strength of the 95 °F-95 °F mixture is reduced compared to the other placement conditions.

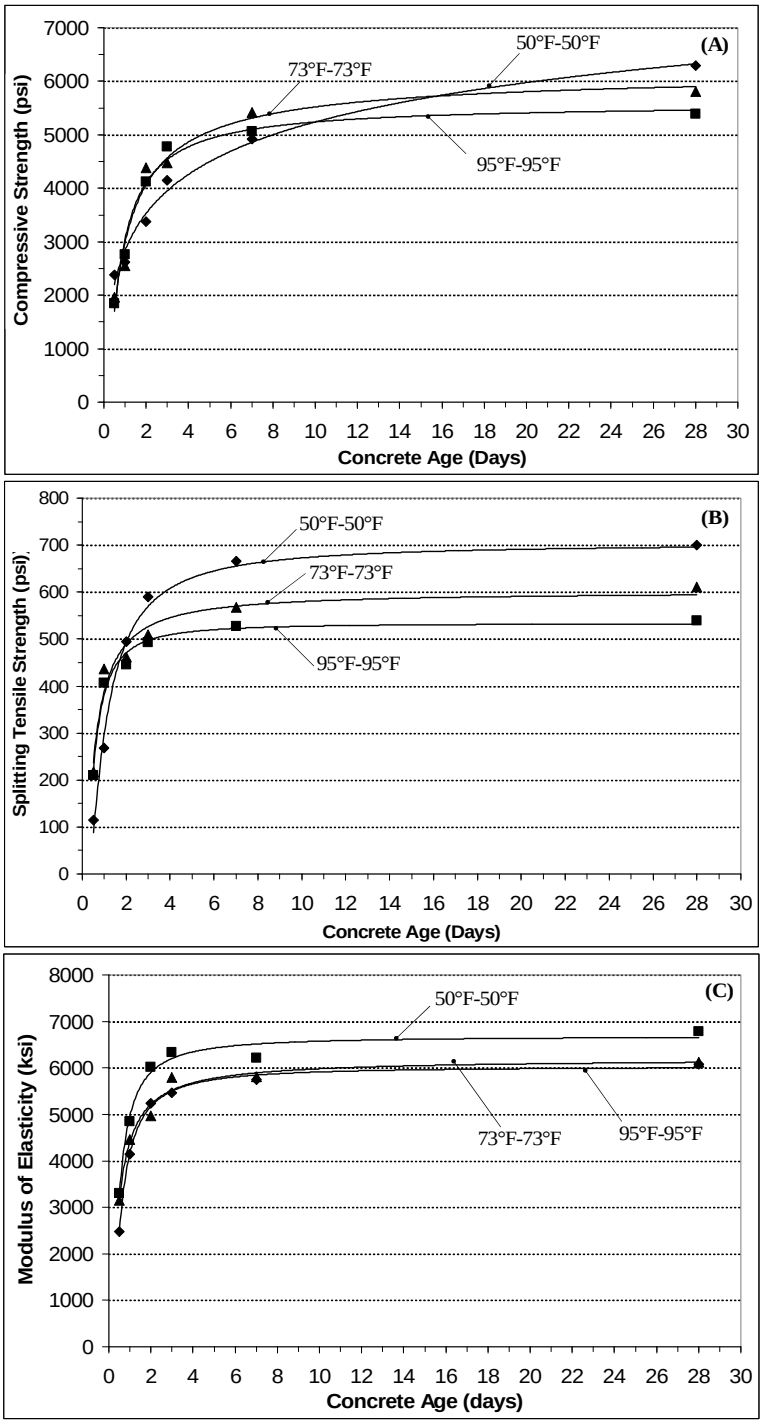

Figure 4-1: Development of early-age mechanical properties of the control mixture (Mix ID = I-CTRL) (A) Compressive strength, (B) tensile strength, and (C) modulus of elasticity

4.2.1.2 SCM Mixtures

The early-age development of mechanical properties for all the SCM mixtures, as compared to the control mixture, when placed at 95 ^{o}F, is presented in Figure 4-2. Supplementary cementing materials such as fly ash and GGBF Slag, slightly increase the compressive strength at 7 days. The fly ash mixtures have lower early-age compressive and splitting tensile strength, and stiffness up to 7 days, compared to the control and slag mixture. The Class C fly ash mixture has very low strength properties at a very early-age of 12-24 hours. This is due to retardation in setting due to high replacement percentage of 30%. The slag mixture had higher strengths and stiffness at early ages, when compared to the fly ash mixtures.

4.2.1.3 Limestone Mixtures

Concrete mixtures using dolomitic limestone were also studied in this work. Mixtures were prepared using only Type I cement, and tested at two different curing conditions. Figure 4-3 illustrates the early-age behavior of the limestone mixture as compared to the control mixture having river gravel. It is seen that the tensile strengths for limestone mixture are comparatively lower than the control mixtures. The modulus of elasticity and compressive strength values for these mixtures are similar as shown in Figure 4-3(A) and 4-3(C).

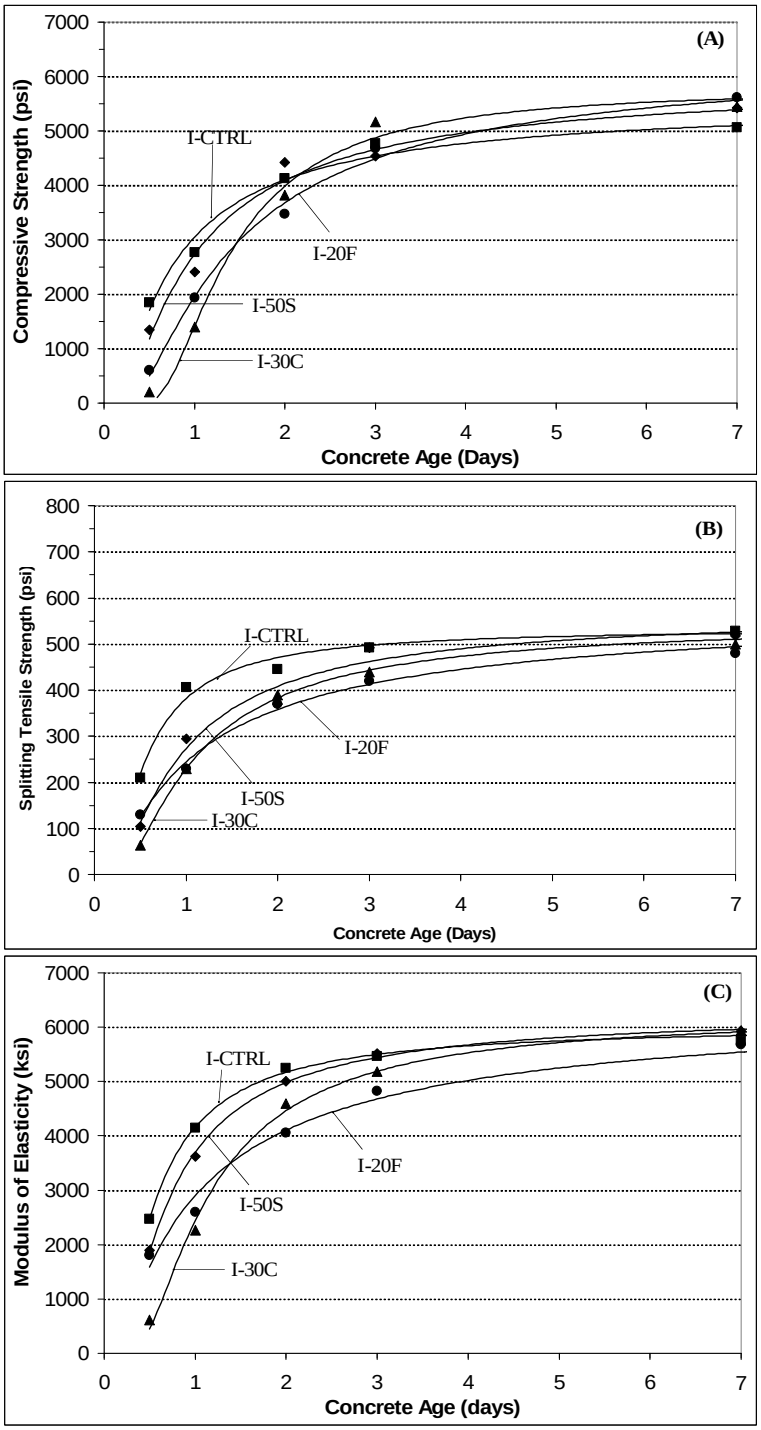

Figure 4-2: Development of early-age mechanical properties (Mix ID = I-CTRL, I-30C, I-20F and I-50S at 95 °F) (A) Compressive strength, (B) tensile strength, and (C) modulus of elasticity

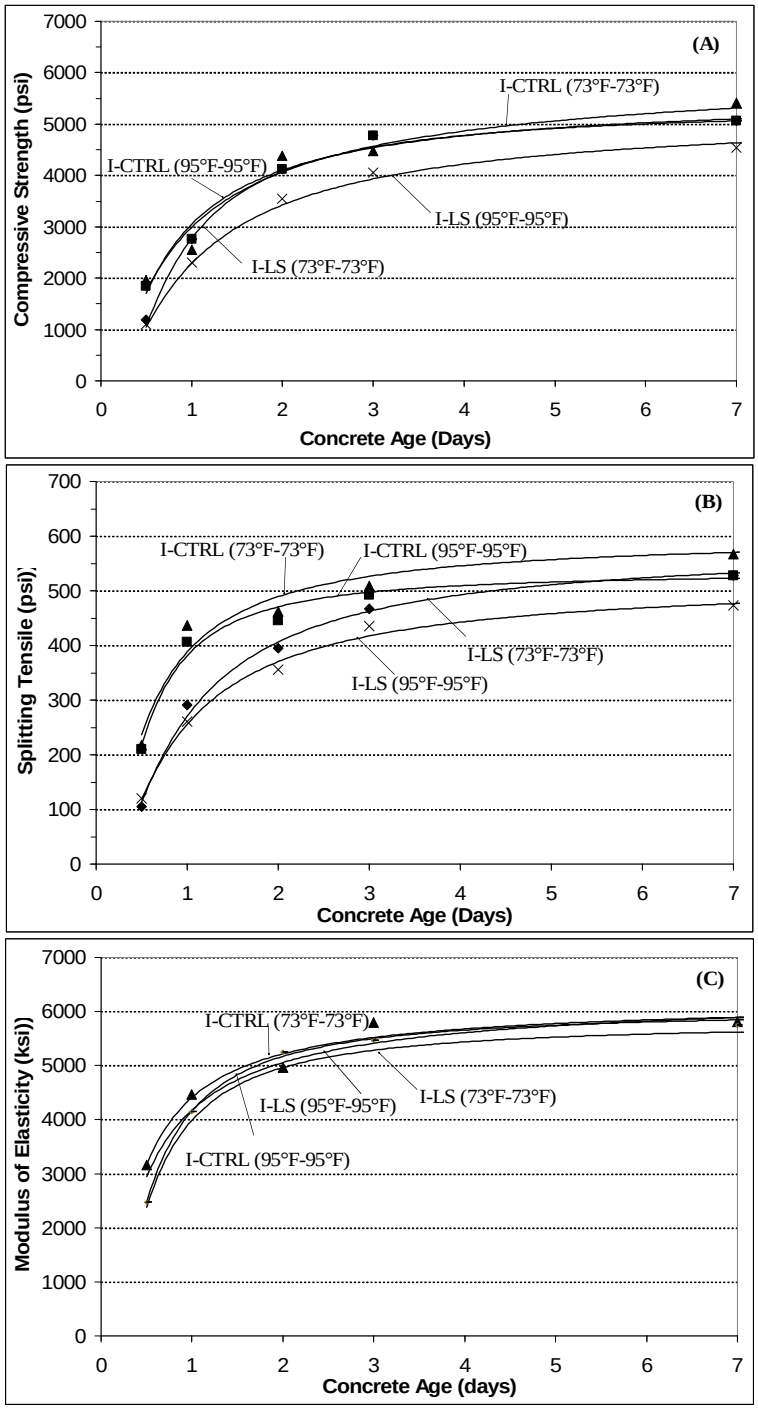

Figure 4-3: Development of early-age mechanical properties (Mix ID = I-CTRL and I-LS at 73 °F and 95 °F) (A) Compressive strength, (B) tensile strength, and (C) modulus of elasticity

4.2.2 DRYING SHRINKAGE

The drying shrinkage results were obtained using procedures outlines in ASTM C 157. The specimens were prepared with the same concrete batch as the rigid cracking frames, but were allowed to hydrate naturally under room conditions instead of being match-cured. The specimens were placed in a moist-curing room and demolded twenty-four hours later. The specimens were placed in a lime-saturated bath for seven days, including the period in the molds, in accordance with ASTM C 157. After curing, the specimens were placed in a temperature and humidity-controlled room and readings were taken for up to 64 weeks.

Since the rigid cracking frames and the free shrinkage frame were sealed, drying shrinkage was eliminated from causing restraint stresses; however, drying shrinkage deformations must be considered when determining the total restraint stresses that may occur in a structure exposed to ambient conditions.

The effect of placement temperature on drying shrinkage of control mixtures is shown in Figure 4-4. The fresh concrete placement temperature did not affect the magnitude of drying shrinkage. All mixtures produced approximately the same magnitude of drying shrinkage at 224 days.

Dolomitic limestone mixtures had similar drying shrinkage magnitudes, to that of control mixtures at both placement temperatures, as shown in Figure 4-5. Hence change in aggregate type does not seem to affect, the drying shrinkage of the control mixture.

Figure 4-5 illustrates the reduction in drying shrinkage when SCMs are applied as mitigation measure for the control of early-age restraint stresses. The use of SCMs had a

substantial effect on the magnitude of drying shrinkage. The Class C fly ash reduced the overall shrinkage much more than the GGBF slag.

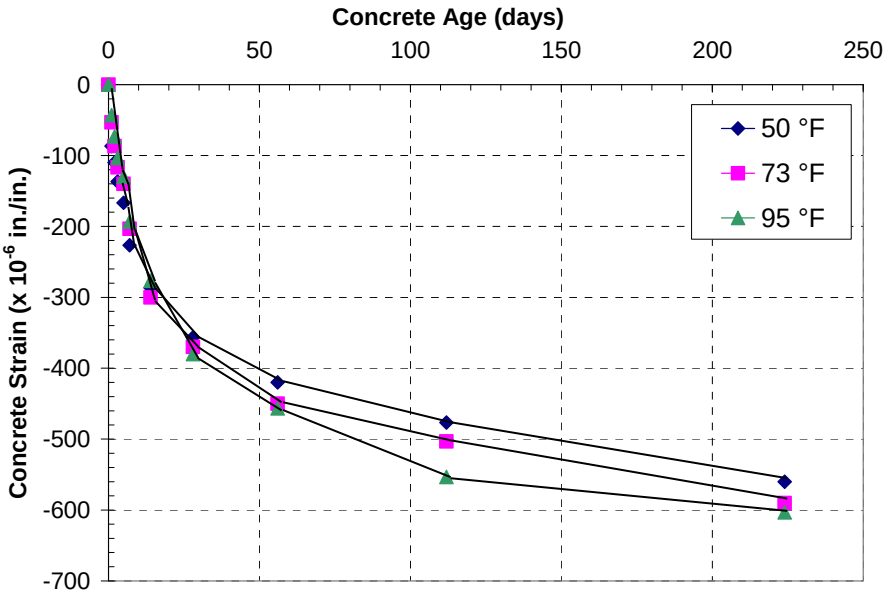

Figure 4-4: Effect of placement temperature of control mixture on drying shrinkage

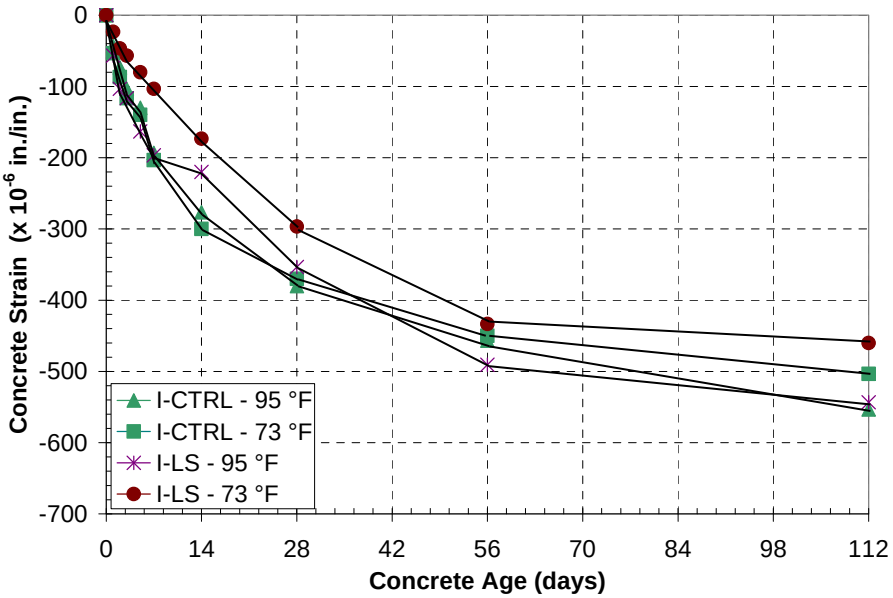

Figure 4-5: Effect of aggregate type on drying shrinkage

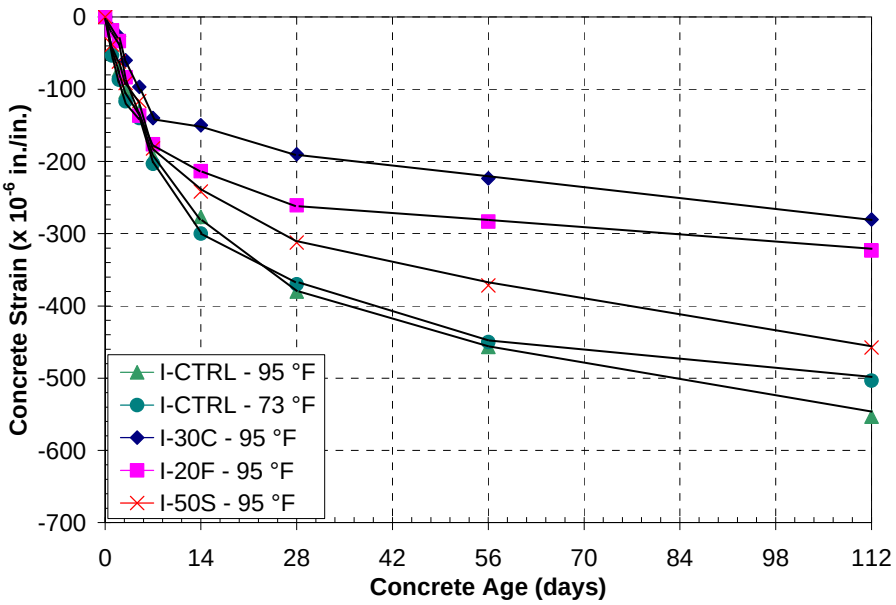

Figure 4-6: Effect of SCMs on drying shrinkage

4.3 RESTRAINED STRESS DEVELOPMENT UNDER MATCH-CURED CONDITIONS

4.3.1 CONTROL MIXTURES

The temperature profile and stress development for the control mixture can be seen in Figures 4-6A and 4-6B, respectively. The control mixture is used as a standard mixture to evaluate how the variables affect the cracking tendency of concrete. By varying the placement and ambient temperature, the effects of temperature with respect to stress development and cracking can be studied. From Figures 4-7A and 4-7B, it is seen that summer conditions cause early-age cracking at an age of 42 hours. However, spring/fall placement delays the cracking to approximately 48 hours. In addition, winter placement delays the cracking further to approximately 75 hours. The fluctuation of stress levels

observed in the initial period (zero to 12 hours) for summer and spring/fall placement is caused due to irregular temperature control in the circulator temperature, which caused the concrete in the cracking frame, to undergo temperature fluctuations. However, for the winter placement conditions, such fluctuations in the circulator temperature did not occur, since the temperature change was gradual.

4.3.2 SCM MIXTURES

The effect of fly ash and GGBF Slag as a replacement for cement was evaluated. These mixtures were only simulated at 95 °F as the placement temperature and ambient condition. The temperature profile and stress development for these mixtures can be found in Figures 4-8A and 4-8B.

It is clear that by using fly ash and GGBF Slag, the maximum temperature reached is decreased. In addition, it is also observed that the use of SCMs significantly increases the time of cracking, which indicates that their use reduces the cracking tendency of the control mixture.

4.3.3 LIMESTONE MIXTURES

The temperature and stress development for the limestone mixtures can be found in Figures 4-9A and 4-9B. These mixtures were simulated at 73 °F and 95 °F as the placement temperature and ambient condition. As the placement and ambient temperatures rise, the mixtures crack later than the control mixture.

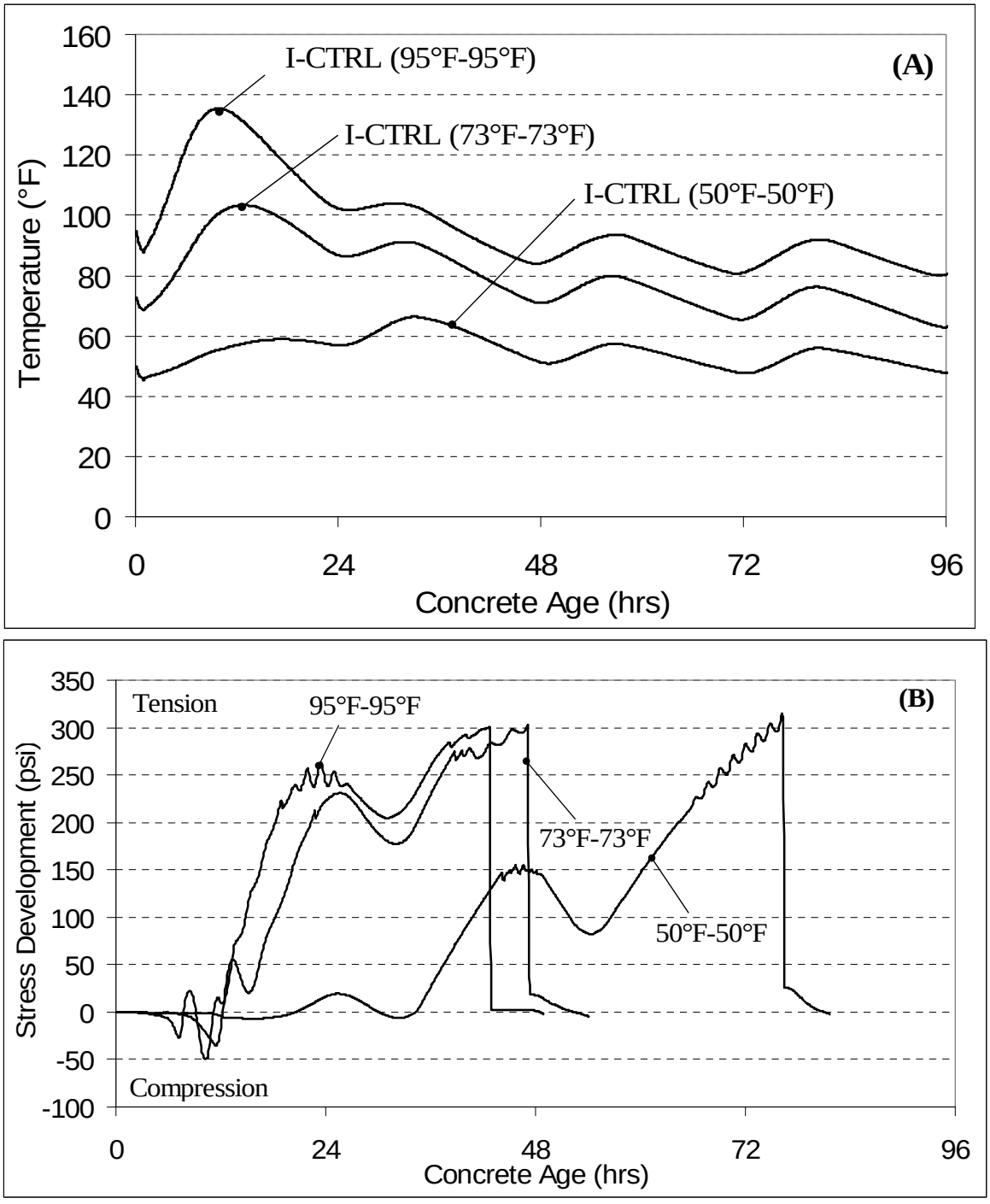

Figure 4-7: Test results for the control mixtures (Mix ID = I-CTRL) (A) Temperature development and (B) stress development

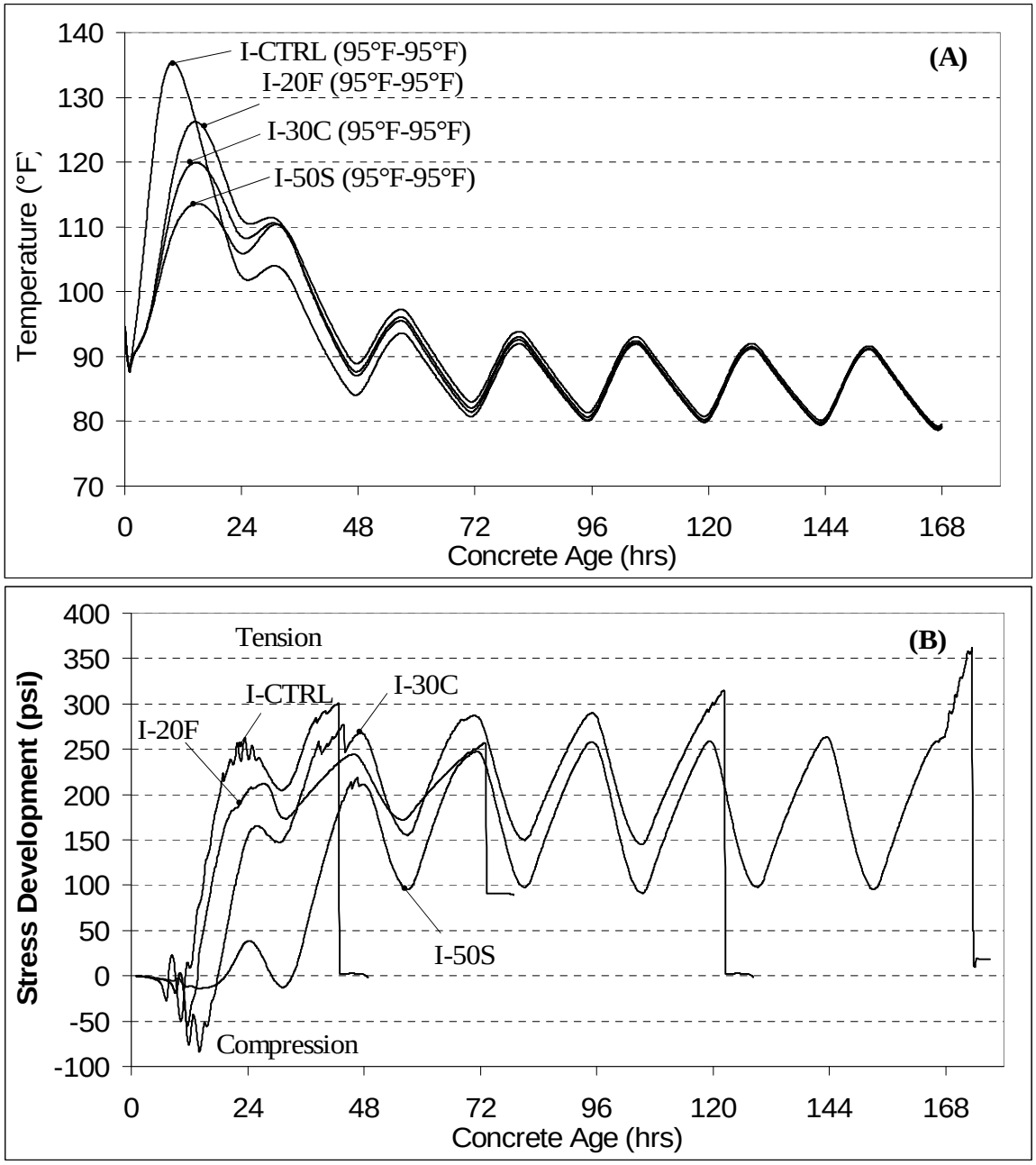

Figure 4-8: Test results for the SCM Mixtures (A) Temperature profile and (B) stress development

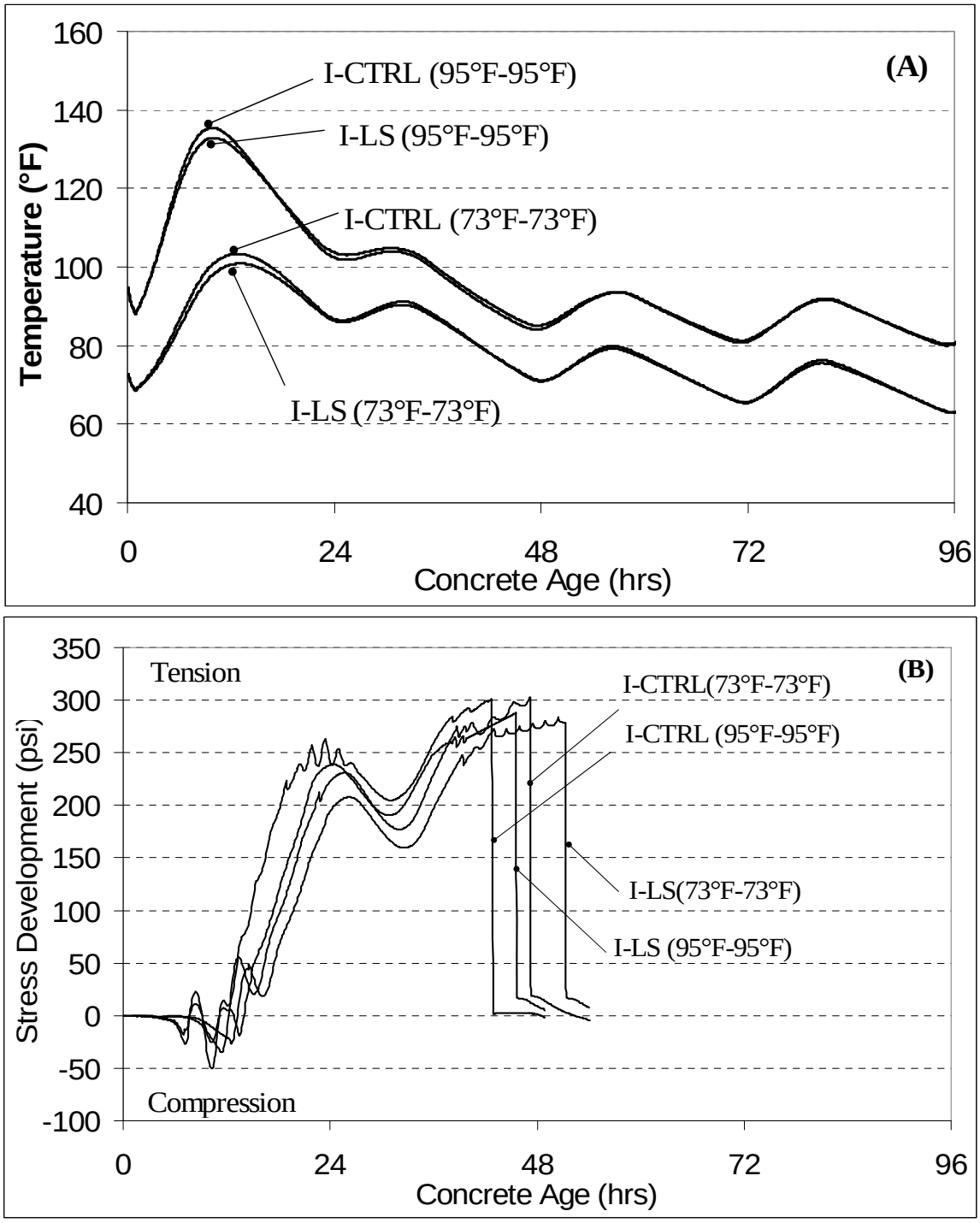

Figure 4-9: Test results for the limestone mixtures (A) Temperature profile and (B) stress development

4.4 FREE DEFORMATION UNDER MATCH-CURED CONDITIONS

The free shrinkage frame is designed to measure the free shrinkage of a concrete specimen i.e. under unrestrained conditions. Negative values indicate contraction and positive values indicate expansion. All shrinkage values start when the concrete reaches initial set. The specimen is match-cured to the same temperature profile as the match-cured rigid cracking frame, as discussed in Chapter 3. Figure 4-10A, 4-10B and 4-10C presents the test results collected, from the match-cured free shrinkage frame, for the control mixture, SCM mixtures and limestone mixtures, respectively. It is observed that SCMs considerably reduce the free shrinkage of the specimen at high-temperature placement conditions. In addition, the control mixtures and the limestone mixtures had quantitatively similar shrinkage.

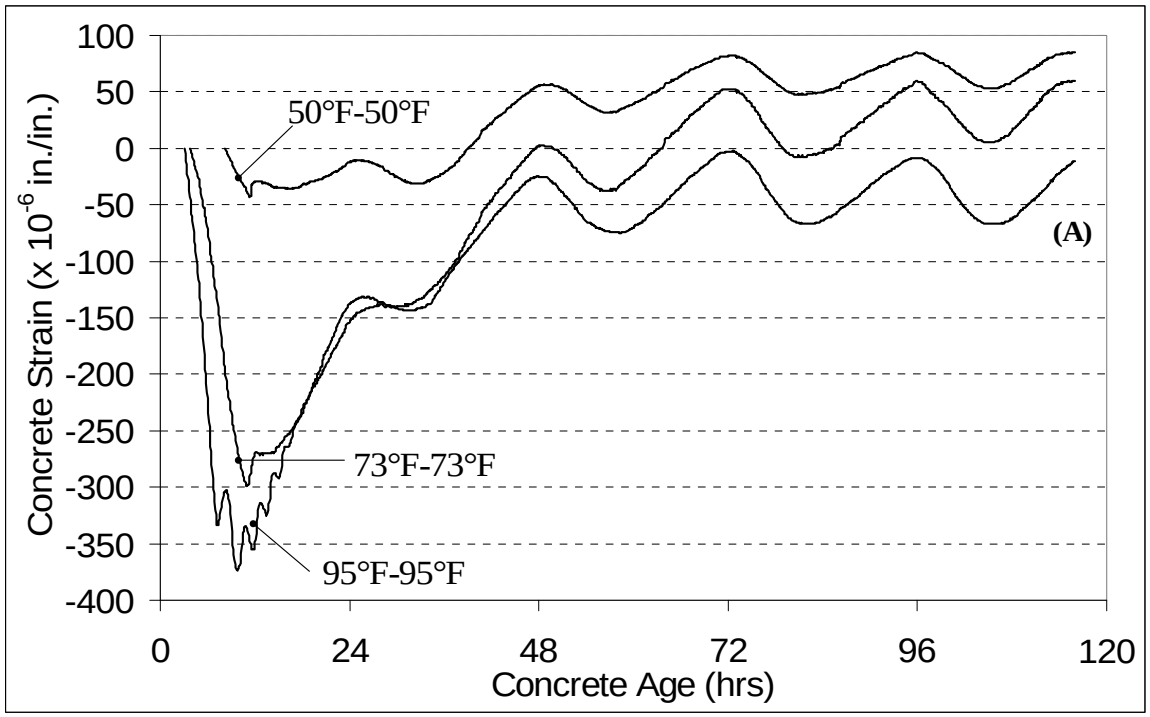

Figure 4-10: Match cured free shrinkage frame results for (A) Control Mixtures

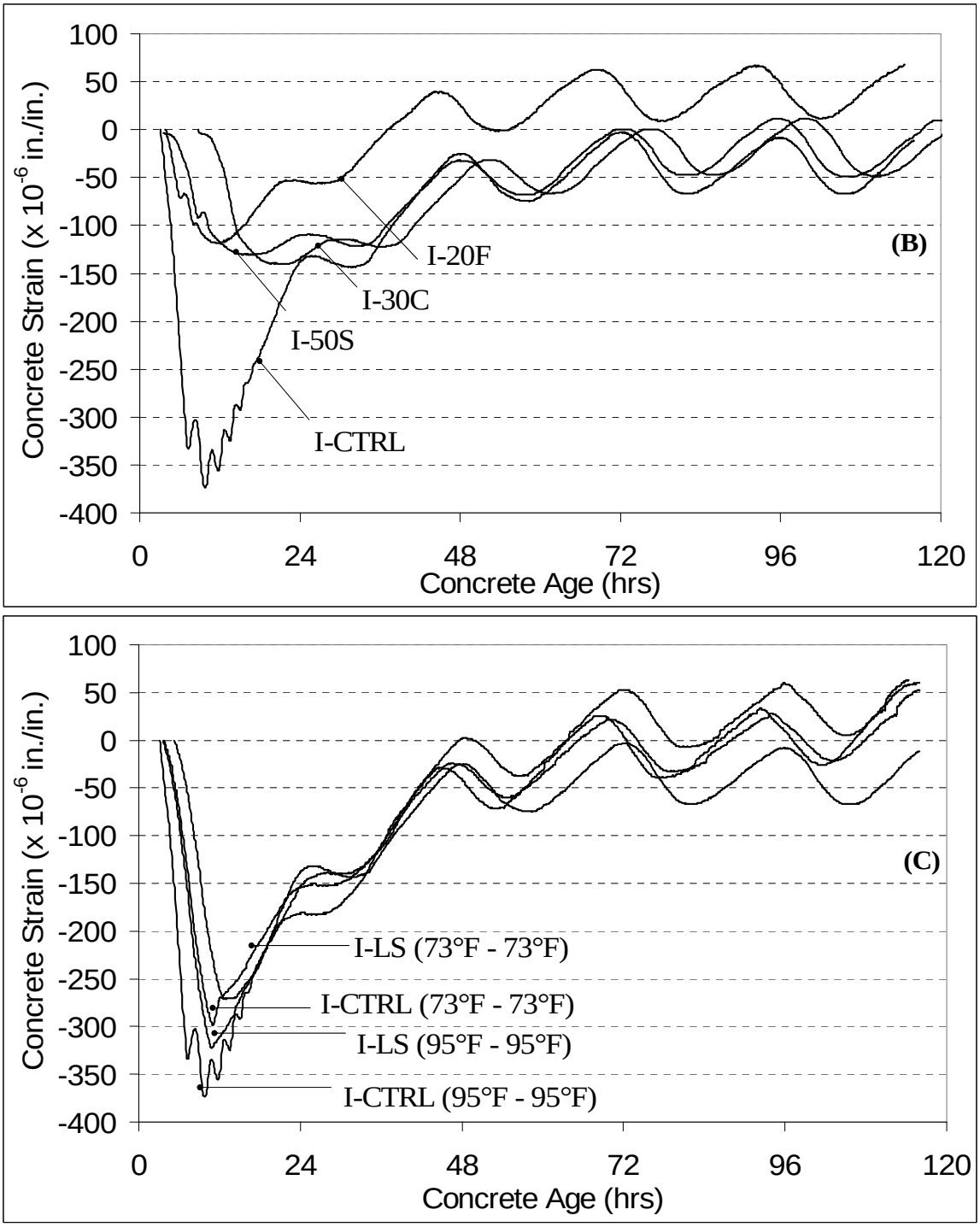

Figure 4-10: Match-cured free shrinkage frame results for (B) SCM mixtures (at 95 ^{o}F)

(C) Limestone mixtures

4.5 RESTRAINED STRESS DEVELOPMENT UNDER ISOTHERMAL CONDITIONS

When the concrete in the rigid cracking frame was cured under isothermal conditions, then it was used to measure the stress development due to only autogenous shrinkage effects. The isothermal rigid cracking frame tests were conducted at three temperatures determined by the target placement temperature of the concrete. These temperatures were 50 °F, 73 °F, and 95 °F. This section presents the results obtained from the isothermal rigid cracking frame. Discussion of the results presented in this section will be provided in Chapter 5.

This section presents the effect of temperature, coarse aggregate type and SCMs on stress development of the isothermal rigid cracking frame.

4.5.1 CONTROL MIXTURE

As discussed in Chapter 3, three temperatures were chosen to conduct the isothermal rigid cracking frame test in order to determine the effect of temperature on autogenous shrinkage. These temperatures reflect seasonal temperatures that may occur during concrete placement. As shown in Figure 4-11, it is observed that the placement temperature has an influence on the overall magnitude of stress development. However, since the w/c ratio for these mixes were relatively high (i.e. 0.44), the autogenous stress values are relatively low and within 50 psi from each other. In addition, the fluctuations in the stresses are due to the irregular temperature control of the circulator.

4.5.2 SCM MIXTURES

As discussed in Sections 4.3.1 and 4.3.2, SCMs improve the early-age cracking resistance of concrete by mitigating temperature development. SCMs also reduce the autogenous stress in the rigid cracking frame, as shown in Figure 4-12, because they reduce the rate of hydration, which in turn reduces the rate of internal relative humidity decrease.

4.5.3 LIMESTONE MIXTURES

The autogenous shrinkage stress values for the control mixture and the limestone mixtures are as shown in Figure 4-13. Not much of a difference in the value of autogenous stress is observed between the control and limestone mixtures at the end of 7 days. However, limestone mixtures develop autogenous stresses at a slower rate than the control mixtures.

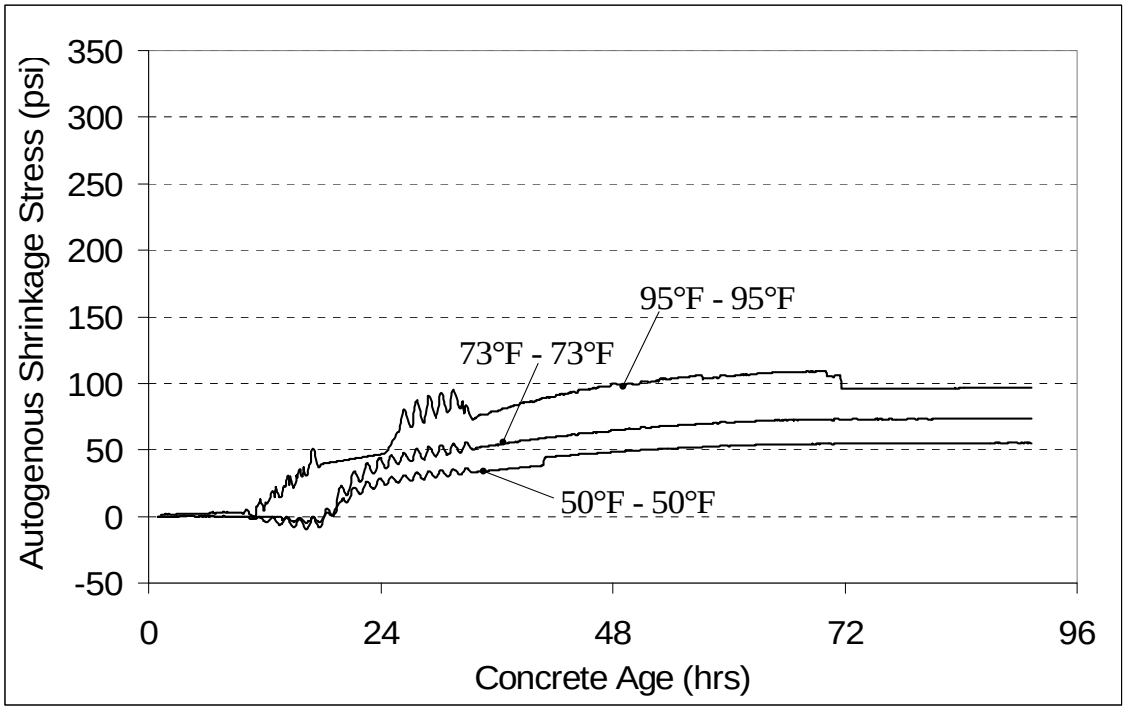

Figure 4-11: Autogenous shrinkage stress results for the control mixtures (I-CTRL)

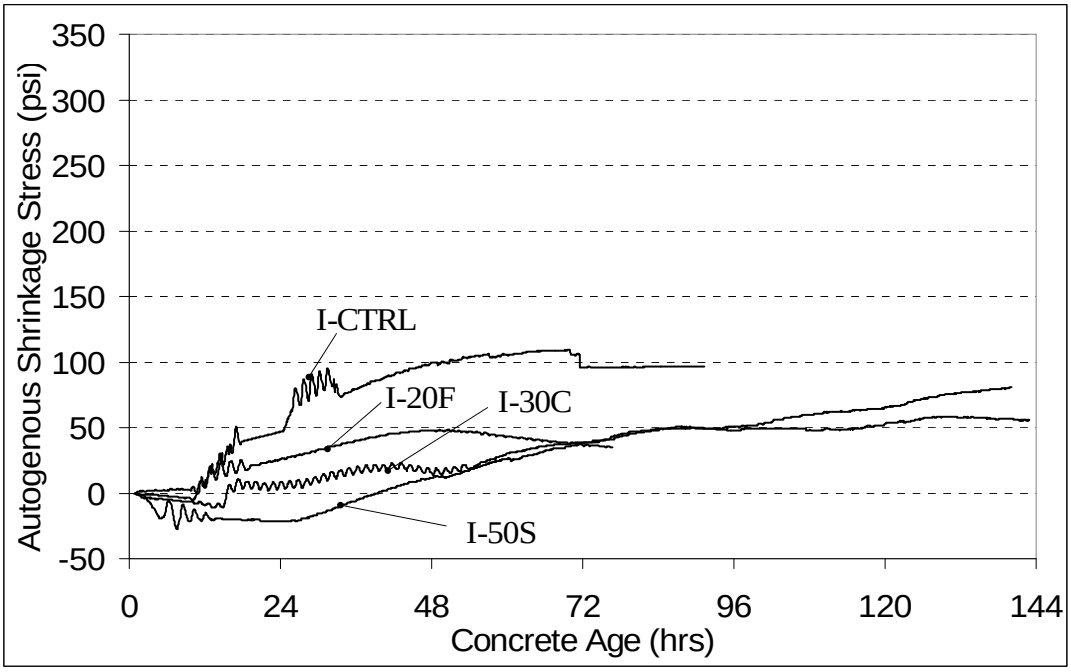

Figure 4-12: Autogenous shrinkage stress results for the SCM mixtures (Mix ID = I-CTRL, I-30C, I-20F, and I-50S) at 95 °F

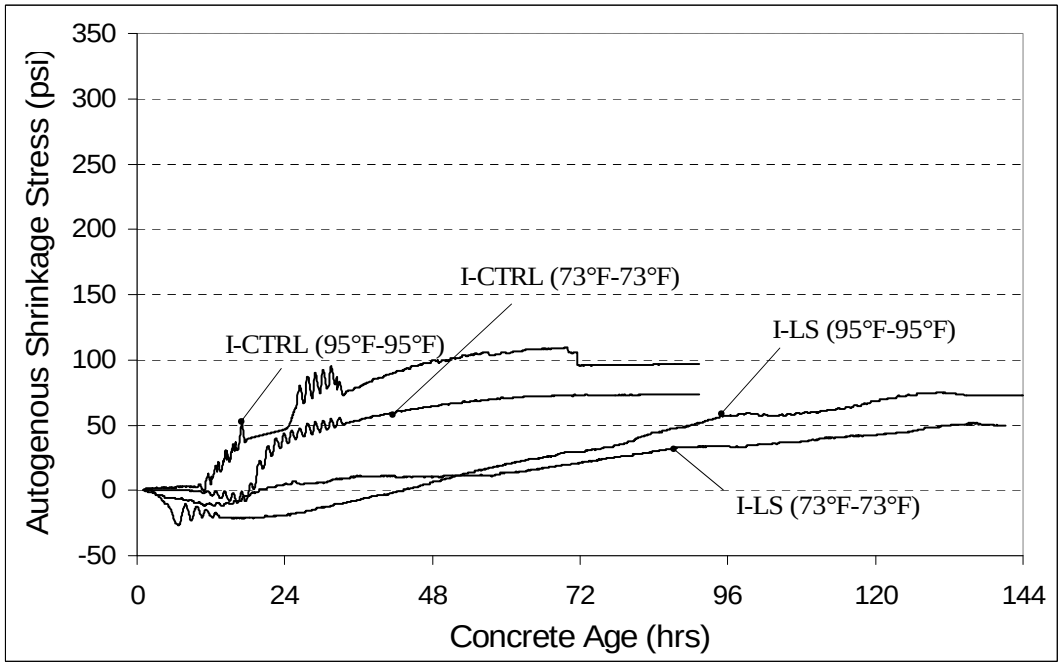

Figure 4-13: Autogenous shrinkage stress results for the control mixtures (I-CTRL) and limestone mixtures (I-LS) at 73 °F and 95 °F

4.6 FREE DEFORMATION UNDER ISOTHERMAL CONDITIONS

In addition to the testing program described in Meadows (2007), in this study, the free shrinkage frame specimens were also tested under isothermal conditions whenever the cracking frame test was performed under isothermal conditions. This allowed the assessment of autogenous shrinkage development of the concrete mixtures. Figure 4-14A, 4-14B and 4-14C shows the results of the isothermal free shrinkage frame for control, SCMs and limestone mixtures respectively. Reduction in the autogenous shrinkage, with placement temperature, was observed for control mixtures. In addition, for limestone mixtures, the magnitude of the autogenous shrinkage was similar to the control mixtures. However, it may be seen that SCMs have a beneficial effect of reducing the autogenous shrinkage strain. However, all the autogenous strain magnitudes are small, since all these concrete mixtures have a relatively high w/c ratio of 0.44.

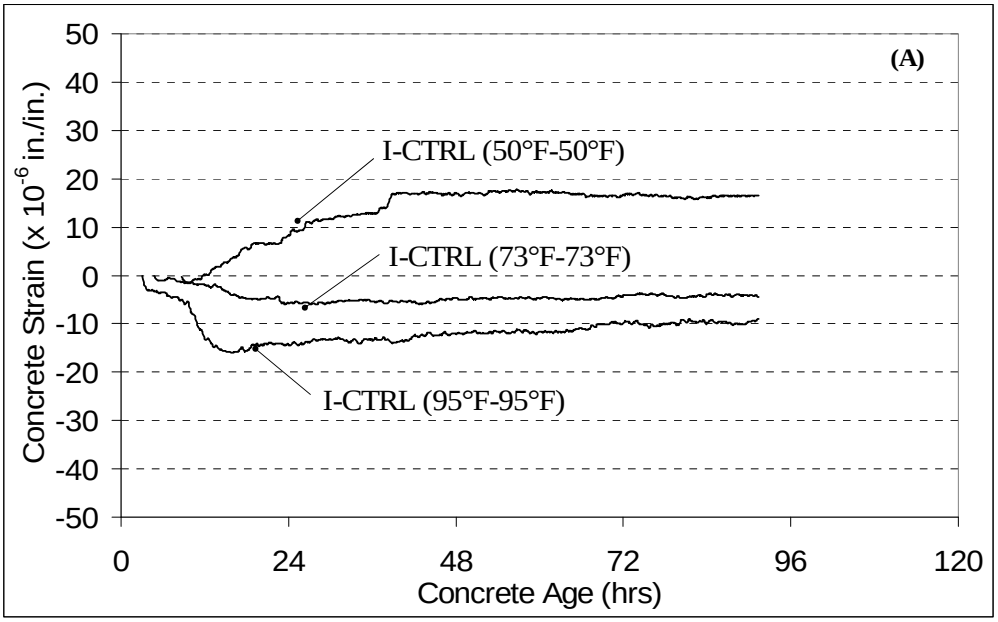

Figure 4-14: Autogenous shrinkage results for the (A) Control mixture (I-CTRL) using the isothermal free shrinkage frame

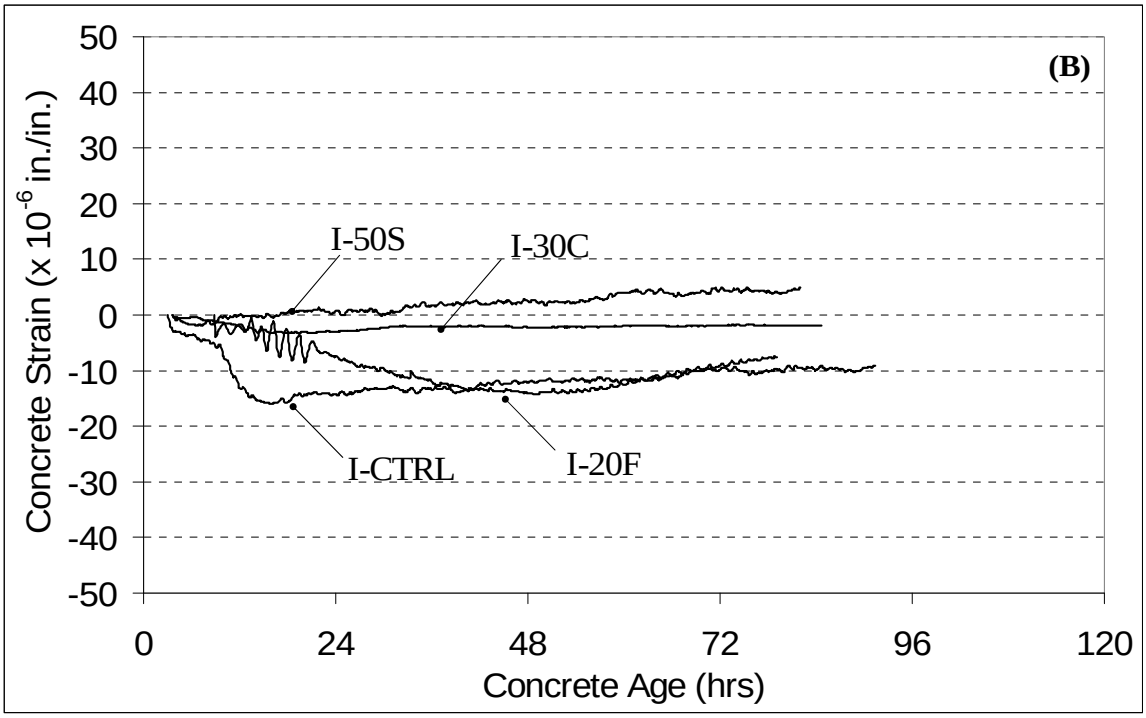

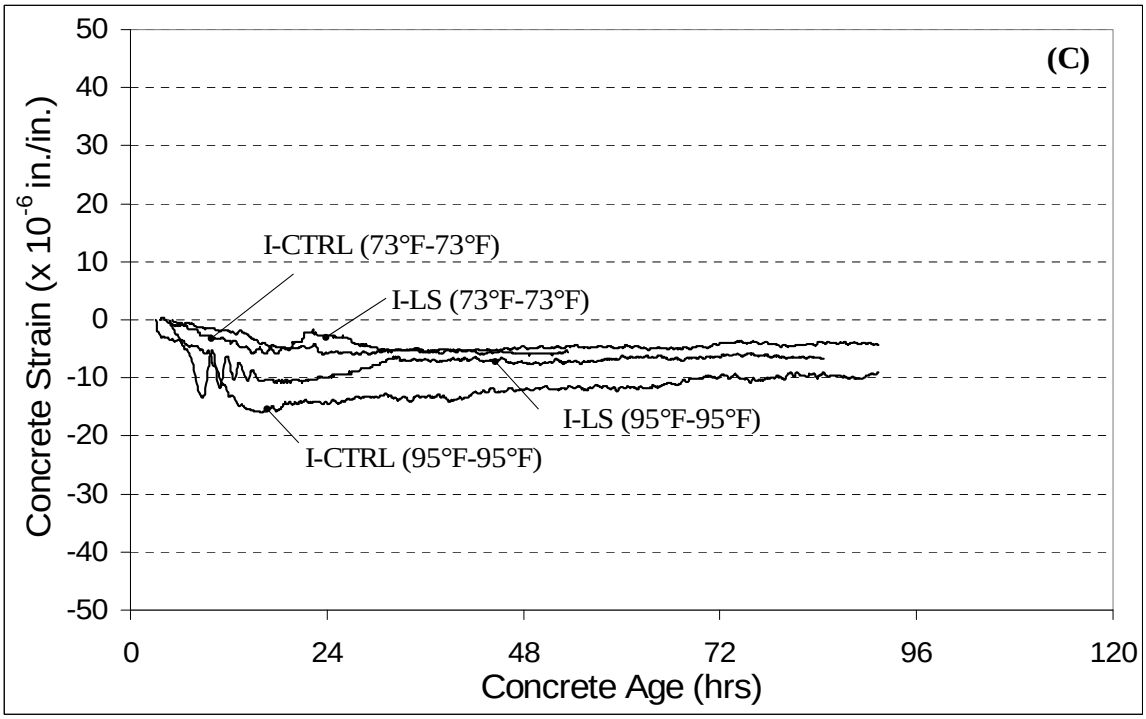

Figure 4-14: Autogenous shrinkage results for (B) SCM mixtures and (C) limestone mixtures using the isothermal free shrinkage frame

CHAPTER 5

DISCUSSION OF RESULTS

The results presented in Chapter 4 are discussed in this chapter. The effects of placement temperature, supplementary cementitious material types and coarse aggregate types on the cracking tendency of concrete mixtures are discussed. The notation used throughout this chapter is consistent with the notation described in Section 3.2 of Chapter 3.

5.1 DETERMINATION OF STRESS-TO-STRENGTH RATIOS

To better understand the cracking sensitivity of the concrete mixtures evaluated in this study, stress-to-strength ratios have been calculated for each mixture. To obtain the stress-to-strength ratio, at a given age, the stress developed by the concrete in the match-cured rigid cracking frame is divided by the splitting tensile strength. At the time of cracking, one might expect the stress-to-strength ratio to be approximately 100 percent. However, due to the specimen size of the cracking frame relative to the test cylinder, rate of loading, and type of loading, the values of the stress-to-strength ratios fall between 50 to 80 percent.

The concrete specimen in the rigid cracking frame has a much higher volume than the splitting tensile test cylinder, which produces a higher probability of a flaw in the concrete. The rates of loading in the two specimens are also different. The splitting

tensile test specimen is loaded until failure, which occurs in less than 5 minutes. However, the rigid cracking frame specimen is under stress for approximately 5 days before failure. In addition to the rate of loading, the nature of the loading also differs. The concrete specimen in the rigid cracking frame is under direct tension loading. However, the splitting tensile test does not measure tensile strength directly.

5.2 EFFECT OF SEASONAL TEMPERATURE CONDITIONS

The effect of ambient temperature on the cracking tendency of concrete is evaluated using the following mixtures: I-CTRL, I-30C, I-20F, I-50S and I-LS. The control mixture I-CTRL was placed at 50 °F, 73 °F, and 95 °F and simulated using an ambient temperature of 50 °F, 73 °F, and 95 °F surrounding a typical 8-inch thick bridge deck as shown in Section 3.1.2 of Chapter 3. These temperatures were chosen to represent typical seasonal conditions such as winter, spring/fall, and summer. The SCM mixtures with 30% Class C fly ash, 20% Class F fly ash and 50% GGBF Slag were placed at 95 °F and simulated using summer placement conditions. The concrete mixture with dolomitic limestone coarse aggregates (mixture I-LS) was placed at 73 °F and 95 °F and simulated with spring/fall and summer placement conditions. The mechanical properties, temperature development, and stress development of all these mixtures can be found in Sections 4.2 and 4.3 of Chapter 4.

5.2.1 CRACKING SENSITIVITY

The seasonal temperature condition surrounding a concrete element affects the rate of hydration. As mentioned previously, elevated temperatures amplify the rate of temperature rise, as shown in Figures 4-7, 4-8 and 4-9.

In addition, the rate of development of the modulus of elasticity is more affected by the use of SCMs than the increase in seasonal temperature conditions, as shown in Figure 4-2.

5.2.1.1 Control Mixtures

As the seasonal temperature decreased, the cracking temperatures decreased, as shown in Figure 5-1. According to Springenschmid and Breitenbücher (1998), the cracking temperature provides an indication of the cracking sensitivity of the mixture. The lower the cracking temperature, the lower the risk of cracking for the given concrete mixture and its placement/curing conditions. From Figure 5-1, a very clear trend can be identified between the placement temperature and the cracking temperature. The cracking temperature continues downward from the 95 °F to the 50 °F condition. When compared to the 95 °F – 95 °F condition, the cracking temperatures were reduced by approximately 40 °F by the decrease in seasonal temperature conditions. The seasonal temperature conditions thus had a substantial impact on the cracking tendency of the control mixtures.

Figure 5-2 shows the stress-to-strength plot for the control mixtures. From Figure 5-2, it is seen that the seasonal temperature changes had only small impacts on the slopes of the stress-to-strength ratio development of the 95 °F – 95 °F and 73 °F – 73 °F mixtures, even though the cracking temperature was reduced.

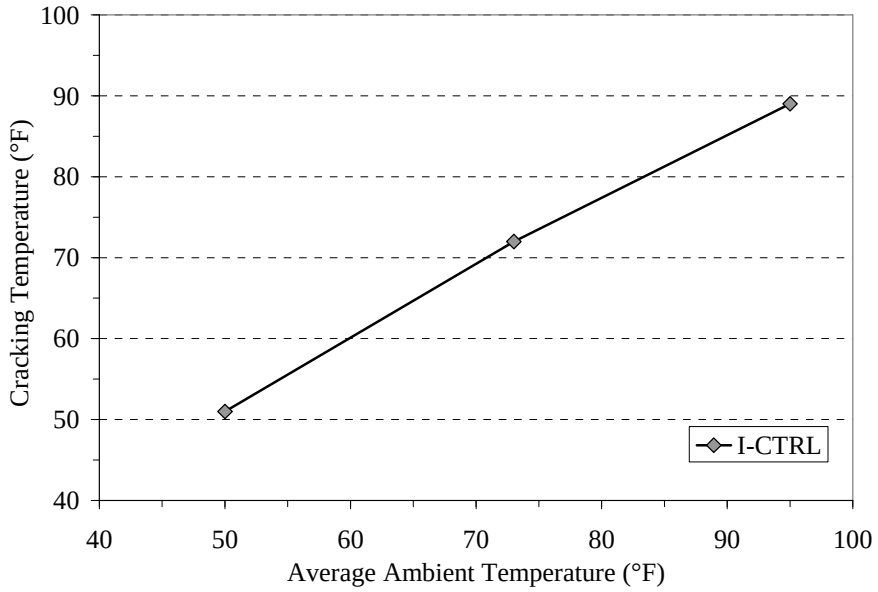

Figure 5-1: Effect of seasonal temperature conditions on control mixtures

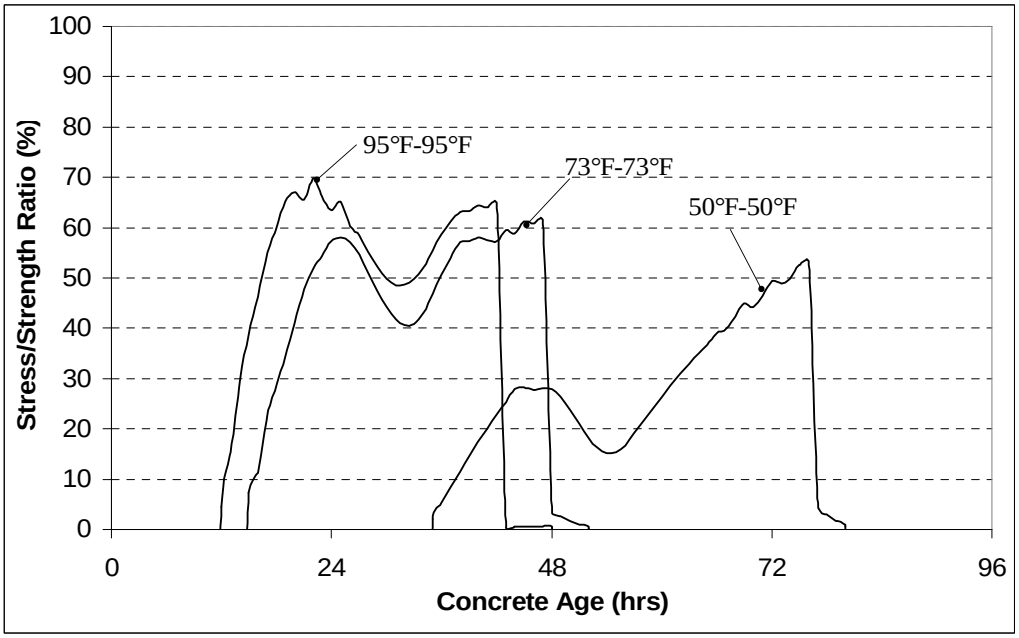

Figure 5-2: Effect of seasonal temperature conditions on the stress-to-strength ratio of the control mixtures

However, the rate of stress-to-strength development was lower for the 50 °F – 50 °F mixture.

5.2.1.2 Limestone Mixtures

Limestone mixtures showed behavior, similar to that of control mixtures. In these mixtures too, as the average seasonal temperature reduced, the cracking temperatures decreased, as shown in Figure 5-3. In these mixtures too, the cracking temperature continues downward from the 95 °F to the 73 °F condition. When compared to the 95 °F – 95 °F condition, the cracking temperatures were reduced by approximately 20 °F decreasing the average seasonal temperature to 73 °F. Although the cracking temperature was reduced, the seasonal temperature changes only had a small impact on the slopes of the stress-to-strength ratio development, as shown in Figure 5-4.

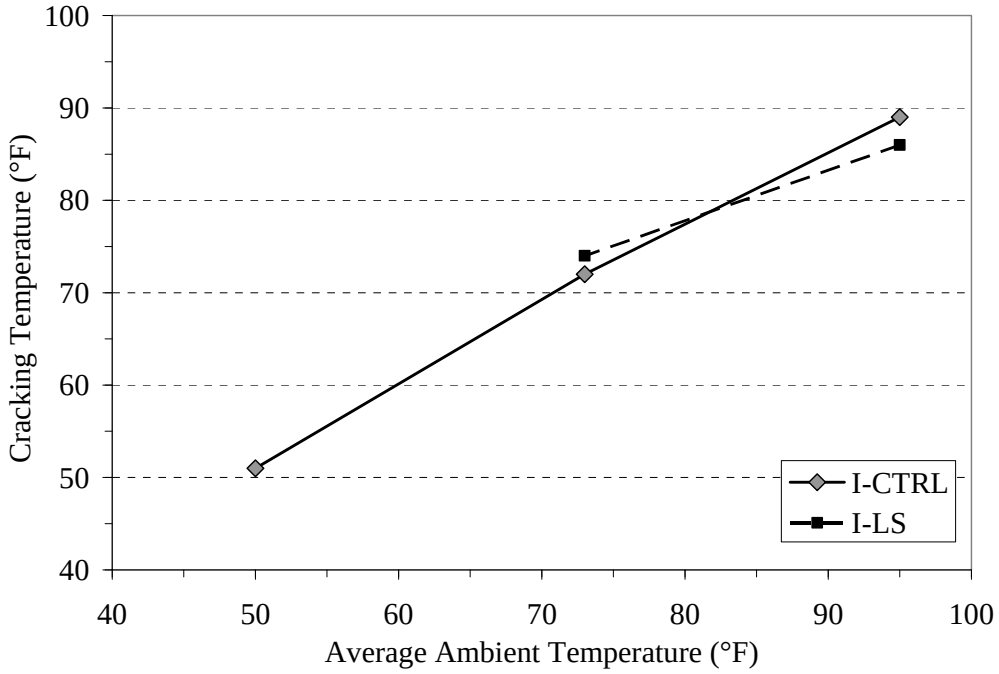

Figure 5-3: Effect of seasonal temperature conditions on limestone mixtures

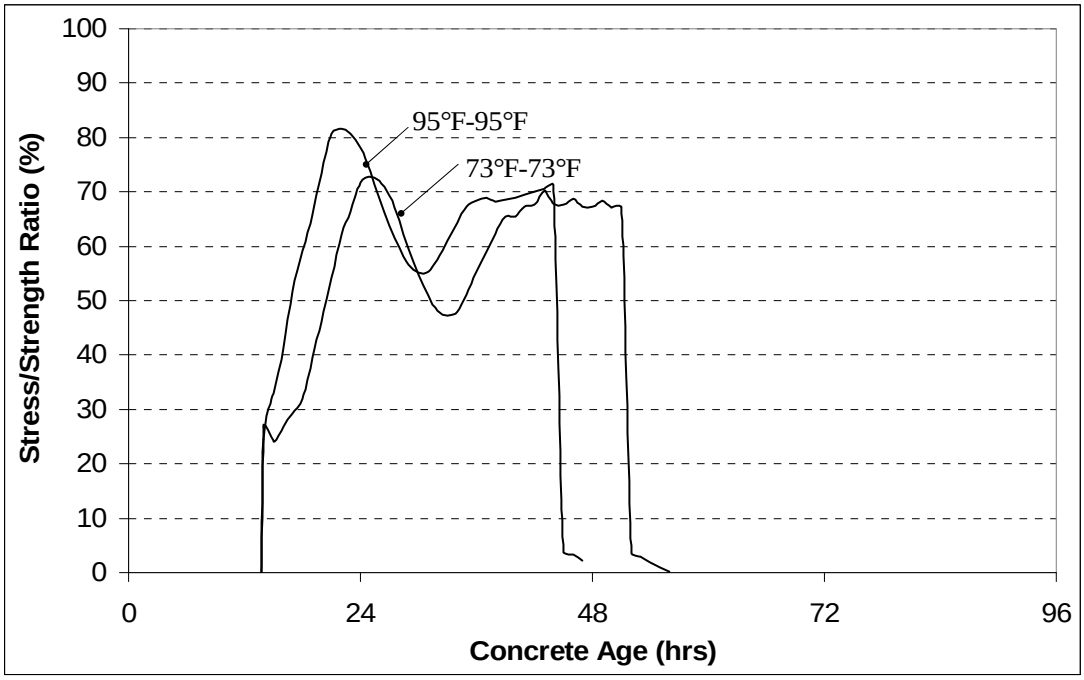

Figure 5-4: Effect of seasonal temperature conditions on the stress-to-strength ratio of the limestone mixtures

5.2.2 AUTOGENOUS SHRINKAGE STRESSES

Due to the nature of the laboratory testing program, the isothermal temperature conditions were selected based on the fresh concrete placement temperature. All the concrete mixtures were tested under isothermal conditions. None of the mixtures cracked under these isothermal conditions by the end of testing.

5.2.2.1 Control Mixtures

The magnitude of the autogenous stress was found to be dependent on the isothermal temperature conditions. The reduction in seasonal temperature conditions affected the

magnitude of autogenous stresses for the control mixtures, as shown in Figure 4-10. However, all these stress values are within 50 psi.

5.2.2.2 Limestone Mixtures

Limestone mixtures exhibited a similar relationship with the isothermal conditions as that of the control mixtures, as shown earlier in Figure 4-14. The magnitude of autogenous stress is dependent on the isothermal temperature. However, the stress values are within 25 psi of each other.

5.3 EFFECT OF AGGREGATE TYPE

The effect of aggregate type on the cracking tendency is evaluated using the two mixtures i.e. I-CTRL and I-LS placed at 73 °F and 95 °F. The mechanical properties of these mixtures can be found in Sections 4.2 and 4.3.

5.3.1 CRACKING SENSITIVITY

The stress-to-strength plot for the control mixture (I-CTRL) and the limestone mixture (I-LS) is given in Figure 5-5. It is observed that the time to cracking of the limestone mixtures are similar to that of control mixtures for both placement conditions.

5.3.2 AUTOGENOUS SHRINKAGE STRESSES

The autogenous shrinkage stress values for control mixture and limestone mixtures are as shown in Figure 4-13. Not much of a difference in the value of autogenous stress is observed between the control and limestone mixtures at the end of 7 days.

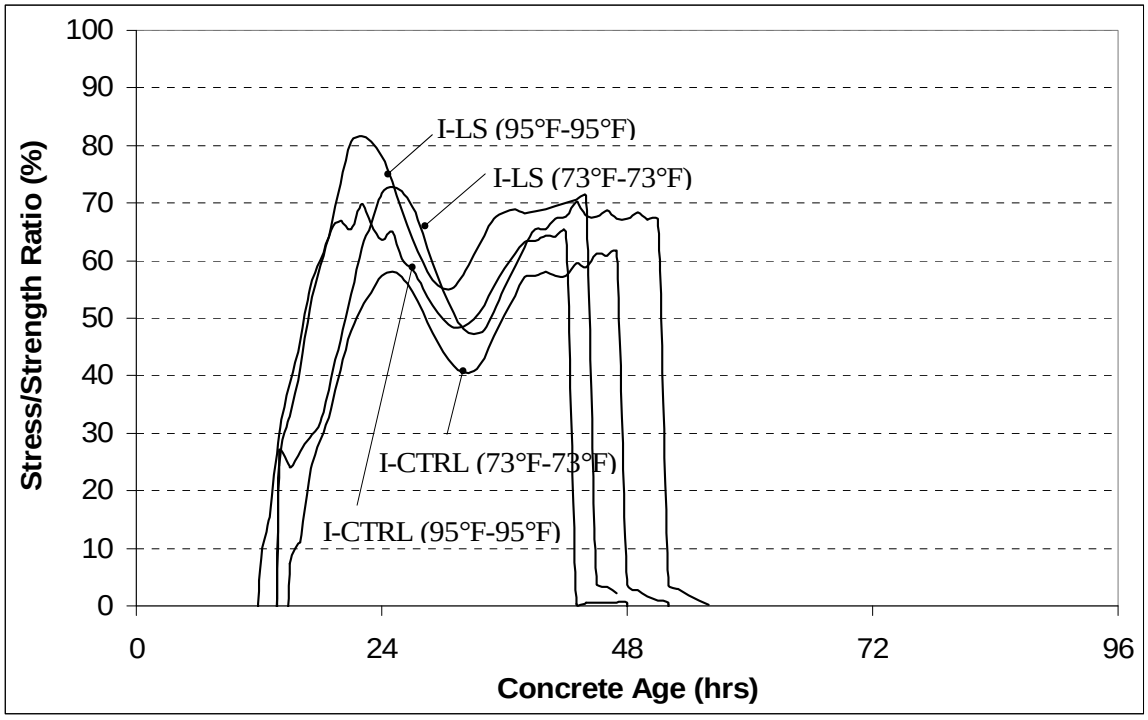

Figure 5-5: Effect of change in aggregate type on cracking sensitivity of control mixtures

5.4 EFFECT OF SUPPLEMENTARY CEMENTING MATERIALS

The effect of supplementary cementing materials on the cracking tendency of concrete was evaluated using the following mixtures: I-CTRL, I-30C, I-20F, and I-50S. These four mixtures were placed at 95 °F and simulated using typical summer ambient temperature conditions. The mechanical properties, temperature development, and stress development of these mixtures can be found in Sections 4.2 and 4.3.

5.4.1 CRACKING SENSITIVITY

Springenschmid and Breitenbücher (1998) stated that it is current practice to reduce the cement content as much as possible in order to reduce the heat development.

Supplementary cementing materials (SCMs) can be used to reduce the heat generation associated with hydration, as discussed in Section 2.1.3. If same cement is replaced by SCMs that have lower heats of hydration, then the temperature rise of the concrete mixture is lower (refer to Figure 2-2, 2-3 and 2-4). These lower temperatures lead to lower zero-stress temperatures and thus lower tensile stresses when cooling to the same temperature. In the present study, the temperature history for the control and SCM mixtures is shown in Figure 4-8A.

Under the 95 °F-95 °F temperature conditions, the maximum temperature reached by the control mixture is 135 °F, by the 20% Class F fly ash mixture is 126 °F, by the 30% Class C fly ash mixture is 119 °F, and by the 50% GGBF Slag mixture is 113 °F. These substantial reductions are caused by the replacement of cement by the SCMs in the concrete mixture.

The restrained stress development of the control mixture and SCM mixtures is shown in Figure 4-7B. The 50% GGBF slag and 30% Class C fly ash mixtures were very effective in mitigating cracking. During testing, the 30% Class C fly ash mixture cracked at about 122 hours. However, the 50% GGBF Slag mixture did not crack even at 7 days (168 hours), and artificial cooling at a rate of 1°C/hr was required to induce cracking. The use of these two mixtures increased the time of cracking by more than 100 percent over the control mixture. Although the 20% Class F fly ash mixture was not as effective in reducing the cracking tendency of the concrete, it too reduced the cracking tendency of the control mixture. It is to be noted here that, the maximum stresses reached for all the mixtures were approximately 250 psi to 350 psi.

A review of the cracking temperatures of the control and SCM mixtures indicate that replacement of cement with SCMs reduces the cracking temperature, and thus the cracking sensitivity of the concrete, significantly. The 50% GGBF Slag mixture caused the maximum reduction of the cracking temperature, as shown Figure 5-6. The specimen cracked at 72 °F after artificial cooling was started.

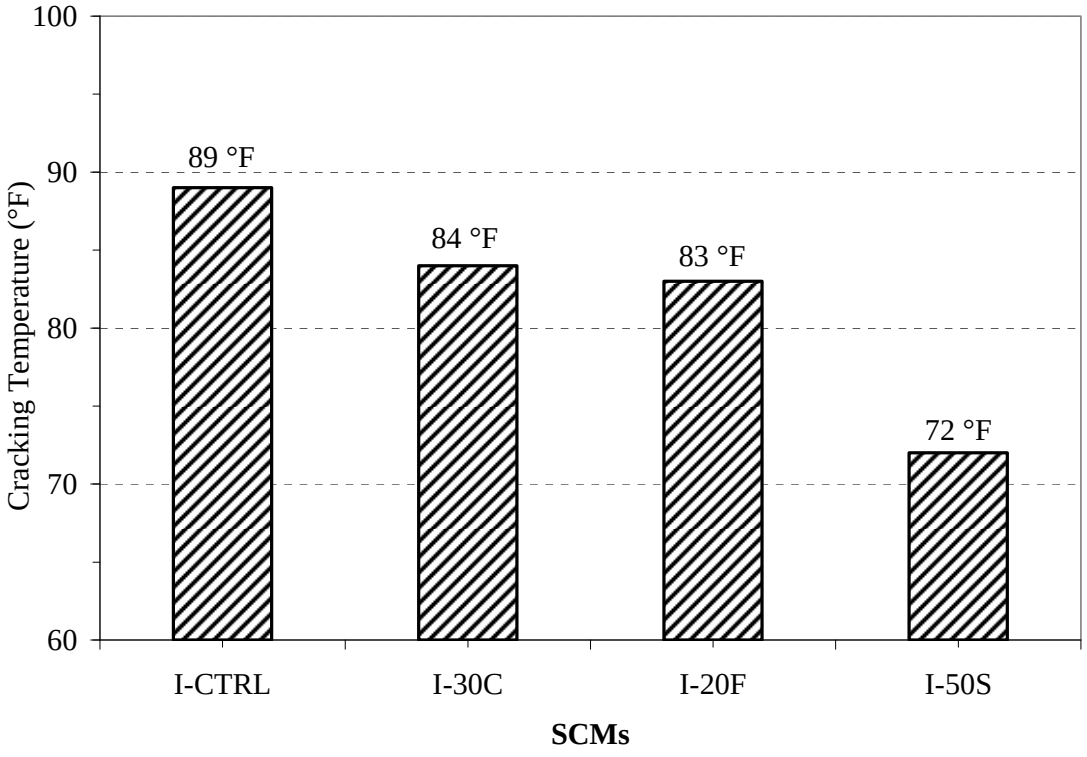

Figure 5-6 Effect of SCMs on cracking temperature under 95 °F - 95 °F curing condition

Springenschmid and Breitenbucher (1998) found fly ash to reduce the cracking temperature due to an increase in tensile strength of the concrete due to the pozzolanic reaction. This should improve the cracking tendency of the concrete. In the present study also, it was found that the use of fly ash and GGBF Slag caused a reduction in the cracking temperature.

In their study, Breitenbucher and Mangold (1994) concluded that GGBF slag lead to reduced temperature rises and reduced tensile stresses. These findings are also valid for the GGBF slag mixtures evaluated in this study. It is important to note that the stress-to-strength ratio of the GGBF slag mixture was only 45% at the time that the I-CTRL mixture cracked as shown in Figure 5-7. Therefore, GGBF slag decreased the cracking tendency of the concrete under summer temperature conditions.

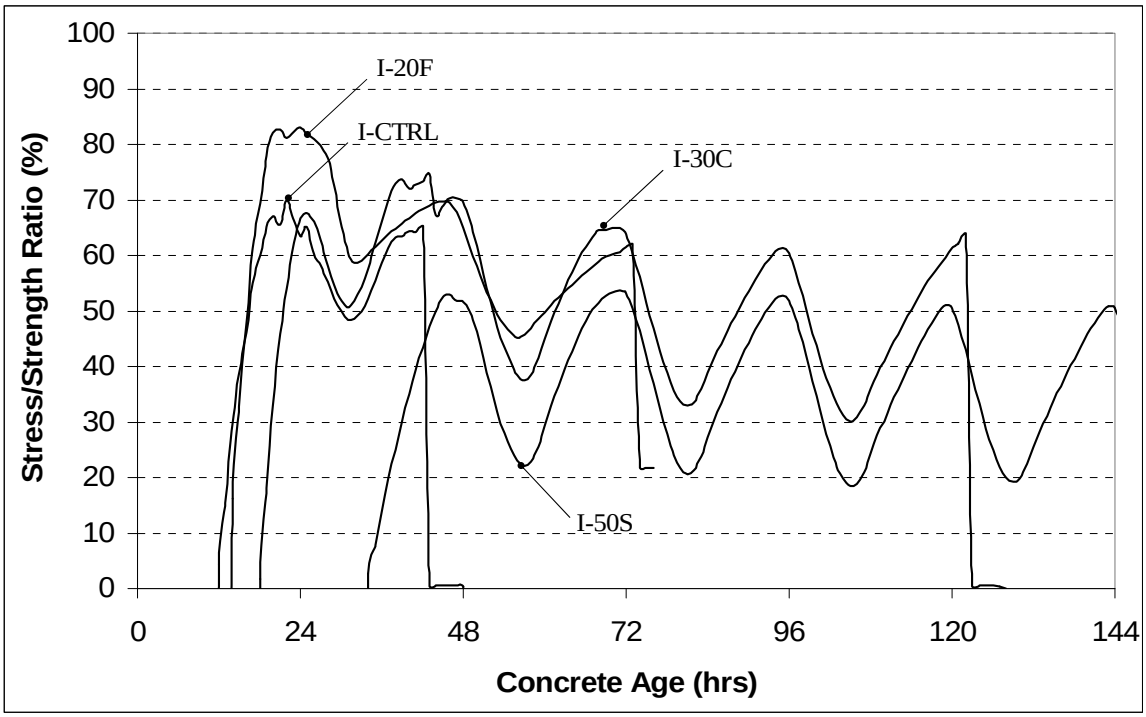

Figure 5-7: Effect of SCMs on the stress-to-strength ratio at 95 °F-95 °F placement

5.4.2 AUTOGENOUS SHRINKAGE STRESSES

The use of SCMs reduces the quantity of portland cement in a concrete mixture, which reduces the early-age volume change associated with chemical shrinkage. Decreasing

chemical shrinkage reduces the magnitude of autogenous stresses as shown in Figure 4-11.

Tazawa and Miyazawa (1997) found autogenous shrinkage to increase when GGBF slag with high fineness is used. This phenomenon could be related to the denser pore structure associated with the use of GGBF slag. These smaller pores may induce higher capillary tension forces during self-desiccation which would lead to higher autogenous shrinkage stresses (Lura et al. 2001). But as Figure 4-12 clearly shows, the replacement of cement with SCMs reduces the magnitude of autogenous shrinkage stresses. The I-50S mixture was the most mixture for reducing autogenous shrinkage stresses, according to the results of the present study.

5.5 SUMMARY

Under the current testing program, two rigid cracking frames were used to evaluate the restrained stress development of various concrete mixtures at early-ages. Eight mixtures were evaluated under both match-cured and isothermal conditions. The effects of seasonal temperature conditions, supplementary cementing materials, and aggregate type on the cracking tendency of concrete mixtures were thoroughly examined.

5.5.1 CRACKING SENSITIVITY

The results obtained from the laboratory testing program reveal that the fresh concrete placement temperature has a substantial impact on the early-age stress development of a concrete specimen in the rigid cracking frame. Lowering of the placement temperature reduced the cracking temperature, which corresponds to the findings of Springenschmid

and Breitenbücher (1998) and Meadows (2007). A placement temperature of 50 °F and 73 °F produced a reduced stress-to-strength ratio relative to a 95 °F placement temperature prior to artificial cooling in the control mixtures. Consequently, the time of cracking was increased, which indicates that cracking tendency was reduced. Mixtures containing limestone coarse aggregate exhibited similar behavior, but had a marginal increase in cracking times.

The 20% Class F fly ash mixture, 30% Class C Fly ash mixture and the 50% GGBF slag mixtures were found to very effective in prolonging cracking under hot weather placement conditions. In addition, GGBF slag mixtures substantially decreased the cracking temperature of the mixture.

5.5.2 AUTOGENOUS SHRINKAGE AND AUTOGENOUS SHRINKAGE STRESSES

The data collected for all the mixtures reveal that autogenous shrinkage stresses were within 50 psi of each other. SCMs were found to slightly reduce autogenous shrinkage stresses with the increase in replacement percentage. The use of SCMs reduces the quantity of portland cement in a concrete mixture, which reduces the volume change associated with chemical shrinkage. Decreasing chemical shrinkage reduces the magnitude of autogenous shrinkage stresses.

CHAPTER 6

CONCLUSIONS AND RECOMMENDATIONS

Early-age cracking in bridge decks is a severe problem that may reduce the functional life of structures. Cracking originates from stresses induced by volume change as a result of thermal, drying, and autogenous shrinkage, coupled with restraint conditions that restrict movement of the concrete. Over time, stresses may exceed the tensile strength of the concrete, which will result in cracking.

The mechanisms driving early-age cracking are influenced by many complex variables, and many of these mechanisms are not clearly understood. In order to better understand the mechanisms driving early-age cracking, the primary variables that influence the cracking sensitivity of the concrete were evaluated in this study.

The experimental testing program utilized a rigid cracking frame, a free shrinkage frame, match-curing system, and a semi-adiabatic hydration drum. The rigid cracking frame was used to evaluate the cracking sensitivity of the concrete mixtures. The free shrinkage frame was used to assess the shrinkage of the concrete mixtures under no restraint conditions. Each concrete mixture was placed and consolidated in the rigid cracking frame. One specimen was subjected to isothermal conditions while another was subjected to a match-cured temperature history in order to distinguish autogenous and thermal stresses. The match-cured temperature profile was created to be representative of

an 8-in thick bridge deck. The free shrinkage frame was also subjected to the match-curing temperature history and isothermal temperatures to measure the volume change under free restraint conditions. Molded cylinders, in the match-curing box, were subjected to the same temperature profile as the match-cured rigid cracking frame so that the mechanical properties and setting times of the concrete in the rigid cracking frame and the free shrinkage frame could be determined.

Eight mixtures were designed to evaluate the effects of placement temperature, seasonal temperature conditions, and concrete constituents on the cracking tendency of concrete mixtures. The effects of placement temperature were investigated by batching concrete mixtures at three different temperatures: 50°F, 73°F, and 95°F. The effects of seasonal temperature changes were investigated, by match-curing each concrete specimen, to a simulated temperature profile based on its unique hydration behavior. The effects of concrete constituents were evaluated by examining different aggregate types, and supplementary cementing materials.

6.1 CONCLUSIONS

The test method developed and discussed in this thesis is a realistic technique for investigating early-age restraint stresses. This testing program provided a means to measure the development of restraint stresses, in concrete bridge decks during early-ages. Results from the experimental laboratory testing program justify the following conclusions:

6.1.1 CRACKING SENSITIVITY

- Lowering of the placement temperature reduces the cracking tendency of the chosen concrete irrespective of the type of aggregate used in the present study.
- When compared to a placement temperature of 95°F, placement temperatures of 50°F and 73°F produced a reduced stress-to-strength ratio. This reduces the likelihood of early-age cracking in structures.
- Use of SCMs such as fly ash and GGBF slag is effective for reducing the temperature rise in the concrete. The GGBF slag mixture was the most effective in reducing the cracking tendency of concrete containing plain Type I cement when placed under summer conditions. However, the cracking tendency when the concrete is cooled and placed needs to be evaluated.
- The GGBF slag mix was very effective in delaying the time to cracking. Even after 7 days of testing, the specimen had not cracked and artificial cooling had to be used to induce cracking. Similarly, 30% replacement of Class C fly ash and 20% replacement of Class F fly ash were found to reduce the magnitude of temperature development and delay cracking.
- The use of dolomitic limestone in place of river gravel does not seem to have a significant effect on the cracking tendency or time of cracking. The limestone mixtures showed very similar temperature history and stress profile to that of the control mixtures.
- SCMs seem to marginally reduce the autogenous stresses (from the isothermal cracking frame). The use of SCMs reduces the quantity of portland cement in a

6.1.2 AUTOGENOUS SHRINKAGE AND STRESS

- Use of SCMs reduces the autogenous shrinkage. However, the water-to-cement ratio is known to be the variable that has the most significant effect on the magnitude of autogenous shrinkage stresses and hence mixtures with lower w/cm need to be investigated.
- Limestone mixtures had approximately similar autogenous stress as the control mixtures. However, they need to be investigated at lower w/c, to clearly understand their effect on the autogenous stress.

6.2 RECOMMENDATIONS

In order to develop a more accurate understanding of early-age behavior of concrete, the following additional research is recommended:

- Further investigations into the effect of concrete constituents on the early-age behavior of concrete such as different cement types, aggregate type and ternary mixtures
- Further investigations into the effect of water-cementitious materials ratio
- Further investigations on cold mixes at hot weather conditions
- Implementation of relative humidity sensors to further study and quantify autogenous shrinkage

Based on the experience gained through the execution of this experimental testing program outlined in Chapter 3 of this thesis, the following equipment modifications are recommended:

- Proper temperature control techniques need to be developed to accurately simulate the temperature history in the cracking frame at early age of concrete. The existing datalogger program code should be modified to control the circulators for proper simulation.
- Relative humidity probes need to be developed that be used to assess the driving mechanism that causes autogenous stresses and shrinkage.
- The datalogger program should be modified for independent use of any unit (i.e. cracking frame, shrinkage frame, match-curing box).

REFERENCES

ACI 116R-12. 1997. *Cement and Concrete Terminology*. Farmington Hills, MI: American Concrete Institute.

ACI 209R. 1997. *Prediction of Creep, Shrinkage, and Temperature in Concrete Structures.* Farmington Hills, MI: American Concrete Institute.

ACI 232.2R. 1997. *Use of Fly Ash in Concrete.* Farmington Hills, MI: American Concrete Institute.

ACI 233.R. 1997. *Ground Granulated Blast-Furnace Slag as a Cementitious Constituent in Concrete*. Farmington Hills, MI: American Concrete Institute.

ACI 318. 2005. *Building Code Requirements for Structural Concrete and Commentary*. Farmington Hills, MI: American Concrete Institute.

ASTM C 1064. 2004. Standard Test Method for Temperature of Freshly Mixed Hydraulic-Cement Concrete. American Society for Testing and Materials. West Conshohocken, PA.

ASTM C 138. 2001. Standard Test Method for Density (Unit Weight), Yield, and Air Content (Gravimetric) of Concrete. American Society for Testing and Materials. West Conshohocken, PA.

ASTM C 143. 2003. Standard Test Method for Slump of Hydraulic-Cement Concrete. American Society for Testing and Materials. West Conshohocken, PA.

ASTM C 157. 2004. Standard Test Method for Length Change of Hardened Hydraulic-Cement Mortar and Concrete. American Society for Testing and Materials. West Conshohocken, PA.

ASTM C 1581. 2004. Standard Test Method for Determining Age at Cracking and Induced Tensile Stress Characteristics of Mortar and Concrete under Restrained Shrinkage. American Society for Testing and Materials. West Conshohocken, PA.

ASTM C 192. 2002. Standard Practice for Making and Curing Concrete Test Specimens in the Laboratory. American Society for Testing and Materials. West Conshohocken, PA.

ASTM C 231. 2004. Standard Test Method for Air Content of Freshly Mixed Concrete by the Pressure Method. American Society for Testing and Materials. West Conshohocken, PA.

ASTM C 33. 2003. Standard Specification for Concrete Aggregates. American Society for Testing and Materials. West Conshohocken, PA.

ASTM C 39. 2003. Standard Test Method for Compressive Strength of Cylindrical Concrete Specimens. American Society for Testing and Materials. West Conshohocken, PA.

ASTM C 469. 2002. Standard Test Method for Static Modulus of Elasticity and Poisson's Ratio of Concrete in Compression. American Society for Testing and Materials. West Conshohocken, PA.

ASTM C 496. 2004. Standard Test Method for Splitting Tensile Strength of Cylindrical Concrete Specimens. American Society for Testing and Materials. West Conshohocken, PA.

ASTM C 670. 2003. Standard Practice for Preparing Precision and Bias Statements for Test Methods for Construction Materials. American Society for Testing and Materials. West Conshohocken, PA.

ASTM C 403. 2004. Standard Test Method for Time of Setting of Concrete Mixtures by Penetration Resistance. American Society for Testing and Materials. West Conshohocken, PA.

Bamforth, P.B. 1980. In Situ Measurement of the Effect of Partial Portland Cement Replacement Using Either Fly Ash or Ground Granulated Blast-Furnace Slag on the Performance of Mass Concrete. *Institution of Civil Engineers*, Part 2, Vol 69: 777-800. London.

Bamforth, P.B. and W.F. Price. 1995. *Concreting Deep Lifts and Large Volume Pours*. Westminster London: Construction Industry Research and Information Association. CIRIA Report 135.

Bažant, Z.P. and E. Osman. 1976. Double Power Law for Basic Creep of Concrete. *Materials and Structures* 9, no. 49: 3-11.

Bažant, Z.P. and J.C. Chern. 1985a. Log Double Power Law for Concrete Creep. *Journal of the American Concrete Institute* 82, no. 5: 665-675.

Bažant, Z.P. and J.C. Chern. 1985b. Triple Power Law for Concrete Creep. *Journal of Engineering Mechanics* 111, no. 1: 63-83.

Bažant, Z.P. and J.C. Chern. 1985c. Concrete Creep at Variable Humidity. *Materials and Structures* 18, no. 103: 1-19.

Bjøntegaard, Ø. 1999. *Thermal Dilation and Autogenous Deformation as Driving Forces to Self-Induced Stresses in High Performance Concrete*. Doctoral Thesis. Norwegian University of Science and Technology, Division of Structural Engineering.

Bogue, R.H. 1929. Calculations of the Compounds in Portland Cement. *Industrial and Engineering Chemistry 1*, no. 4: 192.

Breitenbücher, R. 1990. Investigation of Thermal Cracking with the Cracking-Frame. *Materials and Structures* 23, no. 135: 172-177.

Breitenbücher, R. and M. Mangold. 1994. Minimization of Thermal Cracking in Concrete at Early Ages. In *RILEM Proceedings 25, Thermal Cracking in Concrete at Early Ages*, ed. R. Springenschmid, 205-212. London: E & FN Spon.

Carino, N.J. and H.S. Lew. 2001. The Maturity Method: From Theory to Application. National Institute of Standards and Technology.

Emanuel, J.H. and L. Hulsey. 1977. Prediction of the Thermal Coefficient of Expansion of Concrete. *Journal of the American Concrete Institute* 74, no. 4: 149-155.

Emborg, M. 1989. *Thermal Stresses in Concrete Structures at Early Ages*. Doctoral Thesis. Luleå University of Technology, Division of Structural Engineering.

FDOT. 2002. *Structures Design Guidelines (LRFD).*

Federal Highway Administration High Performance Concrete Website (FHWA). 2005. Located on the World Wide Web at: http://knowledge.fhwa.dot.gov/cops/hpcx.nsf/home?openform&Group=HPC%20Cast-in-Place%20Construction&tab=WIP

Fulton, F.S. 1974. The Properties of Portland Cement Containing Milled Granulated Blast-Furnace Slag. Portland Cement Institute. 4-46. Johannesburg.

Hammer, T.A., and K.T. Fossa. 2006. Influence of Entrained Air Voids on Pore Water Pressure and Volume Change of Concrete Before and During Setting. *Materials and Structures 39*: 801-808.

Hedlund, H. 2000. *Hardening Concrete: Measurement and Evaluation of Non-Elastic Deformation and Associated Restraint Stresses*. Doctoral Thesis. Luleå University of Technology, Division of Structural Engineering.

Hedlund, H. and G. Westman. 1999. Evaluation and Comparison of Sealed and Non-Sealed Shrinkage Deformation Measurements of Concrete. In JCI Proceedings, *Autogenous Shrinkage of Concrete*, 121-132. New York: Routledge.

Holt, E. and M. Leivo. 2004. Cracking Risks Associated with Early Age Shrinkage. *Cement and Concrete Composites* 26, no. 5: 521-530.

Holt, E. 2004. Contribution of Mixture Design to Chemical and Autogenous Shrinkage of Concrete at Early Ages. *Cement and Concrete Research* 35, no. 3: 464-472.

Holt, E. 2001. *Early Age Autogenous Shrinkage of Concrete*. Doctoral Thesis. The University of Washington in Seattle.

Kada, H., M. Lachemi, N. Petrov, O. Bonnequ, and P.-C. Aïtcin. 2002. Determination of the Coefficient of Thermal Expansion of High Performance Concrete from Initial Setting. *Materials and Structures* 35, no. 245: 35-41.

Kosmatka, H., B. Kerkhoff, and W.C. Panarese. 2002. Design and Control of Concrete Mixtures. 14th Edition. Skokie, Illinois. Portland Cement Association.

Krauss, P.D. and E.A. Rogalla. 1996. *Transverse Cracking in Newly Constructed Bridge Decks*. Washington D.C.: Transportation Research Board, National Research Council. NCHRP Report 380.

Lange, D. and S. Altougat. 2002. Early Thermal Changes. In *RILEM Report 25, Thermal Cracking in Concrete at Early Ages*, ed. A. Bentur, 37-38. RILEM Publications S.A.R.L.

Larson, M. 2003. *Thermal Crack Estimation in Early Age Concrete: Models and Methods for Practical Application*. Doctoral Thesis. Luleå University of Technology, Division of Structural Engineering.

Lura, P., K. van Breugel, and I. Maruyama. 2001. Effect of Curing Temperature and Type of Cement on Early-Age Shrinkage of High-Performance Concrete. *Cement and Concrete Research 31*, no. 12: 1867-1872.

Lynam, C.G. 1934. *Growth and Movement in Portland Cement Concrete*. London: Oxford University Press.

Mangold, M. 1994. *The Development of Restraint and Intrinsic Stresses in Concrete Members during Hydration*. Doctoral Thesis. Technical University of Munich.

Mangold, M. 1998. Methods for Experimental Determination of Thermal Stresses and Crack Sensitivity in the Laboratory. In *RILEM Report 15, Prevention of Thermal Cracking in Concrete at Early Ages*, ed. R. Springenschmid, 26-39. London: E & FN Spon.

Mehta, P. K. and P.J.M. Monterio. 2006. *Concrete: Microstructure, Properties, and Materials*. 3rd Edition. McGraw-Hill, Inc. New York, NY.

Meadows, Jason Lee. 2007 *Early age cracking of Mass Concrete Structures,* M.S Thesis submitted to Auburn Univeristy, Alabama.

Mindess, S., J. Young, and D. Darwin. 2002. *Concrete*. 2nd Edition. Prentice Hall. Upper Saddle River, NJ.

Mindess, S., and J.F. Young. 1981. *Concrete*. Prentice Hall. Upper Saddle River,NJ

NCHRP Report 380, *Transverse Cracking in Newly Constructed Bridge Decks,* Transportation research board report, 1996.

Nilsson, M. 2003. *Restraint Factors and Partial Coefficients for Crack Risk Analyses of Early Age Concrete Structures*. Doctoral Thesis 2003:19. Luleå University of Technology, Division of Structural Engineering.

Paulini, P. 1996. Outlines of Hydraulic Hardening – an Energetic Approach. In Workshop NTNU/SINTEF*, Early Volume Changes and Reactions in Paste-Mortar-Concrete*. Trondheim, Norway.

Poole J.L, Riding K.A., Browne R.A., Schindler A.K. 2006. Temperature Management of Mass Concrete Structures. *Concrete Construction Magazine.*

Sakai, E., S. Miyahara, S. Ohsawa, S. Lee, and M. Daimon. 2005. Hydration of Fly Ash Cement. *Cement and Concrete Research* 35, no. 6: 1135-1140.

Schindler, A. and K. Folliard. 2005. Heat of Hydration Models for Cementitious Materials. *Journal of American Concrete Institute 102*, no. 1: 24-33

Sellevold, E., Ø. Bjøntegaard, H. Justnes, and P.A. Dahl. 1994. High Preformance Concrete: Early Volume Change and Cracking Tendency. In *RILEM Proceedings 25, Thermal Cracking in Concrete at Early Ages*, ed. R. Springenschmid, 230-236. London: E & FN Spon.

Sioulas, B. and J.G. Sanjayan. 2000. Hydration Temperatures in Large High-Strength Concrete Columns Incorporating Slag. *Cement and Concrete Research* 30, no.11: 1791-1799.

Springenschmid, R. and R. Breitenbücher. 1998. Influence of Constituents, Mix Proportions and Temperature on Cracking Sensitivity of Concrete. In *RILEM Report 15, Prevention of Thermal Cracking in Concrete at Early Ages*, ed. R. Springenschmid, 40-50. London: E & FN Spon.

Springenschmid, R., R. Breitenbücher, and M. Mangold. 1994. Development of the Cracking Frame and the Temperature-Stress Testing Machine. In *RILEM Proceedings 25, Thermal Cracking in Concrete at Early Ages*, ed. R. Springenschmid, 137-144. London: E & FN Spon.

Tazawa, E. and S. Miyazawa. 1997. Influence of Constituents and Composition on Autogenous Shrinkage of Cementitious Materials. *Magazine of Concrete Research 49*, No. 178: 15-22.

Thielen, G. and W. Hintzen. 1994. Investigation of Concrete Behaviour Under Restraint with a Temperature-Stress Test Machine. In *RILEM Proceedings 25, Thermal Cracking in Concrete at Early Ages*, ed. R. Springenschmid, 145-152. London: E & FN Spon.

Townsend, C.L. 1965. Control of Cracking in Mass Concrete Structures. Engineering Monograph No. 34. Water Resources Technical Publication. U.S. Department of the Interior. Bureau of Reclamation. 1965.

TxDOT. 2004. *Standard Specifications for Construction and Maintenance of Highways, Streets, and Bridges*. Texas Department of Transportation. Austin, Texas. pp 500.

USBR. Concrete Manual. 8th Edition. Water Resources Technical Publication. U.S. Department of the Interior. Bureau of Reclamation. 1975.

Verbeck, G.J. and R.H. Helmuth. 1968. Structure and Physical Properties of Cement Paste. Proceedings of 5th International Symposium on Chemistry of Cement. Tokyo, Part III, p 1-32.

Wade, S. 2005. *Evaluation of the Maturity Method to Estimate Concrete Strength*. Master Thesis. Auburn University, Department of Civil Engineering.

Waller, V., L. d'Aloïa, F. Cussigh, and S. Lecrux. 2004. Using the Maturity Method in Concrete Cracking Control at Early Ages. *Cement and Concrete Composites* 26, no.5: 589-599.

Wang, Ch. And W.H. Dilger. 1994. Prediction of Temperature Distribution in Hardening Concrete. In *RILEM Proceedings 25, Thermal Cracking in Concrete at Early Ages*, ed. R. Springenschmid, 21-28. London: E & FN Spon.

Westman, G. 1999. *Concrete Creep and Thermal Stresses: New Creep Models and their Effects on Stress Development*. Doctoral Thesis. Luleå University of Technology, Division of Structural Engineering.

Whigham, J.A. 2005. *Evaluation of Restraint Stresses and Cracking in Early-Age Concrete with the Rigid Cracking Frame*. Master Thesis. Auburn University, Department of Civil Engineering.

APPENDIX A

FRESH CONCRETE PROPERTIES

The objective of this appendix is to present the fresh concrete properties for each concrete mixture. As discussed in Chapter 3, each mixture was mixed separately on consecutive weeks for temperature history testing and isothermal testing. The first week's mix had two batches (batches A and B) and the second week's mix has one batch (batch A). The temperature, slump, air content, unit weight, and setting times for the concrete mixtures are presented in the following table.

Table A-1: Fresh concrete properties for control mixtures

Mixture	Week	Batch	Temp (°F)	Slump (in.)	Air (%)	Unit Weight (lb/ft^3)	Initial Set (hrs)	Final Set (hrs)
I-CTRL (73°F - 73°F)	1	A	75	4	1.9	148.3	4.5	6.1
		B	75	4	2.1	148.0		
	2	A	74	4.25	2.2	148.4	4.8	6.3
I-CTRL (50°F - 50°F)	1	A	48	4.5	2.2	148.1	8.2	11.1
		B	49	4	2.4	148.3		
	2	A	52	4.5	2.0	148.6	8.1	10.7
I-CTRL (95°F - 95°F)	1	A	98	3	2.1	148.4	3.1	4.1
		B	99	3.5	2.3	150.0		
	2	A	94	3.25	2.1	149.2	3.1	4.2

Table A-2: Fresh concrete properties for SCM mixtures

Mixture	Week	Batch	Temp (°F)	Slump (in.)	Air (%)	Unit Weight (lb/ft3)	Initial Set (hrs)	Final Set (hrs)
I-30C (95°F - 95°F)	1	A	92	3.75	2.2	149.1	8.9	11.5
		B	96	3.5	2.3	149.5		
	2	A	98	4	2.4	148.4	8.2	10.7
I-20F (95°F – 95°F)	1	A	96	3.5	2.3	147.9	3.8	4.9
		B	97	3.25	1.9	148.1		
	2	A	94	3.5	1.9	148.4	3.9	4.7
I-50S (95°F – 95°F)	1	A	97	4	2.2	149.2	3.6	5.8
		B	98	3.25	2.1	148.7		
	2	A	94	3.75	2.3	148.6	3.5	5.6

Table A-3: Fresh concrete properties for limestone mixtures

Mixture	Week	Batch	Temp (°F)	Slump (in.)	Air (%)	Unit Weight (lb/ft3)	Initial Set (hrs)	Final Set (hrs)
I-LS (73°F - 73°F)	1	A	71	4.5	2.4	148.1	5.2	7.5
		B	72	4.5	2.3	148.6		
	2	A	76	4	2.0	149.1	5.0	7.3
I-LS (95°F - 95°F)	1	A	97	3.5	2.0	149.1	3.6	4.8
		B	95	3.75	2.0	149.2		
	2	A	98	3.25	2.2	148.4	3.4	4.5

APPENDIX B

HYDRATION PARAMETERS

Table B-1: List of hydration parameters

Mix ID	Activation Energy J/mol	Tau hours	Beta	Alpha (Ultimate)	Hu J/kg
I-CTRL	27,944	13.542	1.171	0.796	513,000
I-30C	35,050	30.300	1.047	0.764	515,100
I-20F	35,000	25.70	1.157	1.000	393,900
I-50S	41500	42.70	0.889	0.897	473,300
I-LS	43,900	20.51	0.707	0.827	505,840